VYSOKÉ UČENÍ TECHNICKÉ V BRNĚ

BRNO UNIVERSITY OF TECHNOLOGY

FAKULTA STROJNÍHO INŽENÝRSTVÍ
LETECKÝ ÚSTAV

FACULTY OF MECHANICAL ENGINEERING
INSTITUTE OF AEROSPACE ENGINEERING

KONCEPČNÍ STUDIE LEHKÉHO DVOUMOTOROVÉHO PROUDOVÉHO LETOUNU

CONCEPTUAL STUDY OF VERY LIGHT TWIN JET AIRCRAFT

DIPLOMOVÁ PRÁCE
MASTER'S THESIS

AUTOR PRÁCE   Bc. MICHAL SMÝKAL
AUTHOR

VEDOUCÍ PRÁCE   Ing. TOMÁŠ URÍK
SUPERVISOR

BRNO 2015

Vysoké učení technické v Brně, Fakulta strojního inženýrství

Letecký ústav
Akademický rok: 2014/2015

ZADÁNÍ DIPLOMOVÉ PRÁCE

student(ka): Bc. Michal Smýkal

který/která studuje v **magisterském navazujícím studijním programu**

obor: **Stavba letadel (2301T039)**

Ředitel ústavu Vám v souladu se zákonem č.111/1998 o vysokých školách a se Studijním a zkušebním řádem VUT v Brně určuje následující téma diplomové práce:

Koncepční studie lehkého dvoumotorového proudového letounu

v anglickém jazyce:

Conceptual study of very light twin jet aircraft

Stručná charakteristika problematiky úkolu:

Diplomová práce se zabývá studií proveditelnosti lehkého letadla se dvěma proudovými motory. Stěžejní náplní práce je zpracování rešerše letounů obdobného charakteru, stanovení předpisové báze pro návrh a provedení koncepčního aerodynamického návrhu spolu s předběžným výpočet výkonů a vlastností letounu. Součástí práce je i výběr pohonné jednotky, vypracování hmotového rozboru, koncepční návrh hlavních konstrukčních celků a rozbor nákladů na vývoj letounu.

Cíle diplomové práce:

1. Zpracování rešerše letounů obdobného charakteru.
2. Koncepční aerodynamický návrh letounu.
3. Předběžný výpočet výkonů a vlastností letounu.
4. Vypracování hmotového rozboru letounu.
5. Koncepční návrh hlavních konstrukčních celků letounu.
6. Stanovení a rozbor nákladů na vývoj letounu.

Seznam odborné literatury:

[1] Jenkinsin, L. R.: Aircraft design projects for engineering students, AIAA, 2003
[2] Jane´s: All the World's Aircraft (všech vydání)
[3] Torenbeek, E.: Synthesis of Subsonic Airplane Design, Delft University Pres, 1976
[4] Roskam, J.: Airplane Design (Parts), The University of Kansas, 1989
[5] Raymer, D. P.: Aircraft Design: A Conceptual Approach, AIAA American Institute of Aeronautics, 1999

Vedoucí diplomové práce: Ing. Tomáš Urík

Termín odevzdání diplomové práce je stanoven časovým plánem akademického roku 2014/2015.

V Brně, dne 10.11.2014

L.S.

_____   _____
doc. Ing. Jaroslav Juračka, Ph.D.   doc. Ing. Jaroslav Katolický, Ph.D.
         Ředitel ústavu   Děkan fakulty

Summary:

The topic of the thesis is a conceptual study of very light twin jet aircraft. The comparison of present aircrafts is made, as well as their engines, and description of proposed solution, aircraft mass analysis, basic aerostatic calculations, flight and gust envelope, development costs and basic design of main parts of the aircraft.

Key words:

Aircraft concept design, drag polar, performance of the aircraft, flight and gust envelope, development costs.

Abstrakt:

Tématem diplomové práce je koncepční studie lehkého dvoumotorového letounu. Je provedeno srovnání současných letounů, jejich motorů, technický popis navrhovaného řešení, hmotový rozbor, výpočet aerostatických podkladů, výpočet obálky zatížení, nákladů na vývoj a základní konstrukce hlavních součástí.

Klíčová slova:

Koncepční návrh, odporová polára, výkony letounu, obálka zatížení, náklady na vývoj

Bibliographic citation:

SMÝKAL, M. *Koncepční studie lehkého dvoumotorového proudového letounu.* Brno: Vysoké učení technické v Brně, Fakulta strojního inženýrství, 2015. 124 s. Vedoucí diplomové práce Ing. Tomáš Urík.

Affirmation:

I declare that this master's thesis is the result of my own work led by Ing. Tomáš Urík, and all used sources are duly listed in the bibliography.

....

Bc. Michal Smýkal

Acknowledgement

I would like to thank the leader of the thesis Ing. Tomáš Urík for his advice and experiences given to me, which helped me to properly write this thesis. Also I would like to thank Patrick Berry for introduce me this project. And in the end I would like to thank my family for their support during studies.

SUMMARY

NOMENCLATURE

a	$[m \cdot s^{-2}]$		acceleration
AR	$[-]$		aspect ratio
b	$[m]$		span
b_f	$[m]$		flap position
c	$[m]$		chord length
c_D	$[-]$		drag coefficient
c_{Di}	$[-]$		induced drag coefficient
c_L	$[-]$		lift coefficient
D	$[N]$		drag
e	$[-]$		Oswalds coefficient
f	$[-]$		friction coefficient
F	$[N]$		thrust
g	$[m \cdot s^{-2}]$		gravitational accelaration
K	$[-]$		lift-to-drag ratio
l	$[m]$		length, take-off length
l_C	$[m]$		distance canard-wing
l_{VT}	$[m]$		distance vertical tail-wing
m	$[kg]$		weight
m_e	$[kg]$		empty weight
m_{tow}	$[kg]$		maximum take-off weight
MAC	$[m]$		mean aerodynamic chord
n	$[-]$		gust load

P	$[W]$	power
R	$[km], [kn]$	range
Re	$[-]$	Reynolds number
RoC	$[m \cdot s^{-1}]$	rate of climb
S	$[m^2]$	area
SFC	$[kg \cdot N^{-1} \cdot h^{-1}]]$	specific fuel consumption
T	$[h]$	endurance
U	$[m \cdot s^{-1}]$	gust speed
v_A	$[m \cdot s^{-1}], [km \cdot h^{-1}]$	design maneuvering speed
v_C	$[m \cdot s^{-1}], [km \cdot h^{-1}], [kts]$	cruise speed
v_D	$[m \cdot s^{-1}], [km \cdot h^{-1}]$	design diving speed
v_F	$[m \cdot s^{-1}], [km \cdot h^{-1}]$	maximum flap extended speed
v_G	$[m \cdot s^{-1}], [km \cdot h^{-1}]$	design maneuvering speed
v_H	$[m \cdot s^{-1}], [km \cdot h^{-1}]$	maximum horizontal speed
v_S	$[m \cdot s^{-1}], [km \cdot h^{-1}]$	stall speed
V	$[-]$	volume coefficient
V_Z	$[m \cdot s^{-1}]$	descent speed
$\bar{V}_Z$	$[m \cdot s^{-1}]$	climbing speed
x_{CoG}	$[m]$	centre of gravity position x
$\bar{X}_A$	$[\%MAC]$	aerodynamic center with fixed controls
$\bar{X}'_A$	$[\%MAC]$	aerodynamic center with free controls
y_{CoG}	$[m]$	centre of gravity position y

α	$[1 \cdot rad^{-1}]$	lift curve slope
α_0	$[°]$	angle of zero-lift coefficient
δ	$[-]$	Glauert coefficient
δ_f	$[°]$	flap deflection angle
η	$[-]$	taper ratio
μ	$[N \cdot s \cdot m^{-2}]$	dynamic air viscosity
ρ	$[kg \cdot m^{-3}]$	density
σ	$[\%MAC]$	static margin
χ	$[°]$	angle of climb

1 INTRODUCTION

In modern society nothing is more important than time. Time - spend for business travel or vacation. And this time cost money, which nowadays people are able and want to pay. Thus the jet aircrafts came to world. First attempts were regular business jet aircrafts and then with smaller and more efficient jet engines were companies able to build smaller jet planes for personal usage and move from exclusive small single propeller aircraft to small single jet aircraft. This thesis should move it to another level, to show that it is possible to design small two seat plane with jet engine which properties are highly above current two seat category aircraft. However its exclusivity brings higher price and higher operation costs.

The aircraft should be certified under CS-23 regulation and therefore some of the prerequisites are taken from this regulation.

1.1 Historical content

As first representative of business jet category in the world can be marked French Morane-Saulnier MS760, which first flew in 1954. The MS760 was four-seat jet trainer and liaison aircraft used by French Armée del l'Air between 1959 and 1997. Unfortunately it served only in military service, there was effort to sell aircraft as business jet to US market but this attempt failed. However its successor on the market Learjet 23 created completely new market for fast and efficient business aircraft. But it was in late 90's and in the beginning of new millennium when new companies start working on new generation of very light jets. Companies like Cirrus, Diamond or Flaris, came with new design and applied new materials to their constructions.

1.2 What is very light jet?

Very light jet (VLJ) definition by NBAA (National Business Aviation Association) [11]:

Jet aircraft weighing 10,000 pounds or less maximum certificated takeoff weight and certificated for single pilot operations. These aircraft will possess at least some of the following features:

(1) advanced cockpit automation, such as moving map GPS and multi-function displays;
(2) automated engine and systems management;
(3) integrated autoflight, autopilot and flight-guidance systems.

We can add some other features which should VLJ fulfill. Take-off distance less than 3,000 feet, powered by one or two gas turbine engines (turbofan or turbojets), and contain seats for 1-8 passengers and with final price less than $5M per aircraft.

With comparison to other small single or multiple aircrafts in CS-23 category, like Cirrus SR22 or Diamond DA42, has VLJ different systems and capabilities, operates in different flight regimes at higher speeds, and places different demands upon its pilots due to the diversity in previous flying.
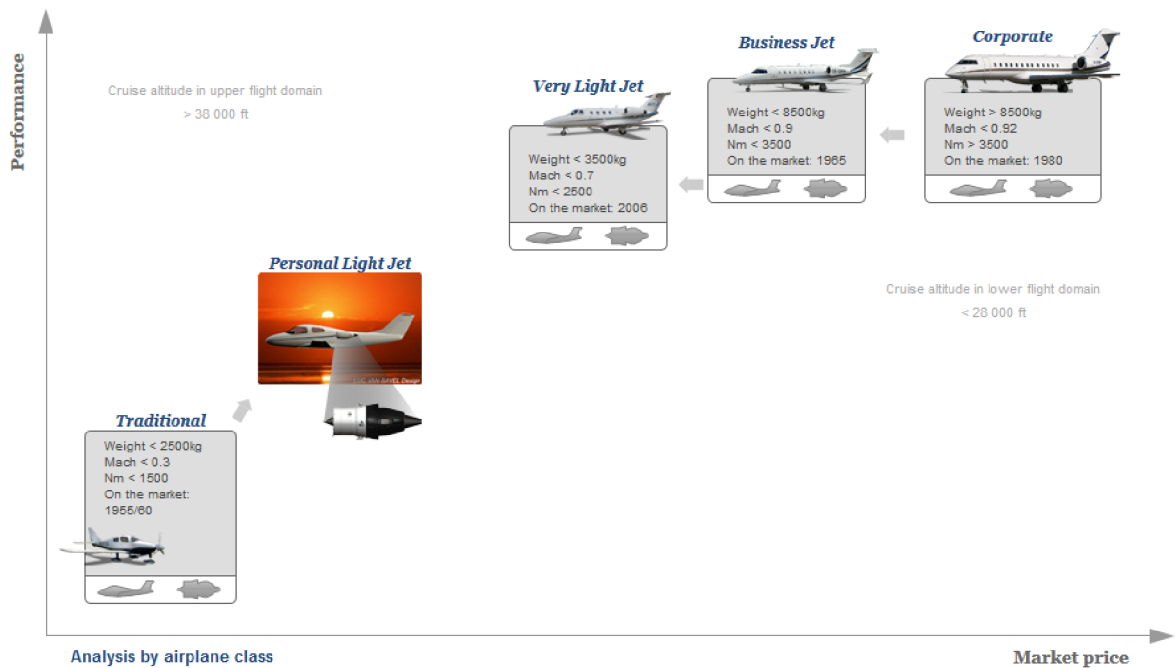
Figure 1.1: Market position of VLJ and Personal Light Jet [12]

1.3 Current very light jets

In last decade there were a lot of attempts to build light jet aircraft but not many of them succeed. However there are still companies which try come to market with something new. This chapter will take a look on some of them.

1.3.1 Cirrus SF50 Vision

The Cirrus SF50 Vision is a single-engine, low-wing, and seven-seat very light jet aircraft produced by Cirrus Aircraft. Vision is the Cirrus first attempt to build jet aircraft and as is usual for the company, they want to be the best and redefine market, company itself call it "personal jet" and not very light jet.

The SF50 is full composite with V-tail and engine placed behind cabin. This configuration produced less noise for passengers and does the travel more comfortable. The engine is Williams International FJ33 with thrust of 1,800 lbf (8 kN). Manufacturer also placed parachute system into the aircraft, which became standard in small aircrafts. Modern cockpit looks more like luxury car than aircraft, and is equipped with advanced avionics – Cirrus Perspective by Garmin avionics. Overall price should be about US$2M.

Figure 1.2: Cirrus Vision SF50 [14]

1.3.2 Flaris LAR 1

The Flaris LAR 1 is a Polish single-engine, four-seat very light jet aircraft currently under development by Metal-Master. The LAR 1 was designed in cooperation with Polish technical universities, Institute of Aviation and Air Force Institute of Technology.

Flaris LAR 1 is full composite, pre-impregnated carbon fibers, with two vertical tails placed on the ends of horizontal tail. It is powered by Pratt & Whitney Canada PW615F with thrust of 1,460 lbf (6.5 kN) and the engine is placed behind cabin to reduce noise. The aircraft is also equipped with parachute system and a cockpit with car-like feeling. Approximate price is about US$1.5M.

Figure 1.3: Flaris Lar 1 [15]

1.3.3 Diamond D-JET

Diamond D-JET is low-wing, single-engine, five-seat very light jet aircraft developed by Diamond Aircraft Industries. Diamond wanted it to aircraft for single-pilot operation and which can compete with the Eclipse 500 and the Cessna Citation Mustang. However this project was suspended in May 2014.

The D-JET is full composite with T-tail configuration. This is caused by the placing the engine into the fuselage. The intakes are placed into the transition between the fuselage and wing. The engine is Williams International FJ33-4A with thrust of 1,900 lbf (8.5 kN). Cabin is pressurized to 5.5 psi, thus cabin altitude is 8,500ft at FL250. Estimated price was about US$1.89M.

Figure 1.4: Diamond D-JET [16]

1.3.4 Epic Victory

The Epic Victory is single-engine, low-wing aircraft with 4-5 seats designed by Epic Aircraft Corporation. The Victory project was the second attempt of very light jet aircraft, nevertheless this project leaded to bankruptcy of the company in 2009.

The Victory is full composite, carbon fiber, with T-tail and engine placed behind aircraft's cabin. The placement of the engine leads to lower noise level in the cabin. It was intended to be powered by Pratt & Whitney Canada PW600. Cabin was designed to overpressure of 6.5 psi. Price was set to less than US$1M.

Figure 1.5: Epic Victory [17]

1.3.5 Sport Jet II

The SportJet II is mid-wing, single-engine, and four-seat very light jet aircraft under development by Sport-Jet, Ltd. Design is based and improved on the Maverick TwinJet aircraft.

The SportJet II has carbon fiber fuselage and aluminum made wings and horizontal tail. Due to design altitude its cabin is full pressurized. SportJet II is powered by one Pratt & Whitney Canada JT15D engine with 2,220 lbf (9.8 kN) thrust. It is mounted in the aft fuselage and the two intakes are placed on the side in the back of the cabin. Manufacturer proclaims that pilot does not need professional jet pilot training or advanced skills to fly. The price tag is US$1.35M.

Figure 1.6: SportJet II [18]

1.3.6 Stratos 714

The Stratos 714 is low-wing, single-engine, and four-seat very light jet aircraft.

The Stratos 714 is made from carbon fiber. The engine is placed in the aft fuselage. Its intakes are on the bottom of the fuselage where the cabin ends. The engine is Williams International FJ44-3AP with thrust of 3,030 lbf (13.5 kN). Pressurized cabin is necessary equipment. Price is set to US$2M.

Figure 1.7: Stratos 714 [19]

1.3.7 Adam A700

The Adam A700 is twin-engine, low-wing, and six-seat very light jet aircraft developed by Adam Aircraft Industries. Its unusual design is based on previous model Adam A500 with two piston-engines in push-pull configuration.

The A700 used carbon fiber to build fuselage and wing. The twin wing-mounted booms supporting aft twin rudders which are linked by high horizontal stabilizer does look this aircraft strange. The A700 is powered by two Williams FJ33-4 turbofan engines with thrust of 1,350 lbf (6 kN) each. These two engines are mounted on the sides of the fuselage. Cabin was designed to overpressure of 6.5 psi. Estimated price was set to US$2.25M.

Figure 1.8: Adam A700 [20]

1.3.8 Eclipse 550

The Eclipse 550 is the low-wing, twin-engine, and six seat very light jet aircraft produced by Eclipse Aerospace. The 550 is developed from previous model 500.

The Eclipse 550 has an all-metal structure with a T-tail. Engines are mounted in the aft fuselage on both sides. The engine is Pratt & Whitney Canada PW610F with thrust of 900 lbf (4 kN) each. The overall price is less than US$3M.

Figure 1.9: Eclipse 550 [21]

1.3.9 Honda Jet

The Honda Ha-420 HondaJet is low-wing, twin-engine, and six-seat very light jet aircraft. The Ha-420 is the first aircraft developed by Honda Aircraft Company.

The HondaJet has composite fuselage and aluminum wings. The biggest difference between HondaJet and other VLJ aircrafts is engine placing. The engines are mounted over-the-wing at HondaJet. This design should achieve lower wave drag at a high Mach number. Honda also developed whole new engine for its plane. Together in cooperation with GE they create GE Honda HF120 engine with thrust of 2,050 lbf (9.1 kN) each. Estimated price is US$4.5M.

Figure 1.10: Honda Ha-420 HondaJet [22]

1.3.10 Cessna Citation Mustang

The Cessna Citation Mustang is low-wing, twin-engine, six-seat very light jet aircraft built by Cessna Aicraft Company. Citation Mustang is the latest model in Cessna's Citation family of business jets.

The fuselage's airframe is made mostly from aluminum alloys. Mustang has high-lift airfoil wing design. On each side of the rear fuselage are two Pratt & Whitney Canada PW615F-A engines. Thrust of each is 1,460 lbf (6.5 kN). Current price is US$3.28M.

Figure 1.11: Cessna Citation Mustang [23]

1.3.11 Embraer Phenom 100

The Embraer Phenom 100 is low-wing, twin-engine, and six seat very light jet aircraft produced by Brazilian company Embraer S.A. The Phenom 100 has bigger variant called Phenom 300.

The Phenom 100's construction contains of 20% carbon-fiber composite and 80% metal. Two Pratt & Whitney PW 617-F engines are mounted to the rear of fuselage and each provide thrust of 1,695 lbf (7.18 kN). Price tag is US$4.5M.

Figure 1.12: Embraer Phenom 100 [24]

1.4 List of engines for VLJ

Situation with small capable engines for VLJs is brighter than we can think. There are several manufacturers producing light but efficient jet engines. In this part we take a look for some main which are used in modern planes. For light jet aircraft we can assume usage of engines with power thrust between 2.9kN and 4.9kN. As it can be seen on Figure 1.13 a lot of new designs rises in last two decades.

Figure 1.13: Engine thrust on year of production dependence [25]

1.4.1 Price Induction DGEN 380/390

The DGEN engine family represents the world's smallest turbofan. It is intended for 4-5 seat twin-engine VLJ flying under 25,000 ft and Mach 0.35. The DGEN is designed with easy integration and maintainability, low fuel consumption and low noise level. The engine control unit as well as the oil & fuel equipment is fully integrated around the engine and controlled by FADEC (Full-Authority Digital Engine Control). A starter-generator device is integrated on the high-pressure spool and allows for the electrical start of the engine before switching to generation mode. The main advantages are an easy and reliable control for the pilot, simplified maintenance and a reduced overall weight. This concept also allows for a continuous engine health and aging monitoring.

The DGEN engine family provides enough thrust for take-off for aircrafts with maximum take-off weight of 1,650 to 2,150 kg. Smaller model, *DGEN 380*, gives 2.5 kN of thrust and the bigger one, *DGEN 390*, gives 3.3 kN of thrust. These engines share 90% of parts. However DGEN 390 is still under development.

Table 1.1: Price Induction DGEN's specification table [13]

	DGEN 380	DGEN 390
Take-off Thrust (lbf)	570 (2.6 kN)	725 (3.2 kN)
Dry Weight (lb)	175 (80 kg)	N/A
Length (in)	53 (1,346 mm)	N/A
Diameter (in)	18.5 (469 mm)	N/A

Figure 1.14: DGEN 380 [13]

1.4.2 Pratt & Whitney Canada PW600

The PW600 turbofan engine family is design for thrust from 950 to 1,750 pounds (4.2kN − 7.9kN). Three models are currently available with this thrust range (PW610F, PW615F and PW617F). The engine core was developed to enable the PW600 family of engines to grow to 3,000 pounds thrust.

The PW600 is a two spool engine with a two-stage high pressure compressor driven by a single-stage high pressure turbine and a single-stage low pressure turbine driving advanced fan. A high efficiency reverse-flow combustor ensures low emissions and fuel consumption. Further a high efficiency exhaust mixes contributes to the engine family's low fuel burn and noise. For relief pilot's workload is installed the latest Full-Authority Digital Engine Control (FADEC) and advanced engine health monitoring/diagnostics. Design features enable fast access to engine externals. The result of all this is a compact, lightweight design powering new generation of light jet aircrafts.

At present time there are three aircrafts using all available versions. Cessna Citation Mustang is using *PW615F-A*, Eclipse 500 *PW610F-A* and Embraer Phenom 100 *PW617F-E*.

Table 1.2: Pratt & Whitney Canada PW600's specification table [26]

	PW610F-A	PW615F-A	PW617F-E
Take-off Thrust (lbf)	950 (4.2 kN)	1,460 (6.5 kN)	1,780 (7.9 kN)
Dry Weight (lb)	259.3 (118 kg)	310 (141 kg)	380 (173 kg)
Length (in)	46 (1,150 mm)	49.5 (1,238 mm)	49.5 (1,238 mm)
Diameter (in)	14 (350 mm)	16 (400 mm)	17.6 (440 mm)
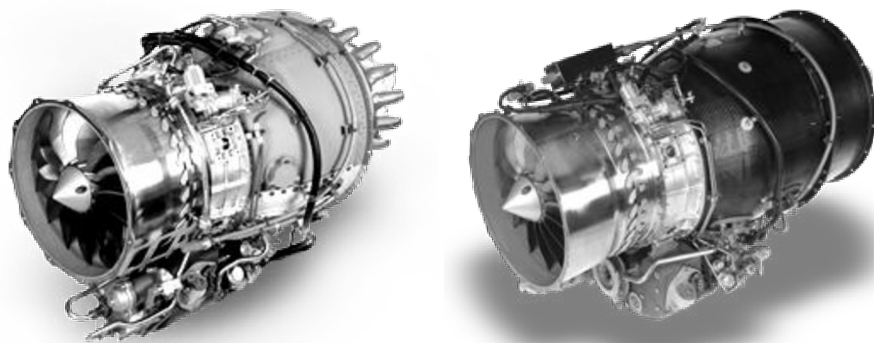
Figure 1.15: Pratt & Whitney PW610F-A (on the left) and PW615F-A (on the right) [26]

1.4.3 GE Honda HF120

The HF 120 was developed in cooperation between General Electric and Honda by the GE Honda Aero Engines. The goal was to create robust, yet simplified design which can deliver greater payload, longer range and outstanding durability. HF120 is a 2,000 (8.9kN) pound to thrust class turbofan engine. The engine has a wide-chord swept fan, two-stage low-pressure compressor and counter rotating high-pressure compressor based on a titanium impeller. Greater fuel efficiency and reduced emissions are two of the goals of the engine's lightweight design.

Another innovation is associated by reducing weight and using innovative 3D aerodynamic designs. The engine components are designed to interact with greater efficiency while optimizing operability. Great engine's advantage is that it is designed to stay on wing over 40% longer than other business jet engines. It is caused by time between overhaul set at 5,000 hours and no need to open the engine for interim hot-section inspection.

A plan for the future is to place this engine not only to Honda HA-420 HondaJet aircraft but also to the Spectrum Freedom, and was also offered to retrofit Cessna Citation's engine Williams FJ44-1.

Table 1.3: GE Honda HF120's specification table [27]

	HF120
Take-off Thrust (lbf)	2,050 (9.1 kN)
Weight (lb)	Less than 400 (182 kg)
Length (in)	44 (1,100 mm)
Diameter (in)	21.2 (530 mm)

Figure 1.16: GE Honda HF120 [27]

1.4.4 Williams FJ44

The FJ44 is a family of small, two-spool engines produced by Williams International/Rolls-Royce. Until the recent boom in VLJ market, the FJ44 was one of the smallest turbofans engines available for civilian applications. At the moment there are four different versions of the FJ44 which can provide thrust from 1,900 to 3,600 lbf.

The *FJ44-1AP* version is improved FJ33-1A jet engine. It provides up to 2,100 lbs of take-off thrust which is 200 pounds more than previous model. It contains from single stage blisk fan plus a single intermediate pressure booster stage, driven by a two-stage low pressure turbine, supercharging a single stage centrifugal high pressure compressor, driven by a single stage uncooled high pressure turbine. It is also equipped with a dual-channel full-authority digital engine control (FADEC).

This engine is highly reliable, designed for simplicity and ease of maintenance. Huge advantage is the unique design allowing hot section disassembly/reassembly and fan removal/replacement while installed on the aircraft. As others modern designed engines FJ44-1AP is also very environmentally friendly, it produces low emissions.

The FJ44-1AP is installed in Cessna CJ1, Cessna CJ1+, Cessna M2 and Saab SK60.

The *FJ44-2* uses the same core and low pressure turbine as the FJ44-1, however it has installed unique fan and compressor sections. The engine maintains the modest turbine temperatures of the FJ44-1 and retains low cost turbofan technology, such as the uncooled, high pressure turbine, effusion-cooled combustor, and high work, two stage low pressure turbine. Available thrust is between 2,300 and 2,400 pounds. It is equipped with single channel full-authority digital engine control (FADEC).

The FJ44-2 is installed in e.g. Beechcraft Premier 1A, Cessna CJ2, Scaled Composited Proteus or Virgin Atlantic Global Flyer.

Further updates leads to *FJ44-3* version which is similar to previous version (FJ44-2). Nevertheless it is improved with increases fan diameter and dual channel FADEC. Thrust was also increased to 3,000 pounds.

The FJ44-3 is installed in Cessna CJ2+, Cessna CJ3+, Nextant 400XTi and Sierra Industries Super II and Super S-II.

The *FJ44-4* is the biggest and most powerful unit from this family. It provides 3,600 pounds of thrust.

There are only three aircrafts using this engine, Cessna CJ4, Hawker 400XPR and Pilatus PC-24.

Table 1.4: Williams FJ44's specification table [28]

	FJ44-1AP	FJ44-2	FJ44-3	FJ44-4
Take-off Thrust (lbf)	1,900-2,100 (8.5-9.3 kN)	2,300-2,400 (10.2-10.7 kN)	3,000 (13.3 kN)	3,600 (16 kN)
Weight (lb)	460 (209 kg)	530 (241 kg)	535 (243 kg)	650 (295 kg)
Length (in)	41.4 (1,035 mm)	47.2 (1,180 mm)	48 (1,200 mm)	52.8 (1,320 mm)
Diameter (in)	20.7 (518 mm)	21.8 (545 mm)	23 (575 mm)	25.3 (633 mm)

Figure 1.17: Williams FJ44-1AP [28]

Figure 1.18: Williams FJ44-4 [28]

1.4.5 Williams FJ33

The FJ33 fanjet is advanced very light engine which expands the option available to airframe manufacturers by providing an engine sized to power light jets in the 5,000 (2,268 kg) to 9,000 (4,082 kg) pound GTOW class. FJ33 is a scaled-down version of the FJ44 engine. This engine is characterized by excellent thrust to weight ration, fuel efficiency, and low acquisition and operating cost with thrust from 1,000 to 1,900 lbf (4.4 – 8.5 kN).

Williams consider this engine as low-noise, third generation wide-sweep fan technology coupled with advanced high work, high efficiency core components which results in a high overall pressure ratio that provides light weight and extraordinary cruise fuel economy.

Right now there are two aircrafts using FJ33 engine, Cirrus Vision SF50 and Diamond D-Jet and was on few other aircrafts which are cancelled now or under development.

Table 1.5: Williams FJ33's specification table [28]

	Williams FJ33
Take-off Thrust (lbf)	1,000-1,900 (4.4-8.5 kN)
Weight (lb)	Less than 310 (141 kg)
Length (in)	38.5 (963 mm)
Diameter (in)	19.03 (476 mm)

Figure 1.19: Williams FJ33 [28]

1.5 Statistical analysis of VLJ

Before any design calculations it is important to take a look for other competitor's aircraft available on today's market and compare their performances. Acquired data comes from the developer's web pages or aircrafts brochures; however some relevant data cannot be obtained, because manufacturer did not publish it.

There are two categories of very light jet aircrafts nowadays, single and two engine aircrafts, made from different material and powered by different engines.

In the first table are shown basic specifications of very light jet aircrafts, like wingspan, length, wing area, empty weight, maximal take-off weight, rate of climb, cruise speed and engine thrust, while in the second some characteristics that are based on these data, dependence of maximum take-off weight on wing area, aspect ratio, thrust on mass dependence and empty weight on maximum take-off weight.

Table 1.6: Aircraft properties overview

	b [m]	l [m]	A [m^2]	me [kg]	mtow [kg]	RoC [m/s]	Vc [km/h]	F [kN]
SF50	11.7	9.0	18.5	1,681	2,727	30	556	8.0
LAR-1	8.7	8.3	10.0	700	1,500	30	704	6.5
D-JET	11.5	10.7	n/a	n/a	2,318	8	444	8.5
VICTORY	11.1	10.2	n/a	1,226	2,497	14	463	4.9
SPORTJET II	10.4	9.1	15.3	1,317	2,384	15	704	9.8
STRATOS 714	12.3	10.9	n/a	1,981	3,273	16	546	13.5
A700	13.4	12.4	13.2	2,520	4,245	12	615	12.0
ECLIPSE 550	11.6	10.2	14.0	1,650	2,724	18	693	8.0
HONDAJET	12.1	13.0	18.5	n/a	4,177	18	693	18.2
CITATION	13.1	12.2	19.51	2,433	3,925	15	630	13.0
PHENOM 100	12.2	12.8	19.58	3,238	4,754	15	720	14.36

Table 1.7: Aircraft specifications overview

	mtow/A [kg/ m²]	AR [-]	F/G [-]	We/Wmtow [-]
SF50	147	7.4	0.299	0.616
LAR-1	150	7.5	0.442	0.467
D-JET	n/a	n/a	0.374	n/a
VICTORY	n/a	n/a	0.200	0.491
SPORTJET II	156	7.0	0.419	0.553
STRATOS 714	n/a	n/a	0.421	0.605
A700	322	13.6	0.288	0.594
ECLIPSE 550	195	9.5	0.299	0.606
HONDAJET	226	7.9	0.444	n/a
CITATION	201	8.8	0.338	0.620
PHENOM 100	243	7.6	0.308	0.681
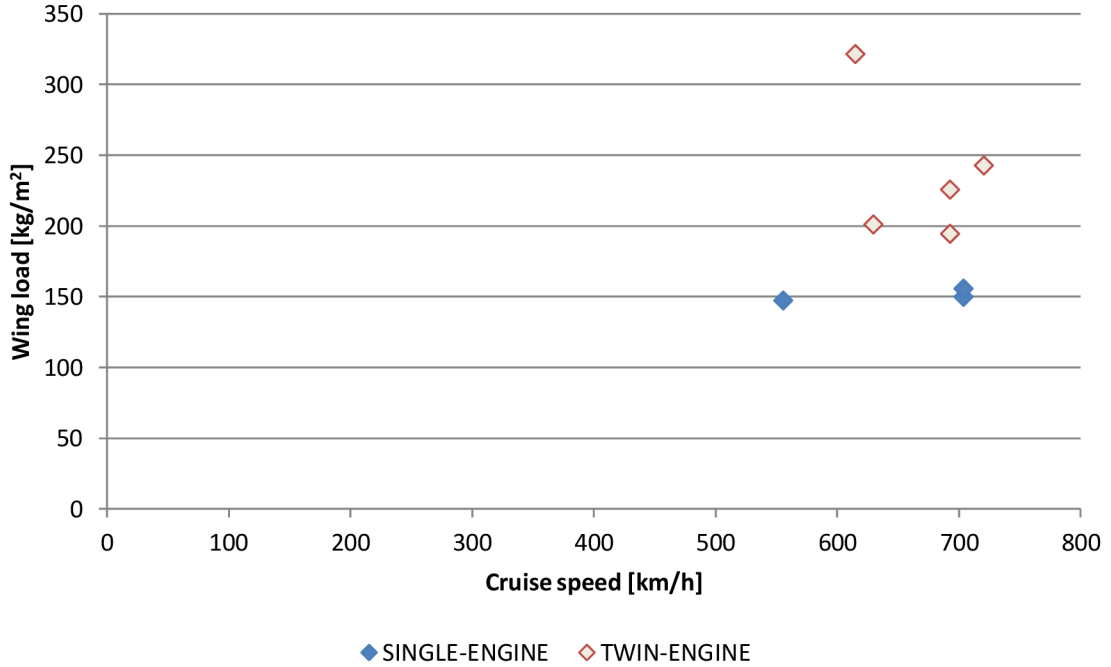
Graph 1.1: Wing load − Cruise speed dependence
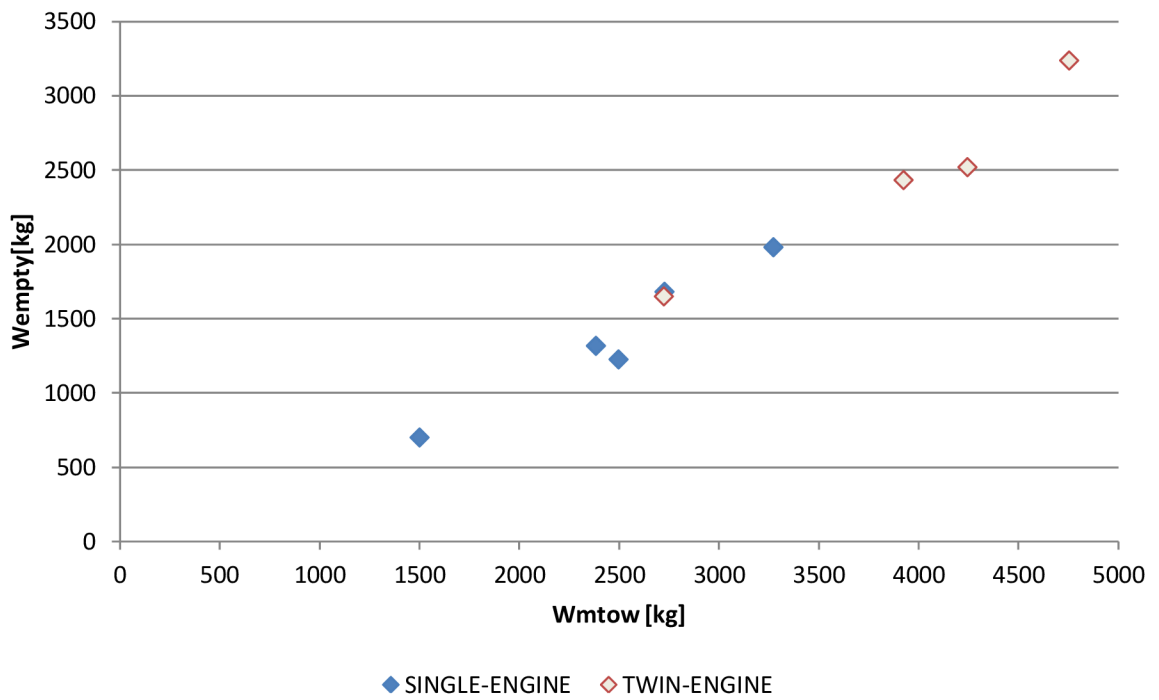
Graph 1.2: Wempty on Wmtow dependence
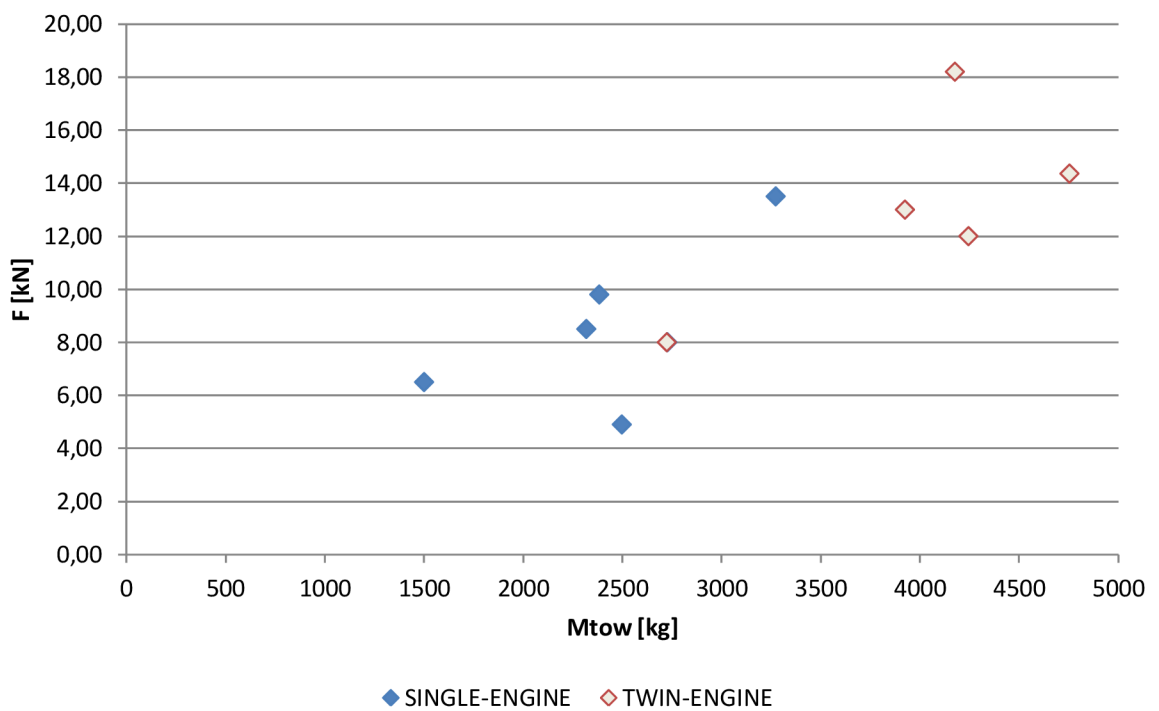
Graph 1.3: Engine thrust on Mtow dependence
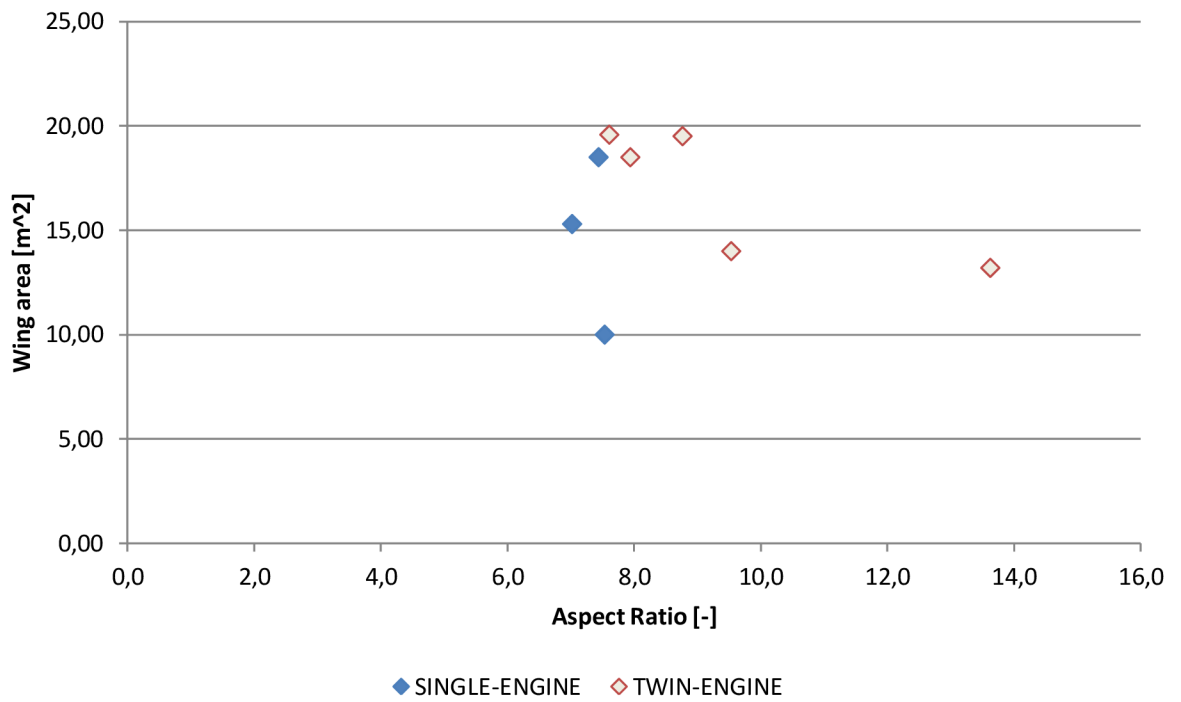
Graph 1.4: Wing area on Aspect ratio
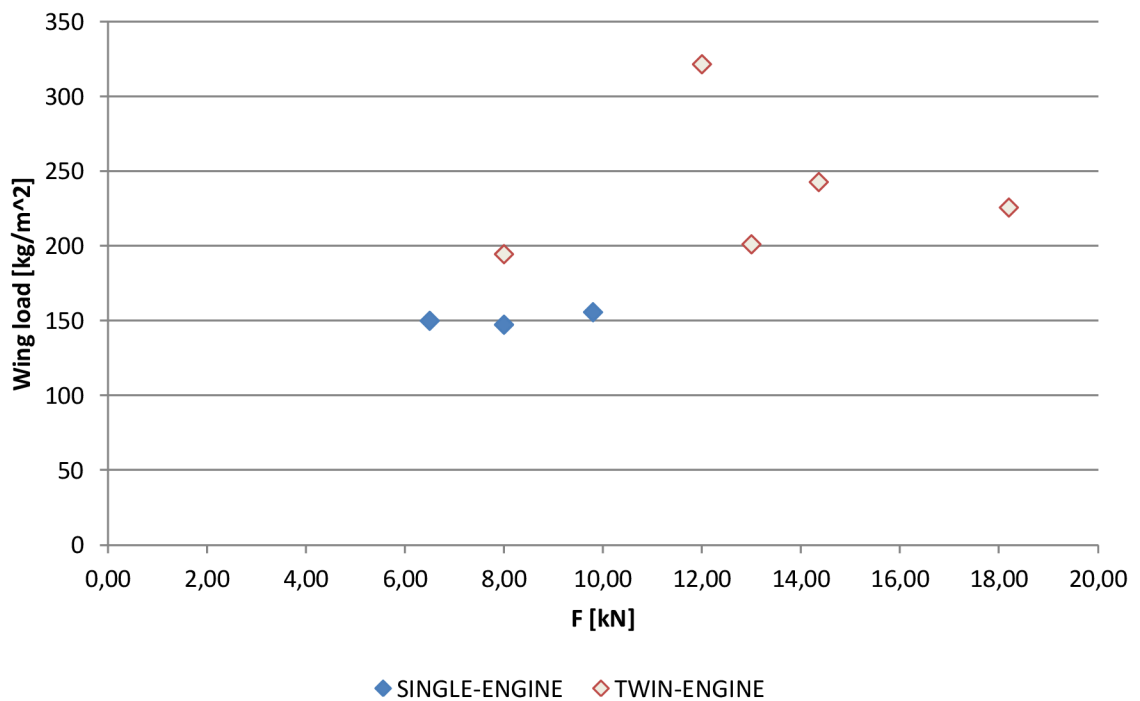
Graph 1.5: Wing load on Engine thrust
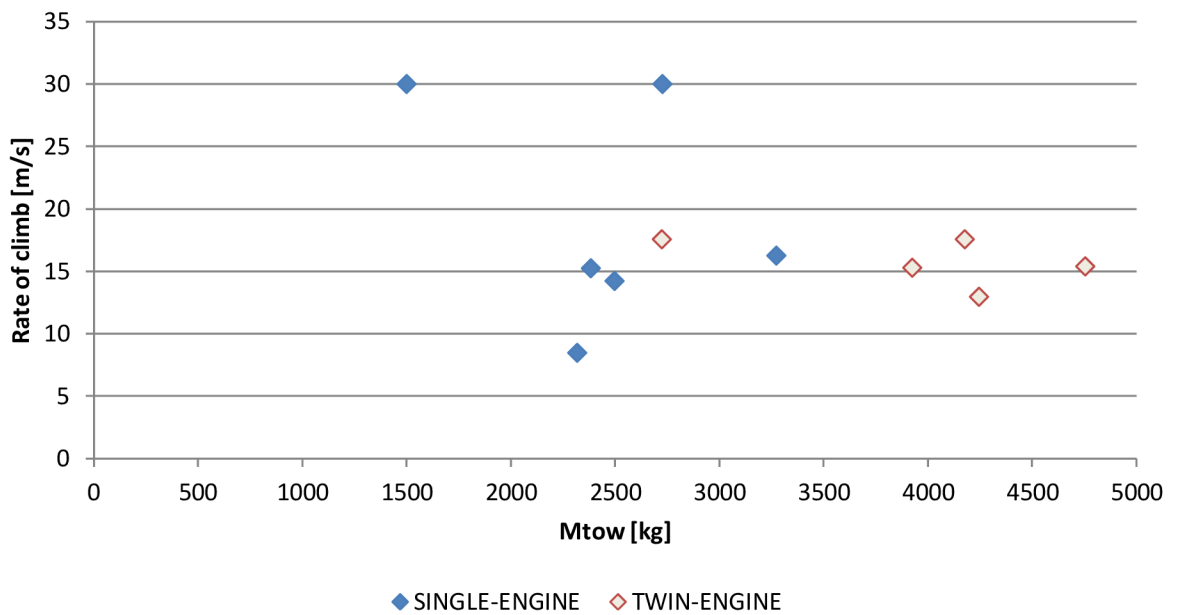
Graph 1.6: Rate of Climb on Mtow

Previous graphs show us some characteristics of very light jet aircrafts divided between single and twin engine. The *Graph 1.1* shows that wing load for single-engine is significantly lower that for twin-engine aircrafts. Same distribution is visible in *Graph 1.5*. However *Graph 1.4* shows that most of the current VLJs have aspect ratio around 8, which is applied for both groups. If we take a look on rate of climb versus mtow (*Graph 1.6*), we can think that single engine aircraft are lighter and thus will have higher climbing speed, nevertheless only two aircrafts much faster in climbing than the rest.

2 CONCEPTUAL DESIGN

2.1 Typical mission

Typical aircraft mission should obtain take-off, climbing to cruise altitude, cruise for the time and distance dependent on pilot's needs and landing.

- Time for taxiing for airplane with possible maximal fuel capacity should take 10 minutes. Take-off distance should be less than 3,000 feet (1,000m).
- Due to the non-pressurized cabin the cruising altitude should not be above 12,500 feet, therefore maximal designed cruise altitude is 12,000 feet (3,658m), flight level FL120. Climbing to the flight level take approximately 15 minutes.
- Horizontal flight at flight level FL120 will be at cruise speed 388 km/h.
- Descent from FL120 to land will take 40 minutes.
- Landing on distance less than 3,000 feet (1,000m) and holding, taxiing should take 23 minutes.
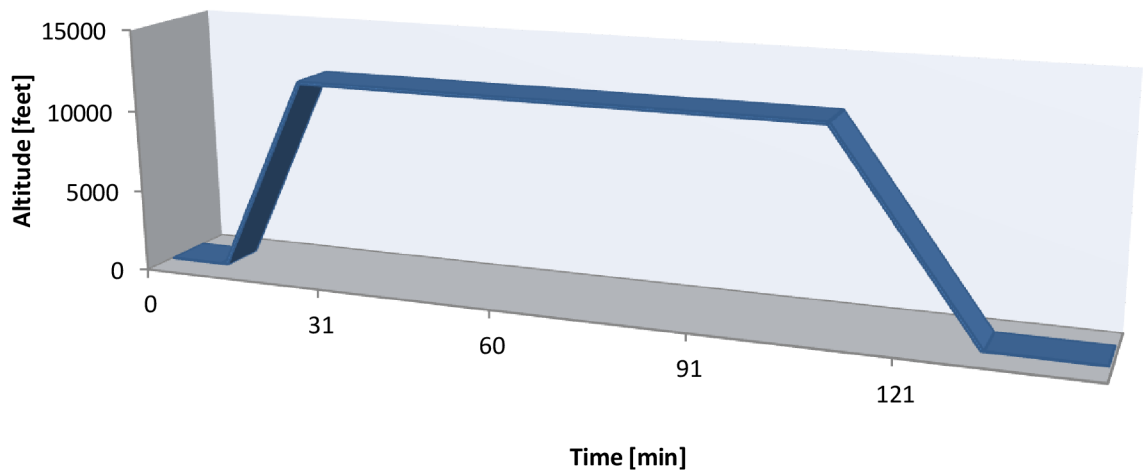
Figure 2.1: Typical mission schematic

2.2 Basic configurations

Design option gives us three basic configurations, classical conception, flying wing and canard configuration. The present very light jet aircrafts stick to the standard configuration of airplane, however this design leads to canard aircraft. These different configurations provide variable advantages and disadvantages. *Classical conception* is the most common and the most widespread configuration where the empennage is in the aft fuselage behind wing. Wing has always higher angle of attack than horizontal tail. The aircraft's center of gravity is located before wing. *Flying wing* is tailless aircraft, where fuselage creates most of the drag (30-40%) and contributes to the empty weight by 8-14%. The design configuration leads to light weight and low efficiency. However the lack of conventional stabilizing surfaces results in instability and difficult controllability. *Canard* configuration has horizontal unit in the fore fuselage before wing. In this case canard has higher angle of attack than wing. Huge advantage is when approaching stall the canard will stall first.
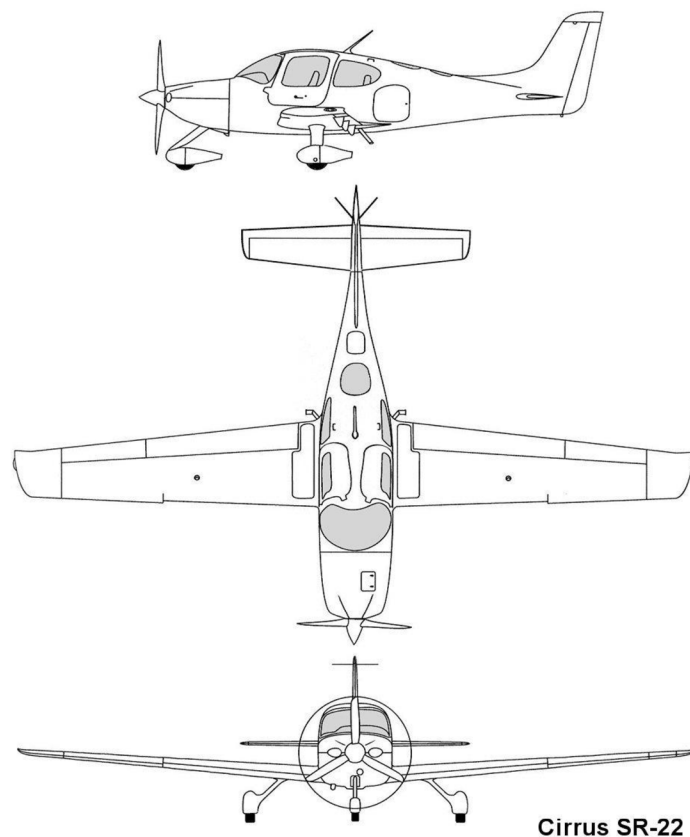
Figure 2.2: Example of classical conception – Cirrus SR-22 [29]
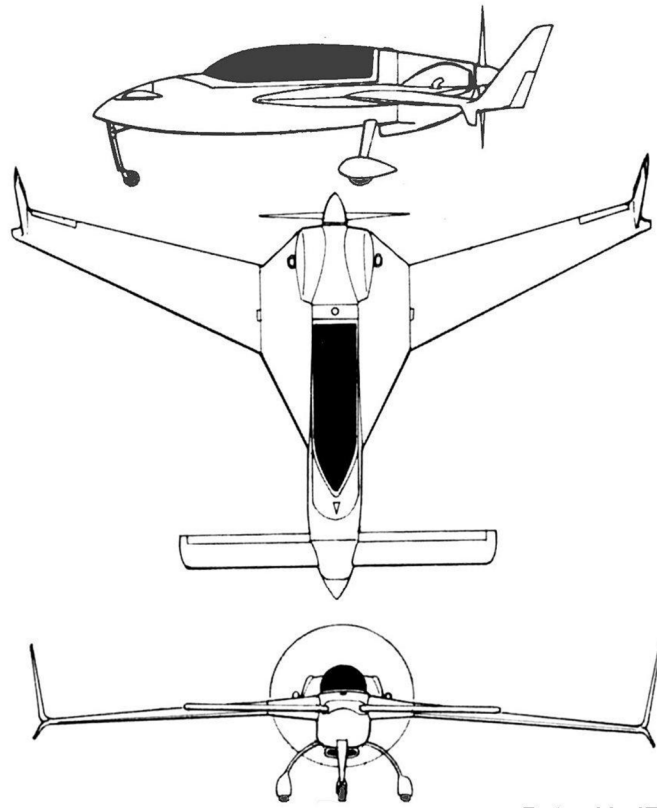
Rutan VariEze

Figure 2.3: Canard conception approach – Rutan VariEze [29]
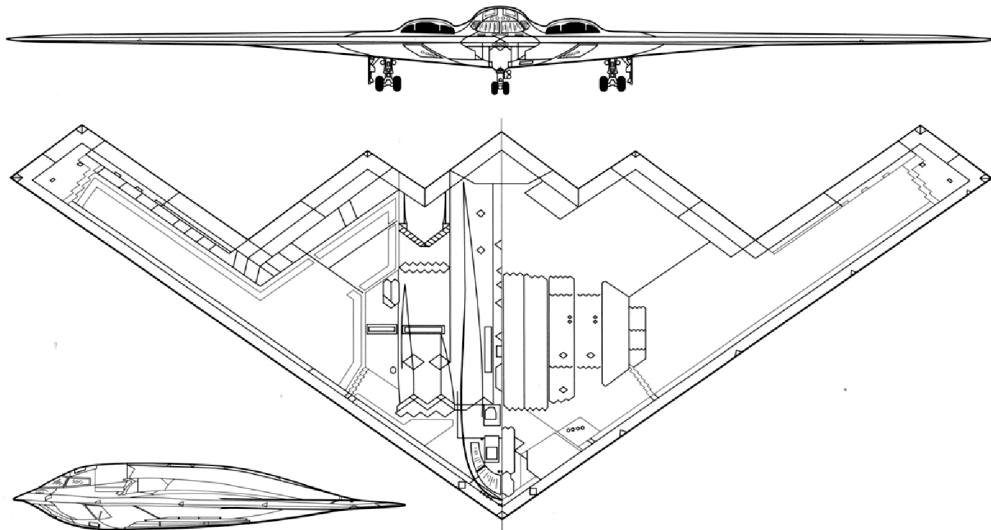
Figure 2.4: Flying wing – Boeing B-2 [30]

2.3 Aircraft layout

The main structural idea is to build the aircrafts with a canard configuration, as it is not common nowadays in the light aircraft industry today. Due to this choice the wing has to be set at the aft of the fuselage with an important back sweep. The chosen solution for the vertical tail is not common; it is decided to have two of them placed at the end of the wing acting as winglets. Therefore canards are placed as much forward as possible and near the lower part of the fuselage. Concerning the fuselage it is emphasized the stream line design and came up with an aerodynamic shape inspired by rain drop that also provides a great visibility to the pilot and passenger.

The two seater market is mostly oriented towards flight training for aero clubs and for customers that are seeking for a sportive, fast and maneuverable aircraft. This is why is was decided to orient this design towards making a fast, good looking and high tech aircraft.

The engine pod is mounted at the rear sides of the fuselage, slightly forward of the wings and higher. Connection with the fuselage is done by using the designed mast that comes with the engines model. In this configuration the engine will be provided with the entire air flow it needs, it will also be protected from any kind of dirt or unwanted objects to be aspirated into the engine. The engine being behind the people onboard and with the use of the latest noise insulation materials so the best comfort for them can be ensured. Nevertheless during design development there were several changes in design, like using only one engine placed on top at the rear of the fuselage (*Figure 2*.5).
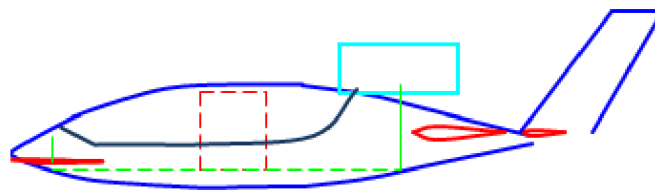
Figure 2.5: First design drawing

Aircraft is equipped with a tricycle landing gear that is fully retractable. The front landing gear has a classic design and is retracted towards the front. The main gear is designed to be retracted to the wing.

2.4 Engine layout

Best available choice on the market right now is French engine DGEN 380 from Price Induction. The DGEN jet engines are two spool, unmixed flow turbofan jet engines with a high bypass ratio. The engine is optimized for a cruise altitude ranging from 15,000 to 20,000 ft and Mach 0.35 with a flight ceiling limited to 25,000 ft. They have low specific fuel consumption.

Fuel equipments are designed to operate with Jet A1 fuel with a specific consumption of 0.78 Kg of fuel/Kg thrust/hour at design point (ISA conditions, cruise setting, 10,000 ft, Mn 0.338).

The DGEN engine is lubricated and oil-cooled in a closed circuit. Each engine has its own regulation group made of a tank, heat exchanger, and pumps. The oil tank capacity should allow operation for more than 300 hours under normal conditions. The oil cooling system is integrated to the engine and does not require the installation of a fuel return line.

The DGEN engine uses modern and high-performance materials allowing the weight of the components to be optimized from both a structural and a functional point of view (composites, light alloys...).

General regulation is carried out by a FADEC that controls the whole engine as well as the electric system in real time. The management of the propulsion group (two engines) is totally under the control of the FADEC. That translates into an extreme ease of use and a much lighter workload for the pilot. Such a layout also allows a continuous engine health and usage monitoring. FADEC and electronics are located in each engine.

The engine starts electrically with the help of an integrated starter-alternator which acts as a generator as soon as the engine reaches autonomy. Regulation accessories for the fuel and oil systems are autonomous and powered by the general electric system.
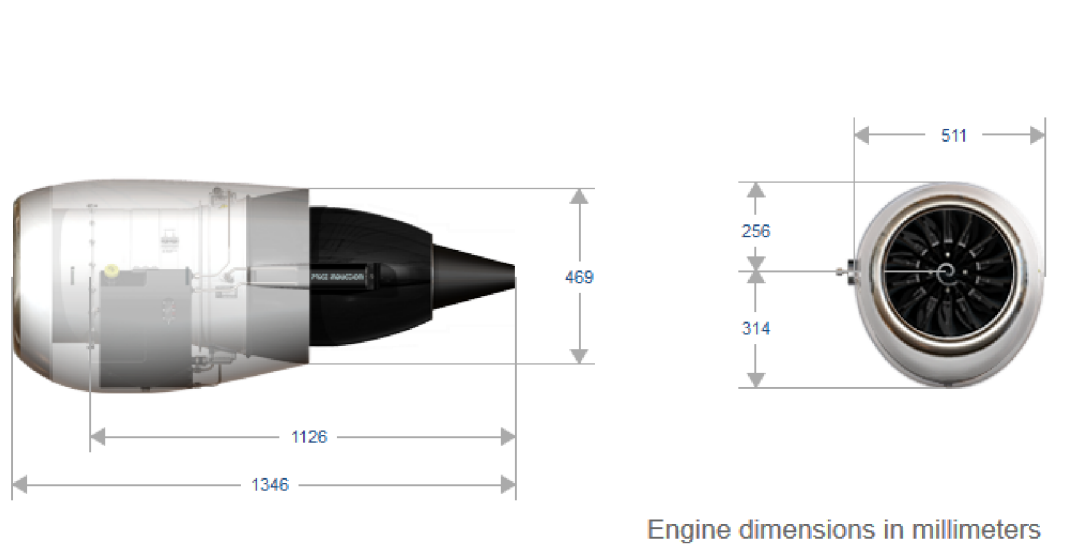
Figure 2.6: DGEN 380 dimensions [12]

PERFORMANCES	DGEN 380			
Thrust at Take Off Power *(ISA SL, Mn 0)* / SFC	255 daN	570 lbf	/	0.44
Thrust at Max Continuous *(ISA, FL100, Mn 0.338)* / SFC	107 daN	240 lbf	/	0.78
Thrust at Max Continuous *(ISA, FL180, Mn 0.4)* / SFC	83 daN	185 lbf	/	0.8
Flight Envelope	< 25,000 ft	ISA ±30		< 250 ktas
Bypass Ratio	7.6			
Dry Weight *(fully equipped, without nacelle)*	80 kg	175 lb		

STANDARD APPLICATIONS	2 seats		4+1 seats	
Aircraft configuration	Single engine applications			
MTOW	900 kg	1,980 lb	1,650 kg	3,640 lb
Wing load	130 kg/m²	25 lb/ft²	125 kg/m²	25 lb/ft²
Wetted surface	35 m²	380 ft²	65 m²	700 ft²
Max airspeed in cruise *(FL120, ISA)*	215 ktas		250 ktas	
Take off distance at 50 ft barrier *(ISA)*	480 m	1,575 ft	580 m	1,900 ft
Fuel on board	250 kg	550 lb	475 kg	1,050 lb
Range *(FL120, ISA, Cruise, 45 min reserve)*	615 Nm		600 Nm	
Range *(FL220, ISA, Cruise, 45 min reserve)*	810 Nm		800 Nm	

Figure 2.7: DGEN 380 performances [12]

2.5 Wing configuration

Wing placement is chosen as mid-wing configuration with back sweep. Wing sweep is important for airplane's balance. The wing swept is 25°. However wing tips are far behind the center of gravity that the vertical tail can be and it actually is located on the wing tips. Their winglets configuration will reduce the induced drag. The wing is double-refracted trapezoid (Figure 2.8), but for most calculation is used reference simple trapezoidal wing. This design was chosen for placing fuel tanks closer to the center of gravity. For calculation basic wing characteristics is necessary to choose some data. Designed maximal take-off weight should be lower than 1,200 kg, stall speed is higher than in classical configuration aircraft, but cannot extend speed required by the regulations, which is 113 km/h. Thus maximal c_L with flaps must be high as well, in configuration with single slotted flaps it is possible to reach $c_{Lmax} = 1,86$.

$$S = \frac{2 \cdot m_{TOW} \cdot g}{\rho_0 \cdot v_{sf}^2 \cdot c_{lwingmax}} = \frac{2 \cdot 1,173 \cdot 9.80665}{1.225 \cdot 31.4^2 \cdot 1.86} = 10.24 m^2 \qquad (2.1)$$

Next step is to determine wingspan which will be $b = 8m$, root chord $c_r = 2.092m$ and tip chord $c_t = 0.6m$.
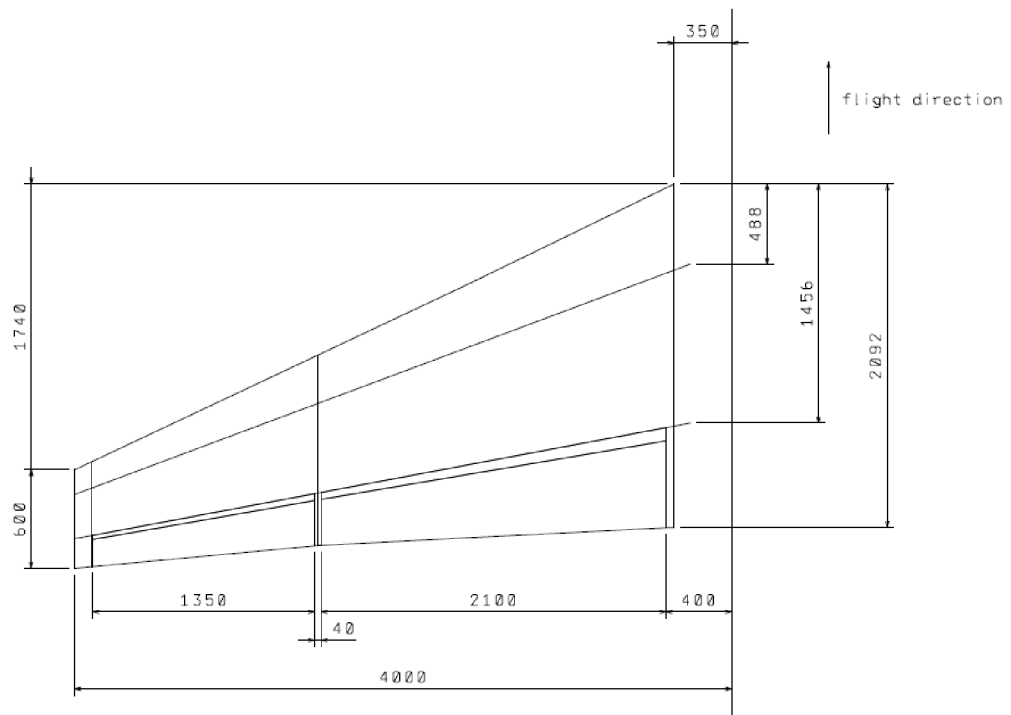
Figure 2.8: Wing drawing

Other characteristics can be obtained from wing geometry design.

Aspect ratio: $\qquad AR = \dfrac{b^2}{S} = \dfrac{8^2}{10.24} = 6.2$ $\hfill$ (2.2)

Taper ratio: $\qquad \eta = \dfrac{c_t}{c_r} = \dfrac{0.6}{2.092} = 0.29$ $\hfill$ (2.3)

Mean aerodynamic chord: $\quad MAC = \dfrac{2}{3} \cdot \dfrac{\eta^2 + \eta + 1}{\eta + 1} \cdot c_r = \dfrac{2}{3} \cdot \dfrac{0.29^2 + 0.29 + 1}{0.29 + 1} \cdot 2.092 = 1.311m$ $\hfill$ (2.4)

MAC position: $\qquad x_{MAC} = \dfrac{b}{6} \cdot \dfrac{\eta + 2}{\eta + 1} \cdot tg\kappa_0 = \dfrac{8}{6} \cdot \dfrac{0.29 + 2}{0.29 + 1} \cdot tg25° = 1.105m$ $\hfill$ (2.5)

$$y_{MAC} = \dfrac{b}{6} \cdot \dfrac{1 + 2\cdot\eta}{1 + \eta} = \dfrac{8}{6} \cdot \dfrac{1 + 2\cdot0.29}{1 + 0.29} = 1.631m \hfill (2.6)$$

$$x_{MAC\,0.25c} = 0.25 \cdot MAC = 0.25 \cdot 1.311 = 0.33m \hfill (2.7)$$

2.5.1 Airfoil selection

For both chord and tip of the wing was chosen same airfoil NACA 63-415. This airfoil has high c_{Lmax} (<1.5) which is important in configuration with canard.
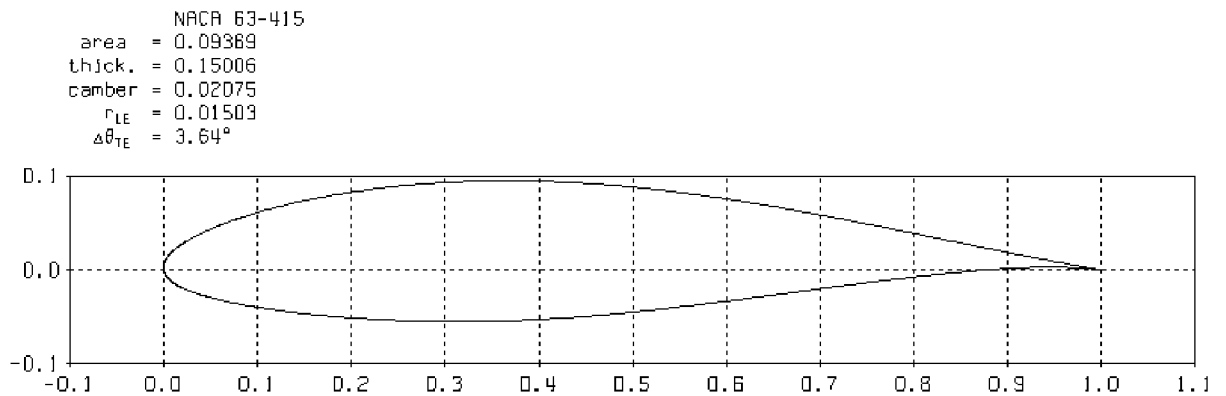
Figure 2.9: NACA 65-415 airfoil from XFoil

2.5.2 Maximum lift coefficient

Lift coefficient is one of the most important parameters that characterize wing. Some of parameters were obtained from Glauert III programme. List of them is below.

Maximal wing lift coefficient: $\qquad c_{lwingmax} = 1.3116$

Glauert coefficient: $\qquad \delta = 0.0114$

Angle of zero-lift coefficient: $\qquad \alpha_{0wing} = -3.00°$

Lift curve slope of the wing: $\qquad \alpha_{wing} = 4{,}8083 rad^{-1}$

Induced drag coefficient: $\qquad c_{Di} = 0.102$

Stall speed: $\quad v_{s1} = \sqrt{\dfrac{2 \cdot m_{TOW} \cdot g}{\rho_0 \cdot S \cdot c_{lwingmax}}} = \sqrt{\dfrac{2 \cdot 1{,}173 \cdot 9.80665}{1.225 \cdot 10.24 \cdot 1.3116}} = 37.39 m/s = 134.6 km/h \qquad (2.8)$
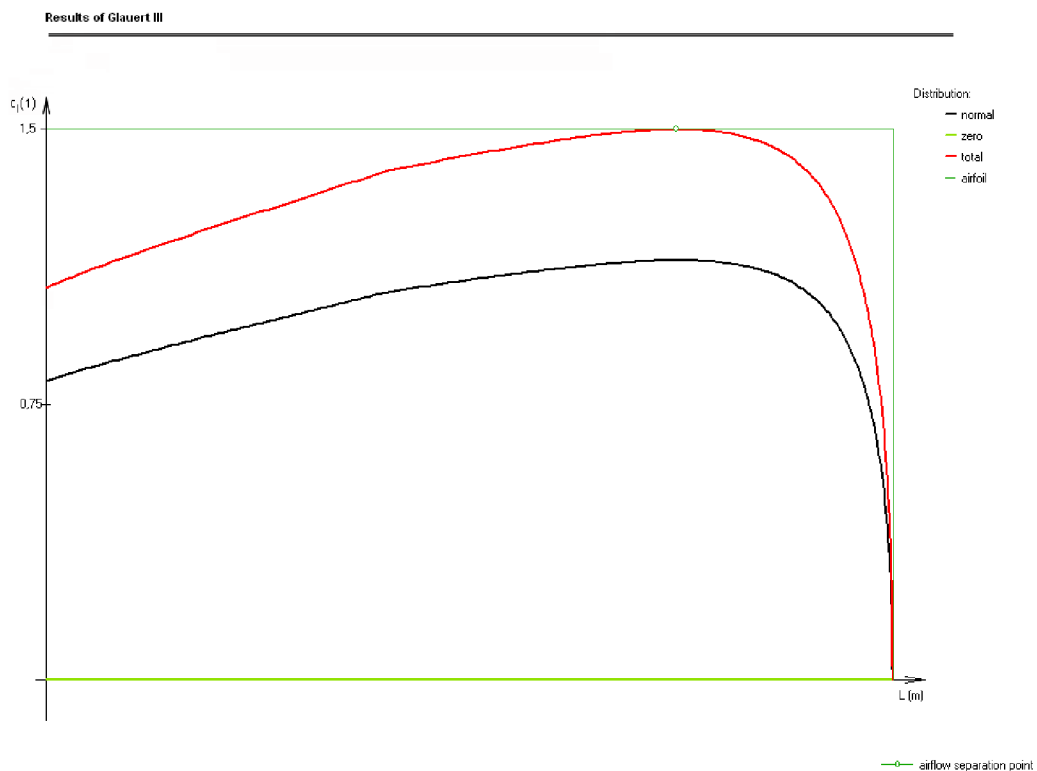
Figure 2.10: Lift coefficient distribution

2.5.3 Maximum lift coefficient with lift devices

For slowing down before landing it is necessary to use lift devices. These are also needed for maintaining current wing area. For required lift was chosen single slotted flap.

Maximal wing lift coefficient with flap at 60°: $c_{lwingmax} = 2.7$

Flap root position: $b_{fr} = 0.4m$

Flap tip position: $b_{ft} = 2.5m$

Chord length: $c_{fl} = 30\%$

Deflection angle: $\delta_f = 60°$

These parameters require enough lift coefficient growth.

Maximal wing lift coefficient in landing configuration: $c_{lwingmax} = 2.0564$

Angle of zero-lift coefficient: $\alpha_{0wing} = -3.00°$

Induced drag coefficient: $c_{Di} = 0.2507$

Stall speed in landing configuration (δ=60°):

$$v_{s0} = \sqrt{\frac{2 \cdot m_{TOW} \cdot g}{\rho_0 \cdot S \cdot c_{lwingmax}}} = \sqrt{\frac{2 \cdot 1,173 \cdot 9.80665}{1.225 \cdot 10.24 \cdot 2.0564}} = 29.86 m/s = 107.5 km/h \qquad (2.9)$$

CS-23 regulation requires stall speed $v_{s0} \leq 113\ km/h$**. This requirement is fulfilled.**
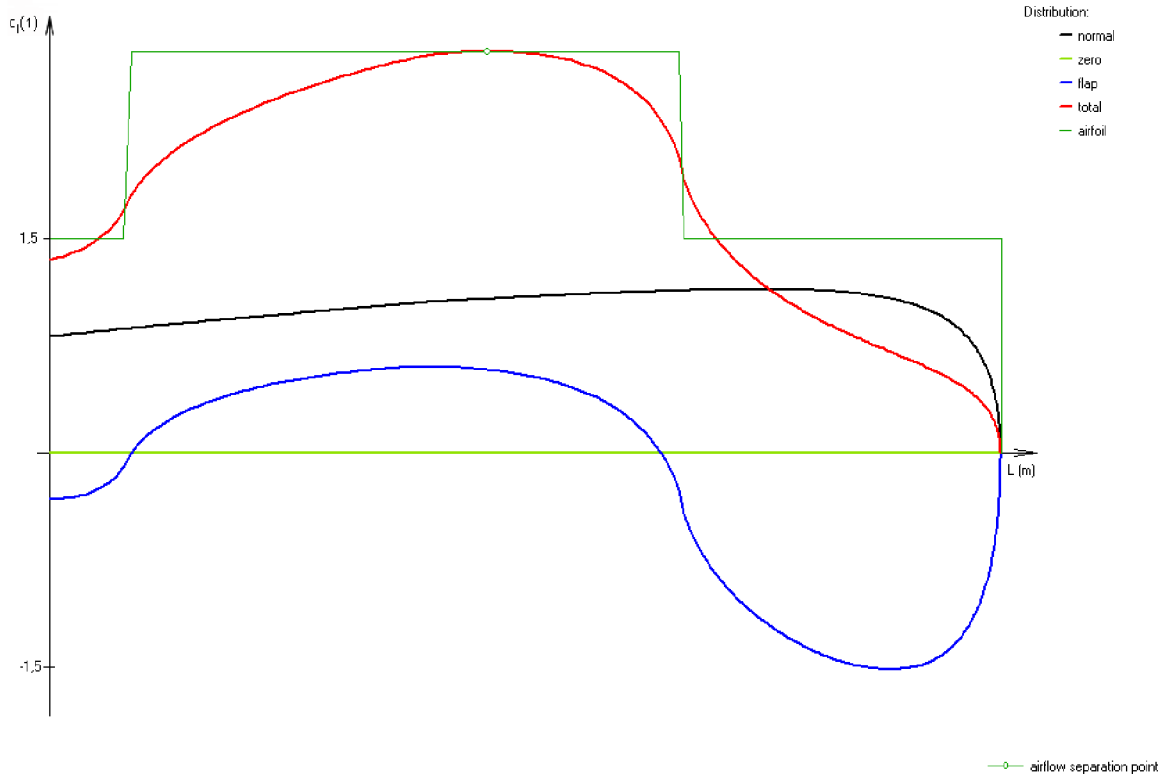
Figure 2.11: Lift coefficient distribution with flaps at 60°

2.6 Canard configuration

Canard is placed in front of the fuselage as low as possible. This placing is important for static margin of entire aircraft. The chosen airfoil is NACA 64-210, which has lower c_{Lmax} ($c_{Lmax} = 1.24$) than wing airfoil and therefore it stall first, and aircraft lowers its nose before pilot will get into trouble. Canard also provides additional lift. Distance between wing and canard is $l_C = 4.91m$. Volume coefficient of canard was chosen $V_C = 0.3$. Canard was designed with swept $\kappa_0 = 20°$.

$$S_C = \frac{V_C \cdot S \cdot MAC}{l_C} = \frac{0.3 \cdot 10.24 \cdot 1.311}{4.91} = 0.82m^2 \qquad (2.10)$$

Canard's geometrical parameters:

Span:	$b_c = 2.5m$
Root chord:	$c_{rc} = 0.5m$
Tip chord:	$c_{tc} = 0.34m$
Area:	$S_c = 0.82m^2$
Aspect ratio:	$AR_c = 7.6$
Taper ratio:	$\eta = \frac{c_{tc}}{c_{rc}} = \frac{0.34}{0.50} = 0.68$

Mean aerodynamic chord:

$$MAC_c = \frac{2}{3} \cdot \frac{\eta^2 + \eta + 1}{\eta + 1} \cdot c_{rc} = \frac{2}{3} \cdot \frac{0.68^2 + 0.68 + 1}{0.68 + 1} \cdot 0.5 = 0.425m \qquad (2.11)$$

MAC position: $x_{MACc} = \frac{b_c}{6} \cdot \frac{\eta + 2}{\eta + 1} \cdot tg\kappa_0 = \frac{2.5}{6} \cdot \frac{0.68 + 2}{0.68 + 1} \cdot tg20° = 0.242m \qquad (2.12)$

$$y_{MACc} = \frac{b_c}{6} \cdot \frac{1 + 2 \cdot \eta}{1 + \eta} = \frac{2.5}{6} \cdot \frac{1 + 2 \cdot 0.68}{1 + 0.68} = 0.585m \qquad (2.13)$$

$$x_{MAC\ 0.25c} = 0.25 \cdot MAC_c = 0.25 \cdot 0.425 = 0.11m \qquad (2.14)$$
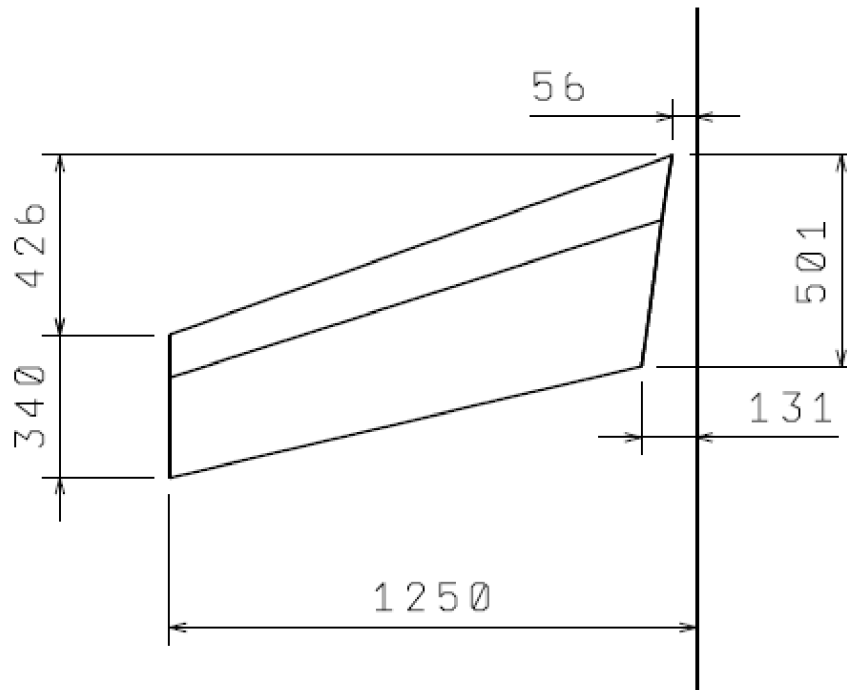
Figure 2.12: Canard drawing

Canard is designed as control-canard which means it pivots as it is necessary for pilot's needs.

2.7 Vertical stabilizer configuration

Vertical tails are placed in the end of wing and works simultaneously like winglet. This is caused by two jet engines placed on the fuselage and therefore their outtakes with hot gases from engines can damage them. Since there is no necessary need for any curved airfoil NACA 0009 was chosen. Distance between wing and vertical stabilizer is $l_{VT} = 1.59m$. Volume coefficient of single stabilizer was chosen $V_V = 0.054$, for double stabilizer is half $V_V = 0.027$.

$$S_{VT} = \frac{V_V \cdot S \cdot b}{l_{VT}} = \frac{0,019 \cdot 10.24 \cdot 8}{1.59} = 1.39m^2 \qquad (2.15)$$

Vertical tail was designed with swept $\kappa_0 = 35°$. Double vertical stabilizer design was chosen due its common usage between canard airplanes where it works simultaneously as stabilizer and as winglet.

Vertical tail's geometrical parameters:

Span: $b_{vt} = 2.1m$
Root chord: $c_{rvt} = 0.82m$
Tip chord: $c_{tvt} = 0.57m$
Area: $S_{vt} = 1.39m^2$
Aspect ratio: $AR_{vt} = 3.3$
Taper ratio: $\eta = \frac{c_{tvt}}{c_{rvt}} = \frac{0.57}{0.82} = 0.70$

Mean aerodynamic chord:

$$MAC_{vt} = \frac{2}{3} \cdot \frac{\eta^2 + \eta + 1}{\eta + 1} \cdot c_{rvt} = \frac{2}{3} \cdot \frac{0.7^2 + 0.7 + 1}{0.7 + 1} \cdot 0.82 = 0.702m \qquad (2.16)$$

MAC position: $\quad x_{MACvt} = \frac{b_{vt}}{6} \cdot \frac{\eta + 2}{\eta + 1} \cdot tg\kappa_0 = \frac{2.1}{6} \cdot \frac{0.70 + 2}{0.70 + 1} \cdot tg35° = 0.427m \qquad (2.17)$

$$y_{MACvt} = \frac{b_{vt}}{6} \cdot \frac{1 + 2 \cdot \eta}{1 + \eta} = \frac{2.1}{6} \cdot \frac{1 + 2 \cdot 0.70}{1 + 0.70} = 0.541m \qquad (2.18)$$

$$x_{MAC\ 0.25c} = 0.25 \cdot MAC_{vt} = 0.25 \cdot 0.702 = 0.18m \qquad (2.19)$$
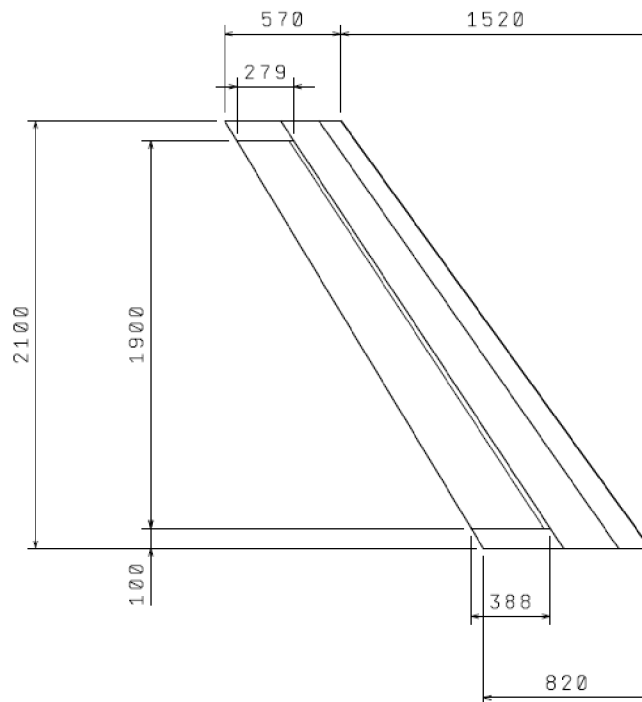
Figure 2.13: Stabilizer drawing

3 WEIGHTS

3.1 Materials

If we look at current VLJs manufacturers we can divide them into two groups. One group consist from companies with long history in aircraft designing and use mostly metals and the second one is formed by new companies which prefer composite materials. Therefore before the weight estimation is necessary to choose materials for the aircraft parts. This information should help for more accurate predictions weight.

3.1.1 Wing

The wing is monocoque two-hollow construction which main parts (skin and main spar) are sandwiches, carbon fibre/epoxy + foam, and rear spar is composite, glass fibre/epoxy. Wing will have minimal number of ribs. The sandwich's skin should provide sufficient dimensional strength. Flaps and ailerons are composite monocoque filled by foam. The fuel tanks are placed in the front of the wing as close to the center of gravity as possible. Between spars is also place for main landing gear and its attachment.

3.1.2 Fuselage

The fuselage is composite monocoque made from carbon fibre/epoxy. Fuselage will be reinforced by composite bulkheads in the placement of wing hinges, canard, front landing gear and engines. Behind the rear seat is also another bulkhead serving as fire bulkhead. The aircraft windshield is made by plexiglass. The control stick is in the middle, and throttle control on the left.

3.1.3 Canard

The canard is monocoque construction made from carbon fibre/epoxy filled by foam. Canard will be control-canard design, which means that main spar is connected to the spigot to could be driven by pilot

3.1.4 Vertical stabilizer

The vertical stabilizer is monocoque carbon fibre/epoxy construction filled by foam.

3.2 Weight estimation

Determining weights is based on statistics [7], or manufacturers manual [12], or are calculated where it was necessary to do. The mentioned values are indicative only, are not known until the aircraft's exact shape.

Table 3.1: Weight estimation table

Nr.	Component	m_i [kg]	m_i/m_{TOW} [%]
1	wing	187	15.94
2	vertical stabilizer	27	2.30
3	canard	15	1.28
4	fuselage	166	14.15
5	windshield	30	2.56
	landing gear		
6	front	10	0.85
7	main	64	5.46
8	hydraulics – front ldg.	2	0.17
9	hydraulics – main ldg.	6	0.51
	power unit		
10	engine	159	13.55
11	engine bed	4	0.34
12	fuel system	10	0.85
13	inexhaustible supply of fuel	3	0.26
	airplane equipment		
14	front seat	3	0.26
15	back seat	3	0.26
16	front seat avionics	15	1.28
17	back seat avionics	15	1.28
18	front seat controls	3	0.26
19	back seat controls	3	0.26
20	batteries	7	0.60
21	electrical components	15	1.28
	empty weight $\sum m_i$	747	63.68

The m_i/m_{TOW} ration for designed aircraft is 64%, similar ratio numbers can be found in chapter 2, Table 1.7.

Table 3.2: Variable weights

Component	m_i [kg]	m_i/m_{TOW} [%]
first pilot	60	5.12
	90	7.67
	0	0
second pilot	60	5.12
	90	7.67
	0	0
fuel	183	15.60
	0	0
baggage	50	4.26
	0	0

For designation of center of gravity it necessary to needs to know weights and location of basic aircraft's parts (Table 3.1). On the other hand there are variables which can change and therefore it can cause change center of gravity location. These components should be placed near to the center of gravity, due to their changes during flight.

Table 3.3: Values for center of gravity calculation

Nr.	Component	m_i [kg]	x_{CoGi} [m]	z_{CoGi} [m]	$m_i \cdot x_{CoGi}$ [kg $\cdot$ m]	$m_i \cdot z_{CoGi}$ [kg $\cdot$ m]
1	wing	187	5.03	1.13	940.66	210.67
2	vertical stabilizer	27	6.36	2.08	171.62	56.18
3	canard	15	0.63	0.80	9.47	12.05
4	fuselage	166	2.91	1.25	482.94	207.36
5	windshield	30	2.52	1.50	75.57	44.91
	landing gear					
6	front	10	1.15	0.22	11.50	2.24
7	main	64	6.00	0.36	384.00	22.93
8	hydraulics – front ldg.	2	1.16	0.61	2.32	1.21
9	hydraulics – main ldg.	6	4.90	1.10	29.39	6.59
	power unit					
10	engine	159	4.40	1.59	699.60	252.02
11	engine bed	4	4.33	1.59	17.32	6.35
12	fuel system	10	4.20	1.15	42.00	11.50
13	inexhaustible supply of fuel	3	4.20	1.15	12.60	3.45
	airplane equipment					
14	front seat	3	2.29	0.94	6.88	2.82
15	back seat	3	3.31	0.96	9.94	2.88
16	front seat avionics	15	1.60	1.30	24.00	19.50
17	back seat avionics	15	2.70	1.30	40.50	19.50
18	front seat controls	3	1.66	0.81	4.99	2.44
19	back seat controls	3	2.76	0.81	8.29	2.44
20	batteries	7	1.00	1.13	7.00	7.88
21	electrical components	15	2.43	0.62	36.42	9.32
		Σm_i			$\Sigma m_i \cdot x_{CoGi}$	$\Sigma m_i \cdot z_{CoGi}$
		747			**2,946.63**	**904.24**

Centre of gravity

$$x_{CoG} = \frac{\Sigma \ m_i \cdot x_{CoGi}}{\Sigma \ m_i} = 3.945 m \qquad (3.1)$$

$$z_{CoG} = \frac{\Sigma \ m_i \cdot z_{CoGi}}{\Sigma \ m_i} = 1.210 m \qquad (3.2)$$

The difference between extended and retracted gear in x-axis are insignificant, thus extended gear will be use for next calculations.

Table 3.4: Variable values for center of gravity calculation

Nr.	Component	m_i [kg]	x_{CoGi} [m]	z_{CoGi} [m]	$m_i \cdot x_{CoGi}$ [kg·m]	$m_i \cdot z_{CoGi}$ [kg·m]
	first pilot	60			126.00	60.00
		90	2.1	1	189.00	90.00
		0			0.00	0.00
	second pilot	60			192.00	60.00
		90	3.2	1	288.00	90.00
		0			0.00	0.00
10	fuel	180	4.2	1.15	756.00	207.00
		0			0.00	0.00
	baggage	50	3.7	1.1	185.00	55.00
		0			0.00	0.00

The final location of the centre of gravity has been calculated with values from Table 3.4 and using equation for centre of gravity. In Table 3.5 is showed the four border cases which determine center of gravity location. Table 3.5 also shows that centre of gravity is placed in front of the MAC position, therefore there are negative marks.

Table 3.5: The resulting center of gravity location

Combination of variable values	Σm_i [kg]	$\Sigma m_i \cdot x_{CoGi}$ [kg·m]	$\Sigma m_i \cdot z_{CoGi}$ [kg·m]	x_{CoG} [m]	x_{CoG} [%MAC]	z_{CoG} [m]
min. fuel + front pilot + no baggage	807	3,072.63	964.24	3.807	-0.246	1.195
min. fuel + both pilots + max. baggage	977	3,608.63	1,139.24	3.694	-0.333	1.166
max. fuel + back pilot + no baggage	987	3,894.63	1,171.24	3.946	-0.140	1.187
max. fuel + both pilots + max. baggage	1157	4,364.63	1,346.24	3.772	-0.273	1.164

Graph 3.1 shows how the weight distribution influences center of gravity location. The front limit is with is almost 33% in front of MAC and the rear limit 14%.
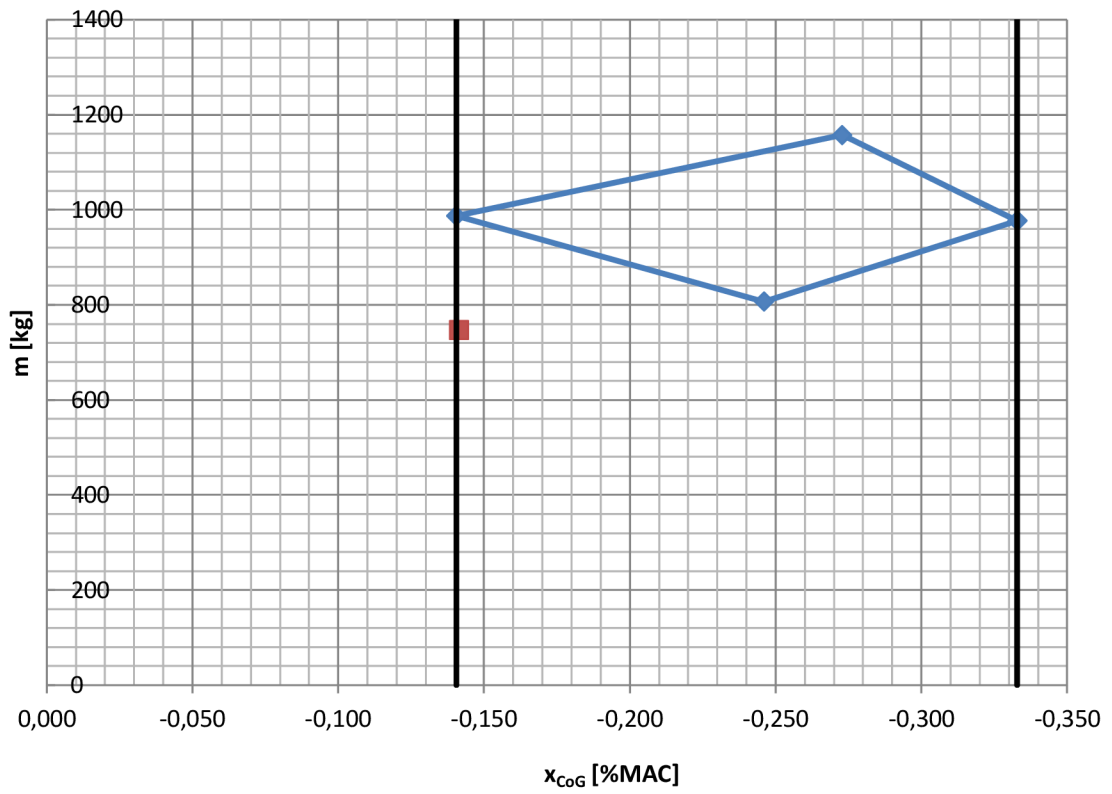
Graph 3.1: Center of gravity location diagram

4 STABILITY

4.1 Aerodynamic center with fixed controls

The location of aerodynamic center is determined by books [7] and [9]. The basic dimension which leads to others is wing's aerodynamic center.

$$\bar{X}_A = \bar{X}_{A_{KT}} + \Delta\bar{X}_{A_{VOP}} \tag{4.1}$$

Fuselage influence:

$$\Delta\bar{X}_{FUS} = -K_{A_{FUS}} \cdot \frac{b_{FUS} \cdot c_r^2}{S \cdot MAC} \tag{4.2}$$

where

$K_{A_{FUS}} = 0.55 -$ value comes from [9, table 2-26] for these values:

$$\frac{l_{a\,FUS}}{l_{FUS}} = \frac{4.003}{6.00} = 0.667$$

and

$$\frac{c_r}{l_{FUS}} = \frac{2.09}{6.00} = 0.35$$

The fuselage influence is then:

$$\Delta\bar{X}_{FUS} = -0.55 \cdot \frac{0.7 \cdot 2.09^2}{10.24 \cdot 1.31} = -0.196$$

Engine nacelle influence:

$$\Delta\bar{X}_{F\,nac} = i_{nac} \cdot k_{nac} \cdot A_{nac} \cdot \frac{a_{nac}}{a_{wing}} \cdot \left(1 - \frac{d\varepsilon}{d\alpha}\right) \tag{4.3}$$

where

i_{nac} is number of nacelles: $\quad i_{nac} = 2$

k_{nac} is nacelle's placement: $\quad k_{nac} = 0.9$

a_{wing} is wing's lift curve slope: $a = 4.8083$

$\frac{d\varepsilon}{d\alpha} \doteq 0.6$ from [7, pg. 111]

$$A_{nac} = \frac{S_{nac} \cdot l_{nac}}{S \cdot MAC} = \frac{0.498 \cdot 1.346}{10.24 \cdot 1.311} = 0.050 \qquad (4.4)$$

and a_{nac} is determined from literature [7, fig. 80].

$$a_{nac} = 2.5$$

The engine nacelles influence is then:

$$\Delta \bar{X}_{F\,nac} = 2 \cdot 0.9 \cdot 0.046 \cdot \frac{2.5}{4.8083} \cdot (1 - 0.6) = 0.0187$$

Canard influence:

$$\Delta \bar{X}_{A\,can} = k_{can} \cdot V_{can} \cdot \frac{a_{can}}{a} \cdot \left(1 - \frac{d\varepsilon}{d\alpha}\right) \qquad (4.5)$$

Aircraft's lift curve slope:

$$a = a_{wing} + a_{can} \cdot k_{can} \cdot \frac{S_{can}}{S} \cdot \left(1 - \frac{d\varepsilon}{d\alpha}\right) \qquad (4.6)$$

where

a_{wing} is wing's lift curve slope: $a_{wing} = 4.8083$

a_{can} is canard's lift curve slope: $a_{can} = 3.51$ from [7, pg. 112, fig. 81]

k_{can} is reduction coefficient of dynamic pressure: $k_{can} = 0.85$ from [7, pg. 113]

Upwash gradient at the canard:

$$\frac{d\varepsilon}{d\alpha} = 1.75 \cdot \frac{a_{wing}}{\pi \cdot A \cdot (\bar{l}_{can.25} \cdot \eta)^{\frac{1}{4}} \cdot (1 + |\bar{h}_{can}|)} \qquad (4.7)$$

where

A is wing's aspect ratio: $A = 6.2$

η is wing's tapper ratio: $\eta = 0.29$

$\bar{h}_{can}$ is comparative height between AC_{can} and AC_{wing}:

$$\bar{h}_{can} = \frac{2 \cdot h_{can}}{b} = \frac{2 \cdot 0.49}{8} = 0.123 \tag{4.8}$$

$\bar{l}_{can.25}$ is comparative distance between AC_{can} and AC_{wing}:

$$\bar{l}_{can.25} = \frac{2 \cdot l_{can.25}}{b} = \frac{2 \cdot 4.911}{8} = 1.228 \tag{4.9}$$

Thus

$$\frac{d\varepsilon}{d\alpha} = 1.75 \cdot \frac{4.8083}{\pi \cdot 6.2 \cdot (1.228 \cdot 0.29)^{\frac{1}{4}} \cdot (1 + |0.123|)} = 0.4954$$

and

$$a = 4.8083 + 3.51 \cdot 0.85 \cdot \frac{0.82}{10.24} \cdot (1 - 0.4954) = 4.929$$

Therefore

$$\Delta \bar{X}_{A_{can}} = 0.85 \cdot 0.3 \cdot \frac{3.51}{4.93} \cdot (1 - 0.4954) = 0.092$$

Propulsion influence:

Propulsion influence can be neglected in this case.

Intakes influence:

Intakes influence can be neglected in this case, due to the anticipated low values.

Outtakes influence:

Outtakes influence can be neglected in this case, due to the anticipated low values.

The final AC location:

$$\bar{X}_A = \bar{X}_{A_{KT}} + \Delta \bar{X}_{A_{VOP}} = 0.25 - 0.196 + 0.0187 + 0.092 = 0.164 \% MAC \tag{4.10}$$

4.2 Static margin with fixed controls

Longitudinal static margin of aircraft is determined as:

$$\sigma = \bar{X}_A - \bar{X}_T \qquad (4.11)$$

where

$\bar{X}_T$ is aircraft's center of gravity related to the length of MAC;

Front limit: $\qquad \sigma_F = \bar{X}_A - \bar{X}_{TF} = 0.164 - (-0.140) = 0.497 = 49.7\% MAC$

Rear limit: $\qquad \sigma_R = \bar{X}_A - \bar{X}_{TR} = 0.164 - (-0.333) = 0.305 = 30.5\% MAC$

4.3 Aerodynamic center with free controls

This is only preliminary calculation due to the lack of input data.

$$\bar{X}'_A = \bar{X}_A + \left(1 + \frac{a}{a\prime}\right) \cdot \frac{l^*_{can}}{MAC} \qquad (4.12)$$

Aircraft's lift curve slope with free controls:

$$C'_{L\alpha} = a' \qquad (4.13)$$

$$C'_{L\alpha} = C_{L\alpha} - C_{L\delta} \cdot \frac{C_{H\alpha}}{C_{H\delta}} \qquad (4.14)$$

$$C_{L\alpha} = a \qquad (4.15)$$

$$C_{H\alpha\,can} = -0.12 \cdot a_{can} \cdot \frac{S_e}{S_{can}} \cdot \left(1 - 3.6 \cdot \frac{S_r}{S_e}\right) \cdot cos\Lambda_e \qquad (4.16)$$

where

S_e is elevator's area, in this case $S_e = S_{can}$

S_r is stabilizer's relief area, in this case $S_r = 0$

Λ_e is canard angle: $\qquad \Lambda_e = 20°$

$$C_{H\alpha\,can} = -0.12 \cdot 3.51 \cdot \frac{0.82}{0.82} \cdot \left(1 - 3.6 \cdot \frac{0}{0.82}\right) \cdot cos20° = -0.4212rad^{-1}$$

$$C_{H\alpha} = C_{H\alpha\,can} \cdot \left(1 - \frac{d\varepsilon}{d\alpha}\right) = -0.4212 \cdot (1 - 0.4954) = -0.2125rad^{-1} \qquad (4.17)$$

$$C_{H\delta} = -0.14 \cdot a_{can} \cdot \left[1 - 6.5 \cdot \left(\frac{S_r}{S_e}\right)^{3/2}\right] \cdot cos^2 \Lambda_e = -0.14 \cdot 3.51 \cdot \left[1 - 6.5 \cdot \left(\frac{0}{0.82}\right)^{3/2}\right] \cdot$$
$$cos^2 20° = -0.4339rad^{-1} \qquad (4.18)$$

$$C_{L\delta} = C_{Lcan_\delta} \cdot k_{can} \cdot \frac{S_{can}}{S} = 1{,}755 \cdot 0.85 \cdot \frac{0.82}{10.24} = 0.1195rad^{-1} \qquad (4.19)$$

Thus

$$a' = a - C_{L\delta} \cdot \frac{C_{H\alpha}}{C_{H\delta}} = 4.8083 - 0.1195 \cdot \frac{-0.2125}{-0.4339} = 4.7498rad^{-1}$$

And therefore

$$\bar{X}'_A = 0.077 + \left(1 + \frac{4.8083}{4.7541}\right) \cdot \frac{5.098}{1.424} = 0.1154$$

$$\bar{X}'_A - \bar{X}_A = 0.1154 - 0.164 = -0.05\%MAC \qquad (4.20)$$

4.4 Static margin with free controls

Longitudinal static margin of aircraft is determined as:

$$\sigma = \bar{X}'_A - \bar{X}_T \quad \text{The main goal og hte}$$
(4.21)

where

$\bar{X}_T$ is aircraft's center of gravity related to the length of MAC;

Front limit: $\qquad \sigma_F = \bar{X}'_A - \bar{X}_{TF} = 0.1154 - (-0.333) = 0.448 = 44.8\%MAC$

Rear limit: $\qquad \sigma_R = \bar{X}'_A - \bar{X}_{TR} = 0.1154 - (-0.140) = 0.256 = 26.5\%MAC$

5 DRAG POLAR

Drag polar is necessary to further performance's calculations. The polar shows dependence between lift and drag coefficients at varying angles of attack. The influence of altitude and velocity is determined by Reynolds and Mach number. The drag polar was determined from literature [5].

5.1 Airfoil polar

Root and tip airfoil have different polar due to the different Reynolds numbers. To calculate airfoil polar I have used Mark Drela's XFoil software program which can calculate polar for given Reynolds number.

Reynolds number:

$$Re = \frac{\rho_0 \cdot c \cdot v}{\mu_0}$$

where

ρ_0 is air density at 0m MSA: $\rho_0 = 1.225 kg \cdot m^{-3}$

μ_0 is dynamic air viscosity: $\mu_0 = 1.79 \cdot 10^{-5} N \cdot s \cdot m^{-2}$

c_r is root chord: $c_r = 2.255m$

c_t is tip chord: $c_t = 0.7m$

v is cruise velocity: $v = 108m \cdot s^{-1}$

Therefore we get these values:

Table 5.1: Final Reynolds number values

	c	v	Re
	[m]	[m/s]	[-]
Root chord	2.255	108	$16.65 \cdot 10^6$
Tip chord	0.7	108	$4.43 \cdot 10^6$

5.2 Wing polar

To create a wing polar in pure configuration it necessary to calculate coefficients affecting wing with different properties at chord and root wing's airfoil.

$$k_r = \frac{1}{3} \cdot \frac{2 \cdot c_r + c_t}{c_r + c_t} = \frac{1}{3} \cdot \frac{2 \cdot 2.092 + 0.6}{2.092 + 0.6} = 0.592 \tag{5.1}$$

$$k_t = \frac{1}{3} \cdot \frac{c_t + 2 \cdot c_r}{c_r + c_t} = \frac{1}{3} \cdot \frac{2.092 + 2 \cdot 0.6}{2.092 + 0.6} = 0.408 \tag{5.2}$$

Drag coefficient of substitute airfoil:

$$c_{DP} = k_r \cdot c_{Dr} + k_t \cdot c_{Dt} \tag{5.3}$$

Lift coefficient of substitute airfoil:

$$c_{Lwing} = k_r \cdot c_{Lr} + k_t \cdot c_{Lt} \tag{5.4}$$

Drag of substitute airfoil including reduce impact surface of the wing by fuselage and wing-fuselage interference:

$$c'_{Dwing} = c_{DP} \cdot \left(1 - k_1 \cdot \frac{S_1}{S}\right) \tag{5.5}$$

where

k_1 is wing-fuselage interference coefficient for mid-wing: $k_1 = 0.85$

S_1 is wing area covered by fuselage: $S_1 = 1.1 m^2$

S is wing area: $S = 10.24 m^2$

Induced drag:

$$c_{Di} = \frac{c_{Lwing}^2}{\pi \cdot \lambda_E} \cdot (1 + \delta) \tag{5.6}$$

where

δ is Glauert coefficient from Glauert III software: $\qquad \delta = 0.0114$

λ_E is wing effective aspect ratio:

$$\lambda_E = \frac{b^2}{S} \cdot \frac{e}{1 - \frac{S_1}{S}} = \frac{8^2}{10.24} \cdot \frac{0.8}{1 - \frac{1.1}{10.24}} = 5.601 \qquad (5.7)$$

where

b is wing span: $\qquad\qquad\qquad b = 8m$

e is span efficiency factor: $\qquad\qquad\qquad e = 0.8$

The total wing drag coefficient:

$$c_{Dwing} = c'_{Dwing} + c_{Di} \qquad (5.8)$$

The total wing drag polar is shown at Appendix 2.

5.3 Drag coefficients

5.3.1 Fuselage drag coefficient

Fuselage drag coefficient is found from [5, pg. 44]:

$$c_{Dfus} = c_{D0fus} + c_{DLfus} \qquad (5.9)$$

Fuselage zero-lift drag coefficient:

$$c_{D0fus} = R_{wf} \cdot c_{ffus} \cdot \left\{ 1 + \frac{60}{(l_f + d_f)^3} + 0.0025 \cdot \left(\frac{l_f}{d_f} \right) \right\} \cdot \frac{S_{wetfus}}{S} \qquad (5.10)$$

where

R_{wf} is wing-fuselage interference factor [5, pg. 24, fig. 4.1]: $\qquad R_{wf} = 1.02$

$c_{f_{fus}}$ is turbulent flat plate skin-friction coefficient of the fuselage [5, pg. 25]:

$$c_{f_{fus}} = 0.0024$$

l_f is fuselage length: $l_f = 6m$

d_f is maximal fuselage diameter: $d_f = 0.7m$

$S_{wet_{fus}}$ is fuselage wetted area: $S_{wet_{fus}} = 13.137m^2$

S is wing area: $S = 10.24m^2$

$$c_{D0_{fus}} = R_{wf} \cdot c_{f_{fus}} \cdot \left\{1 + \frac{60}{(l_f+d_f)^3} + 0.0025 \cdot \left(\frac{l_f}{d_f}\right)\right\} \cdot \frac{S_{wet_{fus}}}{S} = 1.02 \cdot 0.0024 \cdot \left\{1 + \frac{60}{(6+0.7)^3} + 0.0025 \cdot \left(\frac{6}{0.7}\right)\right\} \cdot \frac{13.137}{10.24} = 0.0035$$

Fuselage drag coefficient due to lift:

$$c_{D_{Lfus}} = \eta \cdot c_{d_c} \cdot \alpha^3 \cdot \frac{S_{plf_{fus}}}{S} \tag{5.11}$$

where

η is ratio of the drag of finite cylinder to the drag of an infinite cylinder [5, pg. 47,fig. 4.19]:

$$\eta = 0.655$$

c_{d_c} is experimental steady state cross-flow drag coefficient of a circular cylinder [5, pg. 47,fig. 4.20]:

$$c_{d_c} = 1.2$$

$S_{plf_{fus}}$ is fuselage planform area: $S_{plf_{fus}} = 2.958m^2$

α is the fuselage angle of attack in radians

5.3.2 Empennage drag coefficient

Empennage drag coefficient is found form [5, pg. 66]:

$$c_{D\,emp} = sum_i\left\{\left(c_{D_{o\,emp}}\right)_i + \left(c_{D_{L\,emp}}\right)_i\right\} \tag{5.12}$$

Empennage is divided between canards, which have both part, $c_{D_{o\,can}}$ and $c_{D_{L\,can}}$, and vertical tail, which has only zero-lift drag coefficient $c_{D_{o\,vt}}$.

Canard zero-lift drag coefficient:

Canard zero-lift drag coefficient [5, pg. 23]:

$$c_{D_{o\,can}} = R_{canf} \cdot R_{LS} \cdot c_{f_{can}} \cdot \{1 + L' \cdot (t/c) + 100 \cdot (t/c)^\wedge 4\} \cdot \frac{S_{wet\,can}}{S} \tag{5.13}$$

where

R_{canf} is canard-fuselage interference factor [5, pg. 24, fig. 4.1.]: $R_{canf} = 1$

R_{LS} is lifting surface correction factor [5, pg. 24, fig. 4.2.]: $R_{LS} = 1.06$

$c_{f_{can}}$ is turbulent flat plate friction coefficient of the canard [5, pg. 25, fig. 4.3.]:

$$c_{f_{can}} = 0.0037$$

L' is airfoil thickness location parameter [5, pg. 26, fig. 4.4.]: $L' = 2$

t/c is thickness ratio defined at the mean geometric chord of the canard:

$$t/c = 0.25$$

$S_{wet\,can}$ is wetted area of the canard: $S_{wet\,can} = 2.117 m^2$

S is wing area: $S = 10.24 m^2$

$$c_{D_{o\,can}} = R_{canf} \cdot R_{LS} \cdot c_{f_{can}} \cdot \{1 + L' \cdot (t/c) + 100 \cdot (t/c)^\wedge 4\} \cdot \frac{S_{wet\,can}}{S}$$
$$= 1 \cdot 1.06 \cdot 0.0037 \cdot \{1 + 2 \cdot (0.25) + 100 \cdot (0.25)^\wedge 4\} \cdot \frac{2.117}{10.24} = 0.0015$$

Vertical tail zero-lift drag coefficient:

Vertical tail zero-lift drag coefficient [5, pg. 23]:

$$c_{D_{o_{vt}}} = R_{vtf} \cdot R_{LS} \cdot c_{f_{vt}} \cdot \{1 + L' \cdot (t/c) + 100 \cdot (t/c)\char`^4\} \cdot \frac{S_{wet_{vt}}}{S} \qquad (5.14)$$

where

R_{vtf} is vertical tail-wing interference factor [5, pg. 24, fig. 4.1.]: $\quad R_{vtf} = 1.07$

R_{LS} is lifting surface correction factor [5, pg. 24, fig. 4.2.]: $\quad R_{LS} = 1.03$

$c_{f_{vt}}$ is turbulent flat plate friction coefficient of the vertical tail[5, pg. 25, fig. 4.3.]:

$$c_{f_{vt}} = 0.0034$$

L' is airfoil thickness location parameter [5, pg. 26, fig. 4.4.]: $\quad L' = 2$

t/c is thickness ratio defined at the mean geometric chord of the canard:

$$t/c = 0.12$$

$S_{wet_{vt}}$ is wetted area of the vertical tail: $\quad S_{wet_{vt}} = 3.03 m^2$

S is wing area: $\quad S = 10.24 m^2$

$$c_{D_{o_{vt}}} = R_{vtf} \cdot R_{LS} \cdot c_{f_{vt}} \cdot \{1 + L' \cdot (t/c) + 100 \cdot (t/c)\char`^4\} \cdot \frac{S_{wet_{vt}}}{S}$$

$$= 1.07 \cdot 1.03 \cdot 0.0034 \cdot \{1 + 2 \cdot (0.12) + 100 \cdot (0.12)\char`^4\} \cdot \frac{3.03}{10.24} = 0.0014$$

Canard drag coefficient due to lift

The canard drag coefficient due to lift is found from [5, pg. 68, eqn. 4.51.]:

$$c_{D_{L_{can}}} = \left\{ \frac{(c_{L_{can}})^2}{\pi \cdot A_{can} \cdot e_{can}} \right\} \cdot \frac{S_{can}}{S} \qquad (5.15)$$

where

$c_{L_{can}}$ is canard lift coefficient

A_{can} is canard's aspect ratio: $\qquad A_{can} = 6.6$

e_{can} is Oswald efficiency [5, pg. 69]: $\qquad e_{can} = 0.5$

S_{can} is canard area: $\qquad S_{can} = 0.85 m^2$

Therefore the final empennage drag coefficient:

$$c_{D_{emp}} = c_{D_{o_{can}}} + c_{D_{o_{vt}}} + c_{D_{L_{can}}}$$

5.3.3 Nacelle drag coefficient

Calculating engine nacelle it can be assumed that nacelle is small fuselage, thus it is calculated same way.

Nacelle drag coefficient is found from:

$$c_{D_{nac}} = c_{D_{0_{nac}}} + c_{D_{L_{nac}}} \qquad (5.16)$$

Nacelle zero-lift drag coefficient:

$$c_{D_{0_{nac}}} = R_{f_{nac}} \cdot c_{f_{nac}} \cdot \left\{ 1 + \frac{60}{(l_{nac}+d_{nac})^3} + 0.0025 \cdot \left(\frac{l_{nac}}{d_{nac}} \right) \right\} \cdot \frac{S_{wet_{nac}}}{S} + c_{D_{b_{nac}}} \qquad (5.17)$$

where

R_{fn} is fuselage-nacelle interference factor [5, pg. 24, fig. 4.1.]: $\qquad R_{fn} = 1.75$

$c_{f_{nac}}$ is turbulent flat plate skin-friction coefficient of the nacelle [5, pg. 25, fig. 4.3.]:

$$c_{f_{nac}} = 0.003$$

l_{nac} is nacelle length: $\qquad l_{nac} = 1.34 m$

d_{nac} is maximal nacelle diameter: $\qquad d_{nac} = 0.27 m$

$S_{wet_{nac}}$ is nacelle wetted area: $\qquad S_{wet_{nac}} = 0.498 m^2$

S is wing area: $\qquad S = 10.24 m^2$

$c_{D_{b_{nac}}}$ is nacelle base-drag coefficient

$$c_{D_{b\,nac}} = \left[0.029 \cdot \frac{\left(\frac{d_b}{d_{fn}}\right)^3}{\left\{ c_{D_{o\,nac-base}} \cdot \left(\frac{S}{S_{nac}}\right) \right\}^{0.5}} \right] \cdot \left(\frac{S_{nac}}{S}\right) \tag{5.18}$$

d_b is nacelle base diameter: $\qquad\qquad d_b = 0.071m$

d_{fn} is maximum nacelle diameter: $\qquad\quad d_{fn} = 0.547m$

S_{nac} is nacelle maximum frontal area: $\qquad S_{nac} = 0.235m^2$

$c_{D_{o\,nac-base}}$ is zero-lift drag coefficient of the nacelle exclusive of the base, it is determined from the first term on the right hand side in $c_{D_{0\,nac}}$

$$c_{D_{b\,nac}} = \left[0.029 \cdot \frac{\left(\frac{d_b}{d_{fn}}\right)^3}{\left\{ c_{D_{o\,nac-base}} \cdot \left(\frac{S}{S_{nac}}\right) \right\}^{0.5}} \right] \cdot \left(\frac{S_{nac}}{S}\right)$$

$$= \left[0.029 \cdot \frac{\left(\frac{0.547}{0.071}\right)^3}{\left\{ 0.0079 \cdot \left(\frac{10.24}{0.235}\right) \right\}^{0.5}} \right] \cdot \left(\frac{0.235}{10.24}\right) = 2.51 \cdot 10^{-6}$$

$$c_{D_{0\,nac}} = R_{fnac} \cdot c_{f\,nac} \cdot \left\{ 1 + \frac{60}{(l_{nac} + d_{nac})^3} + 0.0025 \cdot \left(\frac{l_{nac}}{d_{nac}}\right) \right\} \cdot \frac{S_{wet\,nac}}{S} + c_{D_{b\,nac}}$$

$$= 1.75 \cdot 0.003 \cdot \left\{ 1 + \frac{60}{(1.34 + 0.27)^3} + 0.0025 \cdot \left(\frac{1.34}{0.27}\right) \right\} \cdot \frac{0.498}{10.24} + 2.51 \cdot 10^{-6}$$

$$= 0.000391$$

Fuselage drag coefficient due to lift:

$$c_{D_{L\,fus}} = 2 \cdot \alpha^2 \cdot \frac{S_{b\,nac}}{S} + \eta \cdot c_{d_c} \cdot \alpha^3 \cdot \frac{S_{plf\,nac}}{S} \tag{5.19}$$

where

$S_{b\,nac}$ is nacelle base area: $\qquad\qquad S_{b\,nac} = 0.004m^2$

η is ratio of the drag of finite cylinder to the drag of an infinite cylinder [5, pg. 47, fig. 4.19]: $\qquad\qquad\qquad\qquad\qquad \eta = 0.6$

c_{d_c} is experimental steady state cross-flow drag coefficient of a circular cylinder [5, pg. 47, fig. 4.20]:
$$c_{d_c} = 1.2$$

$S_{plf_{fus}}$ is nacelle planform area:
$$S_{plf_{fus}} = 0.498 m^2$$

α is the fuselage angle of attack in radians

5.3.4 Pylon drag coefficient

Calculating engine pylon it can be assumed that pylon is small empennage, thus it is calculated same way.

$$c_{D_p} = sum_i \left(c_{D_{op}} \right)_i \tag{5.20}$$

$$c_{D_{op}} = R_{pf} \cdot R_{LS} \cdot c_{f_p} \cdot \{1 + L' \cdot (t/c) + 100 \cdot (t/c)^4\} \cdot \frac{S_{wet_p}}{S} \tag{5.21}$$

where

R_{pf} is pylon-fuselage interference factor [5, pg. 24, fig. 4.1.]: $R_{pf} = 1$

R_{LS} is lifting surface correction factor [5, pg. 24, fig. 4.2.]: $R_{LS} = 1.75$

c_{f_p} is turbulent flat plate friction coefficient of the pylon [5, pg. 25, fig. 4.3.]:

$$c_{f_p} = 0.0033$$

L' is airfoil thickness location parameter [5, pg. 26, fig. 4.4.]: $L' = 2$

t/c is thickness ratio defined at the mean geometric chord of the pylon:

$$t/c = 0.12$$

S_{wet_p} is wetted area of the pylon: $S_{wet_p} = 0.653 m^2$

S is wing area: $S = 10.24 m^2$

$$
\begin{aligned}
c_{D_{op}} &= R_{pf} \cdot R_{LS} \cdot c_{f_p} \cdot \{1 + L' \cdot (t/c) + 100 \cdot (t/c)^4\} \cdot \frac{S_{wet_p}}{S} \\
&= 1 \cdot 1.75 \cdot 0.0033 \cdot \{1 + 2 \cdot (0.12) + 100 \cdot (0.12)^4\} \cdot \frac{0.653}{10.24} = 0.00046
\end{aligned}
$$

5.3.5 Fuselage-nacelle interference drag factor

The fuselage-nacelle interference drag coefficient may be found [5, pg. 79, eqn. 4.65.]:

$$c_{D_{n_{int}}} = F_{a_2} \cdot \left\{ \left(c_{D_{nac}}\right)' - 0.05 \right\} \cdot \frac{S_{nac}}{S} \tag{5.22}$$

where

S_{nac} is maximum frontal area of the nacelle, excluding the pylon:

$$S_{nac} = 0.235 m^2$$

F_{a_2} is fuselage-nacelle intersection without local area ruling [5, pg. 79]:

$$F_{a_2} = 1$$

c_{D_n}' is drag of the nacelle includes interference [5, pg. 80, fig. 4.42.]:

$$c_{D_n}' = 0.11$$

$$c_{D_{n_{int}}} = F_{a_2} \cdot \left\{ \left(c_{D_{nac}}\right)' - 0.05 \right\} \cdot \frac{S_{nac}}{S} = 1 \cdot \{0.11 - 0.05\} \cdot \frac{0.235}{10.24} = 0.0014$$

5.3.6 Flaps and ailerons drag influence coefficient

Besides the wing drag in pure configuration, there is a drag influence from flaps and ailerons. Values for these drag coefficients were taken from [10].

Flaps: $\quad \Delta c_{Dw} = 0.0009$

Ailerons: $\quad \Delta c_{Dw} = 0.0003$

Therefore final wing drag is: $\Delta c_{Dw} = 0.0012$

5.4 Final drag polar

$$c_{D_{aircraft}} = c_{Dwing} + c_{D_{fus}} + c_{D_{emp}} + c_{D_{nac}} + c_{D_p} + c_{D_{n_{int}}} + \Delta c_{Dw} \qquad (5.23)$$
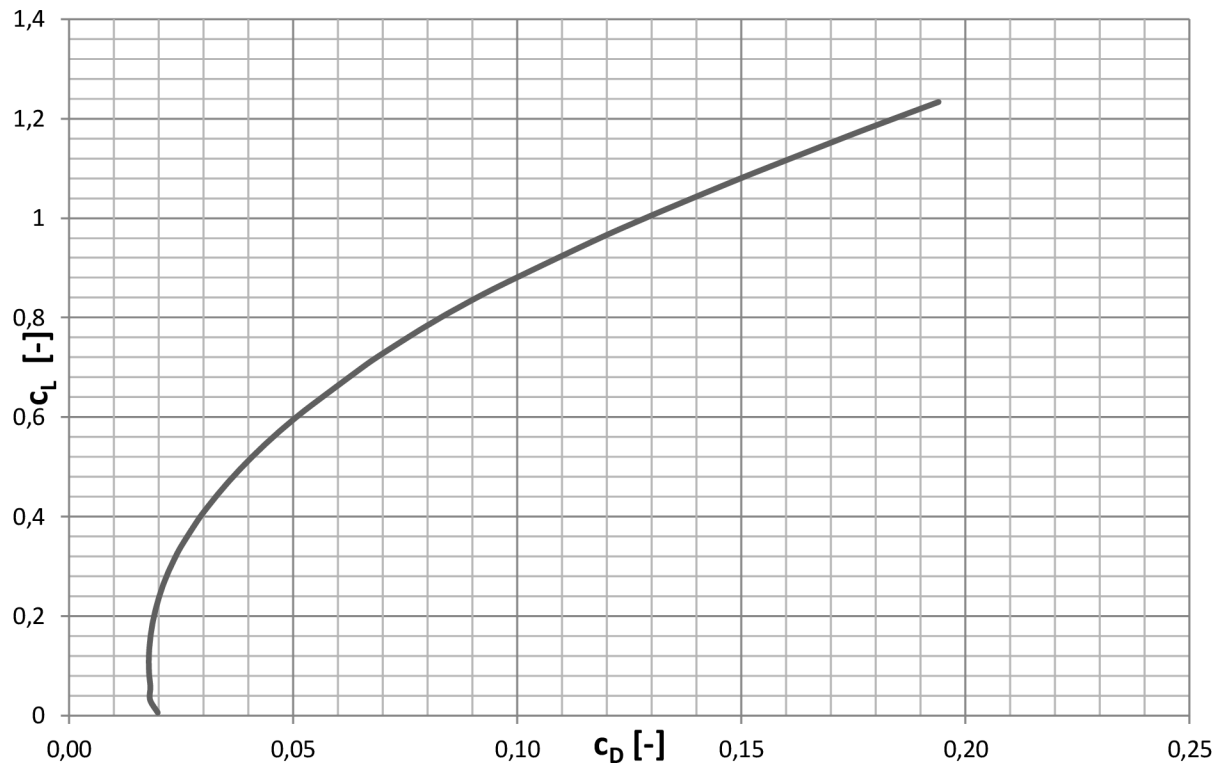
Figure 5.1: Polar drag in pure configuration

5.5 Windmilling drag polar

The polar calculation is going same way as in previous; the difference is only in the windmilling drag coefficient due to the jet engines.

The incremental drag coefficient due to a windmilling jet engine may be estimated from [5, pg. 81, eqn. 4.67.]:

$$\Delta c_{D_{Wmj}} = 0.0785 \cdot \frac{d_{inl}^2}{S} + \frac{2}{1+0.16 \cdot M^2} \cdot \frac{V_{noz}}{U_1} \cdot (1 - \frac{V_{noz}}{U_1}) \cdot \frac{S_{noz}}{S} \qquad (5.24)$$

where

d_{inl} is engine inlet diameter: $\qquad d_{inl} = 0.4m$

S_{noz} is nozzle cross section area: $\qquad S_{noz} = 0.024m^2$

V_{noz}/U_1 is ratio of average flow velocity in the nozzle to the steady state flight speed [5, pg. 81]: $\qquad V_{noz}/U_1 = 0.92$

for the fan airflow of high bypass jet engines

$$\Delta c_{D_{Wmj}} = 0.0785 \cdot \frac{d_{inl}^2}{S} + \frac{2}{1+0.16 \cdot M^2} \cdot \frac{V_{noz}}{U_1} \cdot \left(1 - \frac{V_{noz}}{U_1}\right) \cdot \frac{S_{noz}}{S} = .0785 \cdot \frac{0.4^2}{10.24} + \frac{2}{1+0.16 \cdot 0.35^2} \cdot 0.92 \cdot (1 - 0.92) \cdot \frac{0.024}{10.24} = 0.001564$$
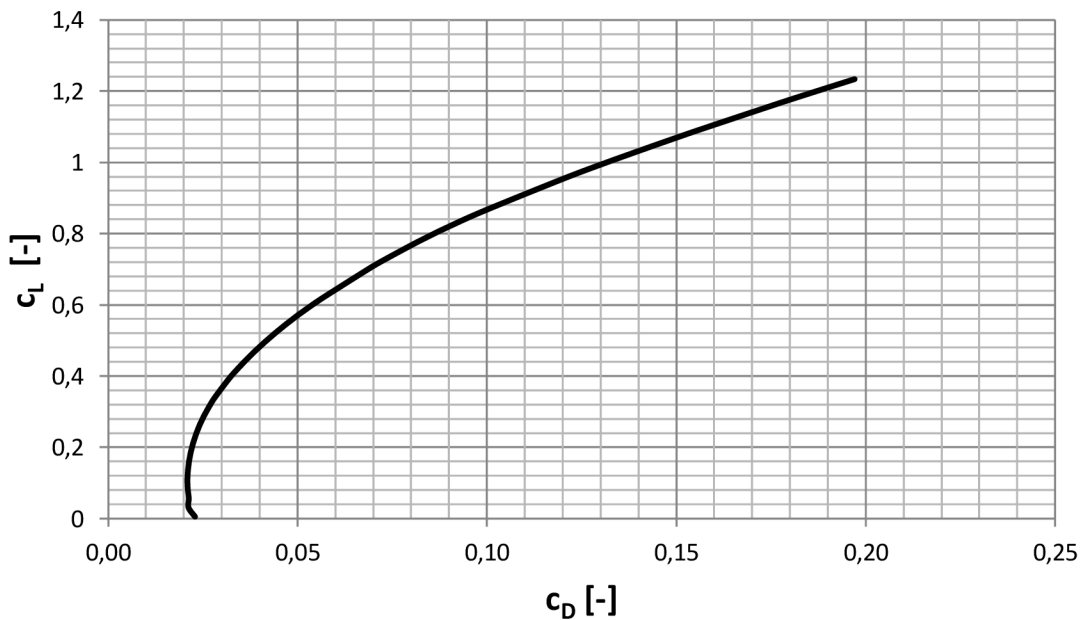
Figure 5.2: Drag polar with stopped engine

5.6 Drag polar in landing configuration

The polar calculation is going same way as in previous; the difference is only in the influence of the flap.

The drag coefficient due to flap deflection may be estimated from [5, pg. 82, eqn. 4.70.]:

$$c_{D_{flap}} = \Delta c_{D_{prof_{flap}}} + \Delta c_{D_{i_{flap}}} + \Delta c_{D_{int_{flap}}} \tag{5.25}$$

where

$\Delta c_{D_{prof_{flap}}}$ is the flap profile drag increment [5, pg. 82, eqn. 4.71.]:

$$\Delta c_{D_{prof_{flap}}} = \Delta c_{d_{p_{\Lambda c0.25}}} \cdot \cos \Lambda_{c0.25} \cdot \frac{S_{wf}}{S} \tag{5.26}$$

where

$\Delta c_{d_{p_{\Lambda c0.25}}}$ is the two-dimensional profile drag increment due to flaps. This increment depends on the type of flaps used. For single slotted flaps: $\Delta c_{d_{p_{\Lambda c0.25}}} = 0.14$

$\Lambda_{c0.25}$ is wing quarter chord sweep angle: $\qquad \Lambda_{c0.25} = 25°$

S_{wf} is the flapped wing area: $\qquad S_{wf} = 7.324 m^2$

$$\Delta c_{D_{prof_{flap}}} = \Delta c_{d_{p_{\Lambda c0.25}}} \cdot \cos \Lambda_{c0.25} \cdot \frac{S_{wf}}{S} = 0.14 \cdot \cos 25 \cdot \frac{7.324}{10.24} = 0.0907$$

$\Delta c_{D_{i_{flap}}}$ is induced drag increment due to the flap [5 pg. 86, eqn. 4.74.];

$$\Delta c_{D_{i_{flap}}} = K^2 \cdot \left(\Delta c_{L_{flap}} \right)^2 \cos \Lambda_{c0.25} \tag{5.27}$$

where

$\Delta c_{L_{flap}}$ is the incremental lift coefficient due to the flap

K is an empirical constant [5, pg. 89, fig. 4.53.]: $\qquad K = 0.28$

$\Delta c_{D\,int_{flap}}$ is the interference drag increment due to the flap [5, pg. 88, eqn. 4.75.]:

$$\Delta c_{D\,int_{flap}} = K_{int} \cdot \Delta c_{D\,prof_{flap}} \tag{5.28}$$

where

$K_{int} = 0.4$ for slotted flaps

$$\Delta c_{D\,int_{flap}} = K_{int} \cdot \Delta c_{D\,prof_{flap}} = 0.4 \cdot 0.0907 = 0.0363$$
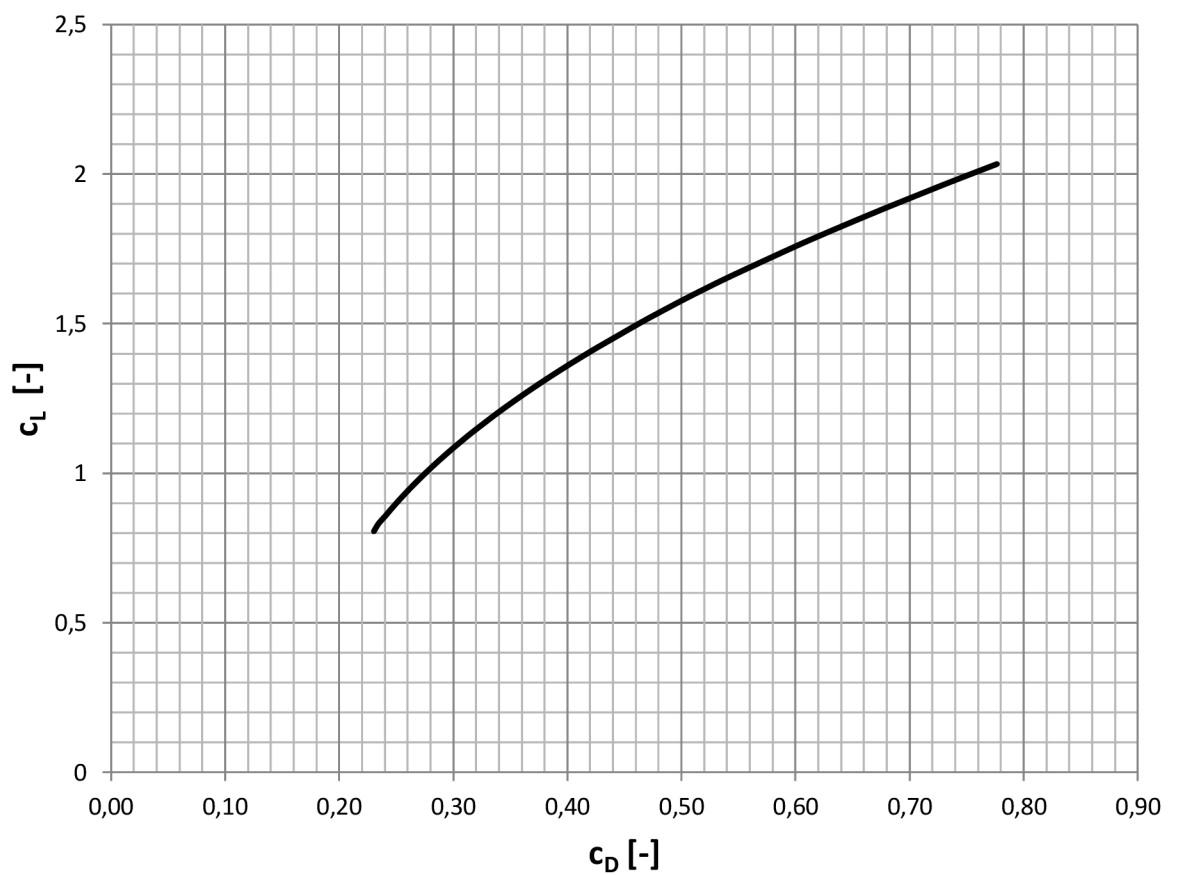
Figure 5.3: Drag polar in landing configuration

6 THE FLIGHT PERFORMANCE AND CHARACTERISTICS

The flight performance is coming from data obtained in previous chapters. Let us assume that engines are working at 74% of their thrust. The other assumption is that all flight's performances are calculating with $m_{TOW} = 1173kg$.

6.1 Maximum horizontal flight speed

The maximum horizontal flight speed is one of the crucial for determining flying envelope. Maximum speed is based on dependence between available and required thrust. Required thrust may be estimated from:

$$D = \frac{1}{2} \cdot \rho \cdot S \cdot c_D \cdot v^2 \tag{6.1}$$

Available thrust is given by engine characteristics and its values are in Appendix 2 as required thrust values.
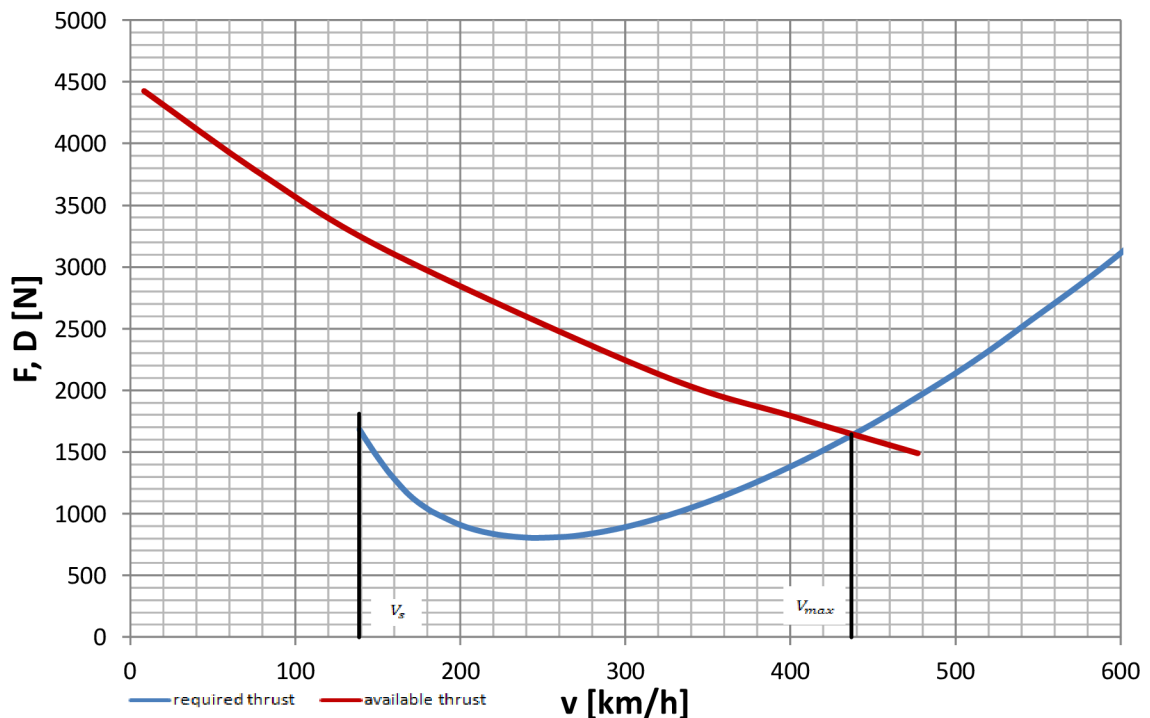
Figure 6.1: Required and available thrust depending on speed

As is visible in Figure 6.1, the maximum horizontal speed is: $v_{max} = 437 km/h$

6.2 Climbing speed

Climbing speed is another performance which determines aircraft performance. The ceiling level is not specified due to the lack of information. However we can assume that it will be limited by pilot's needs and engine limitation.

The climbing speed can be estimated from:

$$\bar{V}_z = \frac{(F-D)\cdot v}{G} = \frac{\Delta P}{G}$$ (6.2)

The angle of climb is then calculated from:

$$\chi = \arcsin\left(\frac{\bar{V}_z}{V}\right)$$ (6.3)
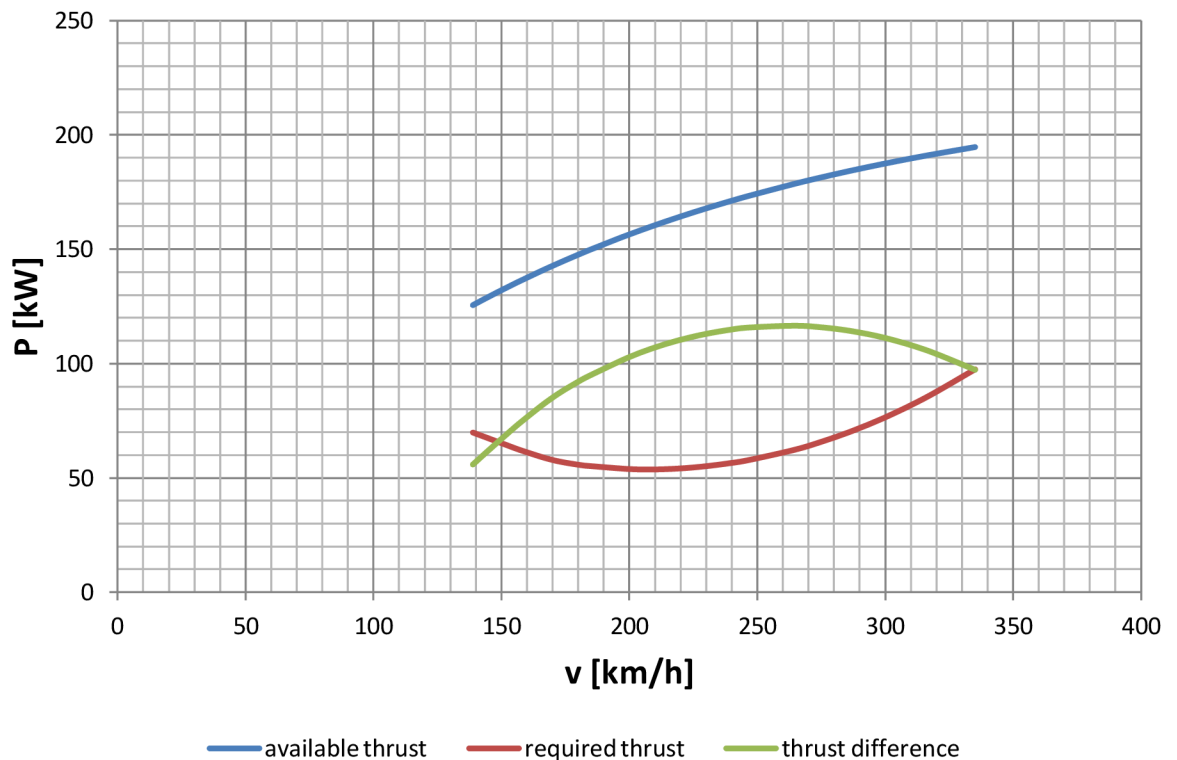
Figure 6.2: Required and available power depending on speed
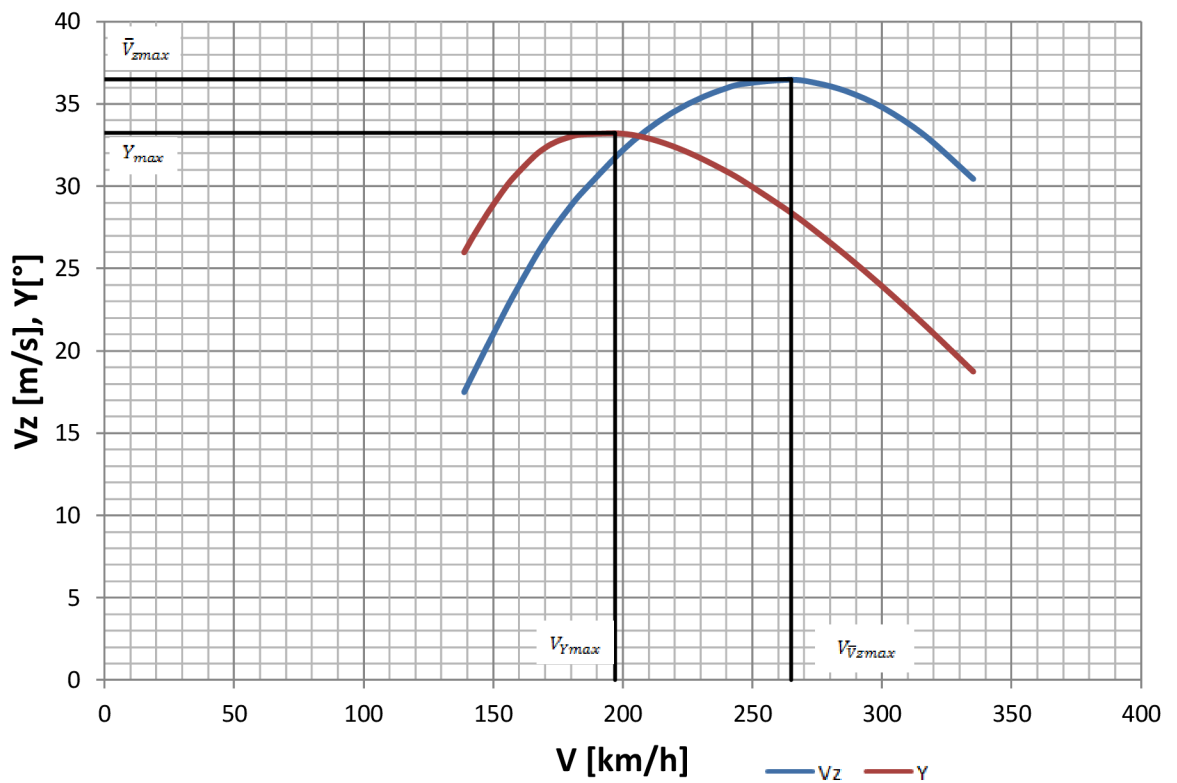
Figure 6.3: Angle of climb and climbing speed depending on speed

The values for maximum climbing speed and maximum angle of climb can be obtained from Figure 6.3:

Maximum climbing speed: $\bar{V}_{zmax} = 36.5 m/s$ at $V_{\bar{V}zmax} = 265 km/h$
Maximum angle of climb: $Y_{max} = 33.25°$ at $V_{Ymax} = 197 km/h$

6.3 Speed polar

Speed polar shows the dependence of aircraft's descent on speed.

Descent speed may be estimated from:

$$V_z = \frac{c_D}{c_L^{3/2}} \cdot \sqrt{\frac{2 \cdot m_{TOW} \cdot g}{\rho_0 \cdot S}}$$

(6.4)

Lift-to-drag ratio:

$$K = \frac{c_L}{c_D}$$

(6.5)
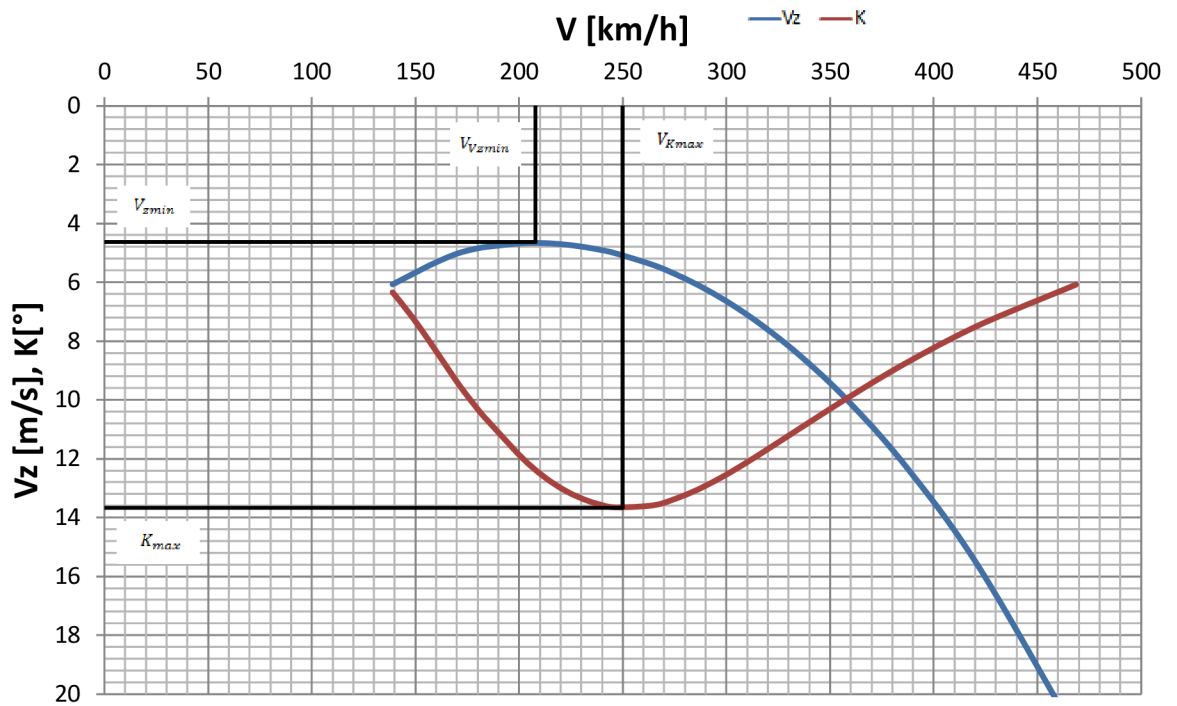
Figure 6.4: Lift-to-drag ratio and descent speed depending on speed in pure configuration

The values for maximum lift-to-drag ratio and minimal descent speed can be obtained from Figure 6.4:

Minimal descent speed: $V_{min} = 4.65 m/s$ at $V_{Vmin} = 208 km/h$

Maximum lift-to-drag ratio: $K_{max} = 13.66$ at $V_{Kmax} = 250 km/h$

Another speed polar was calculated for stopped engines, where the thrust is equal to zero.
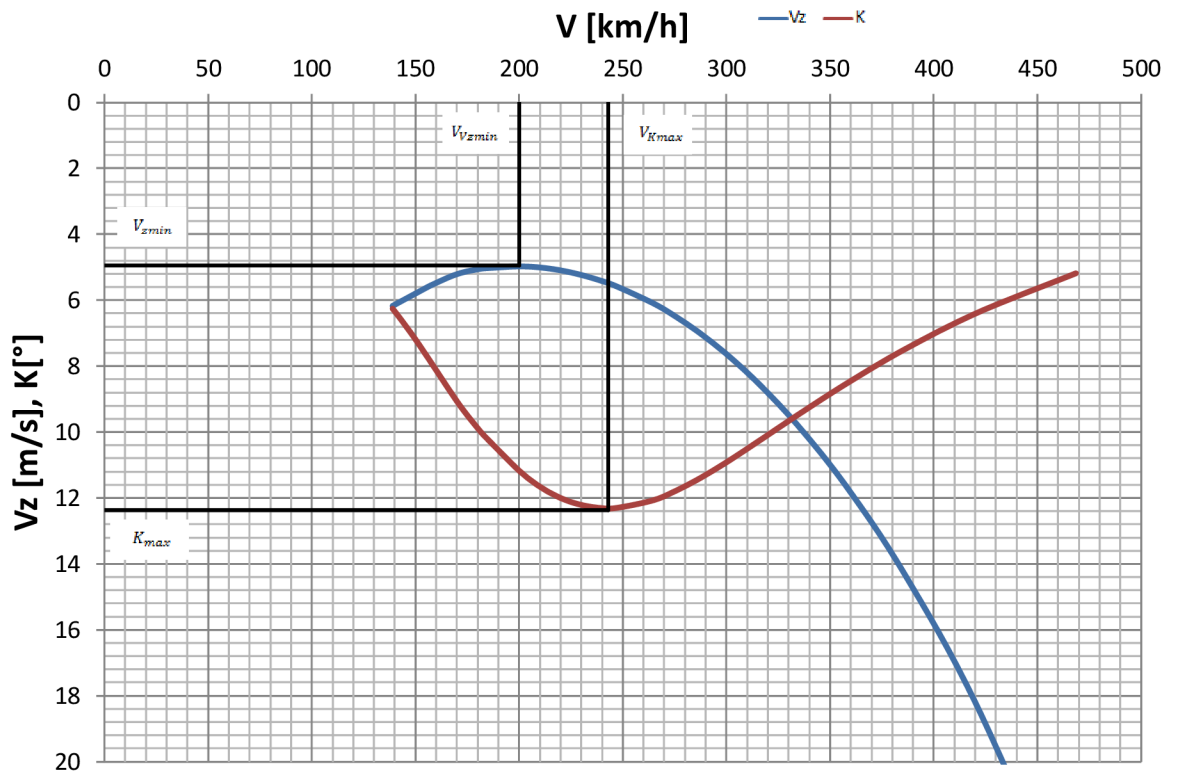
Figure 6.5: Lift-to-drag ratio and descent speed depending on speed with stopped engines

The values for maximum lift-to-drag ratio and minimal descent speed can be obtained from Figure 6.5:

Minimal descent speed: $V_{min} = 4.95 m/s$ at $V_{Vmin} = 200 km/h$
Maximum lift-to-drag ratio: $K_{max} = 12.36$ at $V_{Kmax} = 243 km/h$

6.4 Take-off

The take-off length is calculated for aircraft, which weight is equal to m_{TOW} and drag and lift coefficients, c_{Dopt} and c_{Lopt}, are taken from polar Figure 6.6. The friction coefficient is taken from [3] and for dry asphalt is $f = 0.05$.
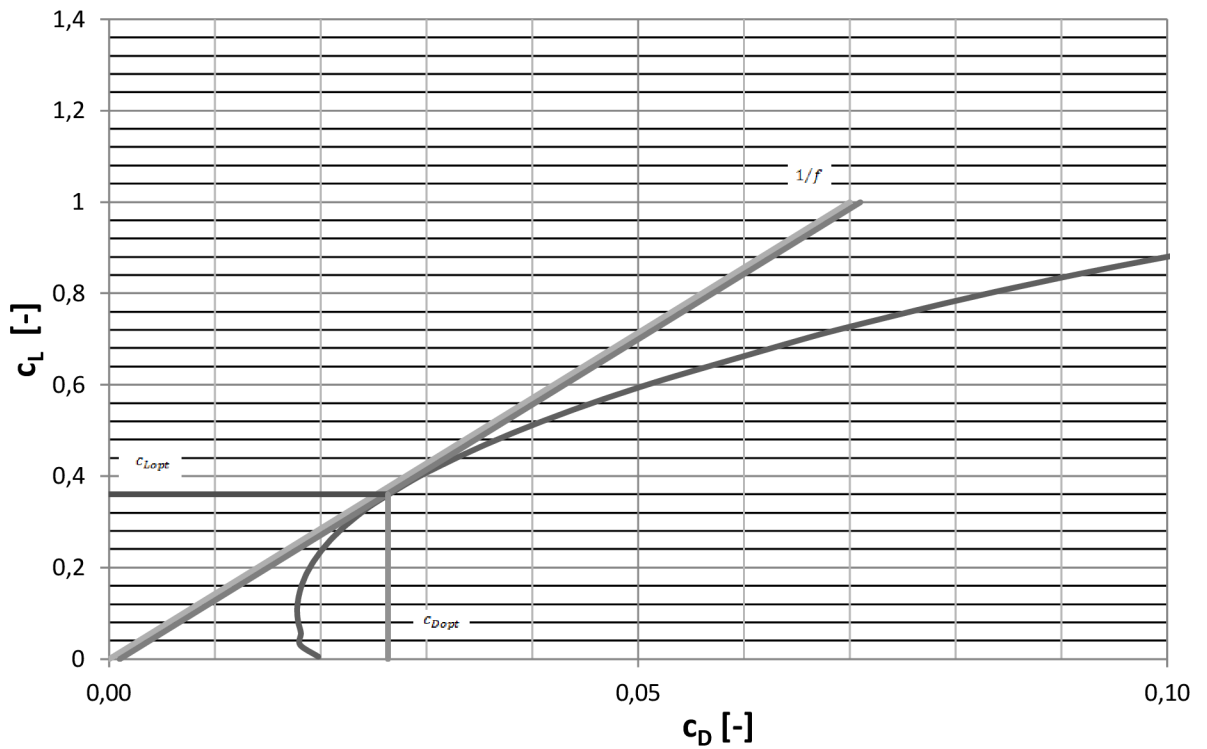
Figure 6.6: Drag and lift coefficient determined from aircraft's drag polar

Start length:

$$l_1 = \int_0^{l_v} dx = \int_0^{V_{LOF}} \frac{V \, dV}{a_{xa}} \tag{6.6}$$

where

acceleration is:

$$a_{xa} = g \cdot \left[\frac{F}{G} - f - \left(c_{dopt} - f \cdot c_{Lopt} \right) \cdot \frac{\rho \cdot V^2}{2 \frac{G}{S}} \right] \tag{6.7}$$

c_{Dopt} is optimal drag coefficient: $\qquad c_{Dopt} = 0.0264$

c_{Lopt} is optimal lift coefficient: $\qquad c_{Lopt} = 0.36$

f is friction coefficient for dry asphalt: $\qquad f = 0.05$

g is gravitational acceleration: $\qquad g = 9.80665 m \cdot s^{-2}$

ρ_o is air density at 0m ISA: $\qquad \rho_o = 1.225 kg \cdot m^{-3}$

G is weight of the aircraft at maximum take-off weight:

$$G = m_{TOW} \cdot g = 11{,}503.2N$$

m_{TOW} is maximum take-off weight: $\qquad m_{TOW} = 1{,}173kg$

$\frac{G}{S}$ is wing loading: $\qquad \frac{G}{S} = \frac{11{,}503.2}{10.24} = 1.123.15N \cdot m^{-1}$

F is engine thrust

Calculation of the take-off velocity:

$$V_{LOF} = 1.1 \cdot V_{s2} = 36.11 m \cdot s^{-1} \qquad\qquad (6.8)$$

The final length for land part of taking-off: $\quad l_1 = 174.75m$

For calculation of air part of taking-off it is necessary to know air speed:

$$V_2 = 1.2 \cdot V_{s2} = 39.39 m \cdot s^{-1} \qquad\qquad (6.9)$$

Mean value of excess thrust:

$$(F - D)_{mean} = \frac{(F-D)_{V2} \cdot (F-D)_{Vlof}}{2} = 3{,}346.3N \qquad\qquad (6.10)$$

The final length for air part of taking-off:

$$l_2 = \frac{G}{(F-D)_{mean}} \cdot \left[\frac{V_2^2 - V_{LOF}^2}{2 \cdot g} + h_s \right] = \frac{1{,}173 \cdot 9.80665}{3{,}346.3} \cdot \left[\frac{39.39^2 \cdot 36.11^2}{2 \cdot 9.80665} + 15 \right] = 95.01m \qquad (6.11)$$

Final taking-off length: $\qquad l = l_1 + l_2 = 174.75 + 95.01 = 269.76m \qquad (6.12)$

$$l = 270m$$

6.5 Range, endurance

To calculate range it is need to know specific fuel consumption SFC, and thus the maximum range distant is calculated for maximum value of $c_L^{1/2}/c_D$. The classical way uses constant SFC, but in this case it is not considered.

Range calculation:

$$R = \frac{2}{SFC} \cdot \sqrt{\frac{2 \cdot m_1}{g \cdot \rho_0 \cdot S}} \cdot \left(\frac{c_L^{\frac{1}{2}}}{c_D} \right) \cdot (\sqrt{m_1} - \sqrt{m_2}) \qquad (6.13)$$

Endurance calculation:

$$T = \frac{1}{g \cdot SFC} \cdot \left(\frac{c_L}{c_D} \right) \cdot \frac{1}{m_1 - m_2} \qquad (6.14)$$

m_1 is aircraft's weight at the beginning (m_{TOW} minus fuel consummated during taxiing and take-off): $\qquad m_1 = 1{,}163kg$

m_2 is aircraft's ending weight: $\qquad m_2 = 998kg$

g is gravitational acceleration: $\qquad g = 9.80665m \cdot s^{-2}$

ρ_o is air density at 0m ISA: $\qquad \rho_o = 1.225kg \cdot m^{-3}$

SFC is specific fuel consumption.
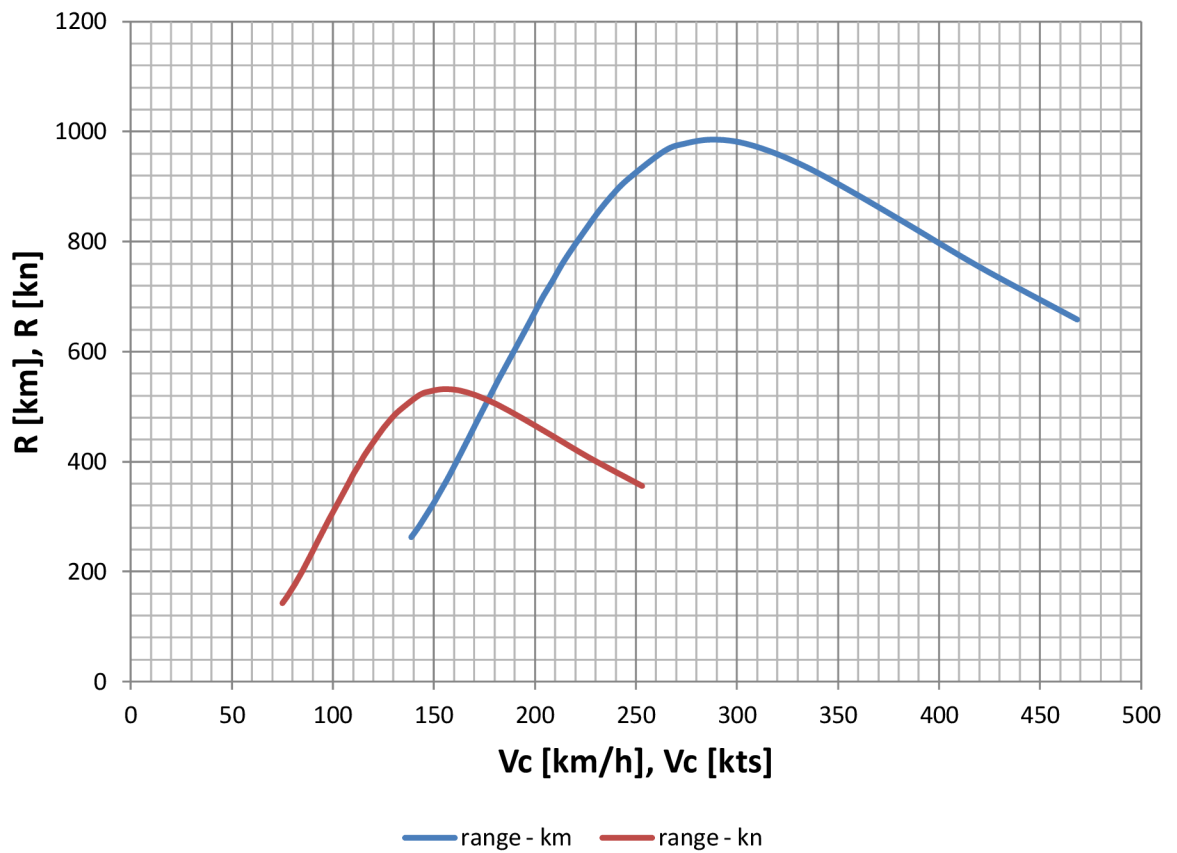
Figure 6.7: Estimated range, both in kilometers and nautical miles

Figure 6.7 shows the range diagram both in metric and imperial units, and it is possible to estimated maximal range.

Maximal range: $R_{max} = 985km$ at $V_{crmax} = 287km/h$ or

$R_{max} = 532nm$ at $V_{crmax} = 155kts$
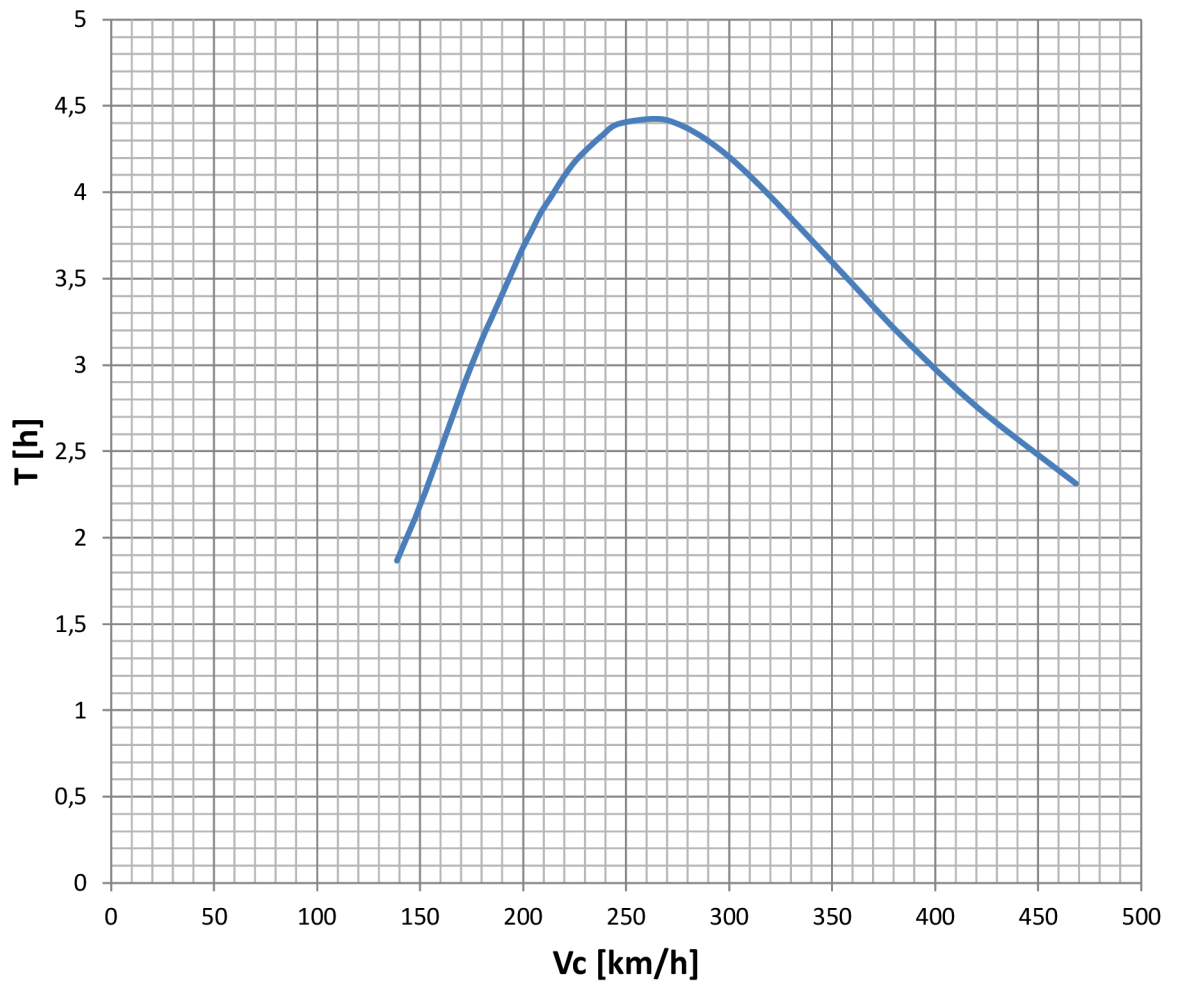
Figure 6.8: Estimated endurance

Figure 6.8 shows the endurance diagram and it is possible to estimated maximal range.

Maximal endurance: $T_{max} = 4.42h$ at $V_{crmax} = 264km/h$

All tables with values used are in Appendix 3.

7 FLIGHT ENVELOPE

The flight envelope is a useful source of information for strength design. It encloses all possible combinations of load and velocity, which can occur during aircraft's lifetime. Background for all calculation is taken from CS-23 regulations.

Design maneuvering speed:

$$v_A = v_{S1} \cdot \sqrt{n_1} \qquad (7.1)$$

v_{S1} is stall speed: $\qquad v_{S1} = 31.40 m/s$

n_1 is load factor: $\qquad n_1 = 3.6$

$$v_A = 72.89\, m/s = 262 km/h$$

Design maneuvering speed:

$$v_G = v_{S1} \cdot \sqrt{|n_1|} \qquad (7.2)$$

v_{S3} is stall speed: $\qquad v_{S3} = 34.96 m/s$

n_1 is load factor: $\qquad n_1 = -1.5$

$$v_G = 42.82\, m/s = 154 km/h$$

Maximum flap extended speed:

$$v_F \geq 1.4 \cdot v_{S1} \qquad (7.3)$$

or

$$v_F \geq 1.8 \cdot v_{S0} \qquad (7.4)$$

v_{S0} is stall speed in landing configuration:

$$v_{S0} = 29.86 m/s$$

then

$$v_F = 1.4 \cdot 31.40 = 52.35 m/s \text{ or } v_F = 1.8 \cdot 29.86 = 53.75 m/s$$

The higher value was chosen: $\qquad v_F = 53.75 \, m/s = 194 km/h$

Design diving speed:

$$v_D \geq 1.2 \cdot v_H \qquad\qquad (7.5)$$

v_H is maximum speed in level flight at maximum continuous power:

$$v_H = 121.39 m/s$$

$$v_D \geq 1.2 \cdot 121.39 = 151.74 \, m/s = 546 km/h$$

Load factor table

Table 7.1: Load factor table

n_1	+3.8
n_2	+3.8
n_3	-1.5
n_4	-1.5

Gust loads:

$$n = 1 \pm \frac{0.5 \cdot \rho \cdot v \cdot k \cdot U_{de} \cdot a}{\frac{m \cdot g}{S}} \qquad\qquad (7.6)$$

$$k = \frac{0.88 \cdot \mu}{5.3 + \mu} \qquad\qquad (7.7)$$

$$\mu = \frac{2 \cdot \frac{m}{S}}{\rho \cdot mgc \cdot a} = \frac{2 \cdot \frac{1,173}{10.24}}{1.225 \cdot 1.36558 \cdot 4.8083} = 28.4775 \qquad\qquad (7.8)$$

$$k = \frac{0.88 \cdot \mu}{5.3 + \mu} = \frac{0.88 \cdot 28.4775}{5.3 + 28.4775} = 0.74192 \qquad\qquad (7.9)$$

Table 7.2: Loads table

velocity	v	n	U	n − gust
	[m/s]	[-]	[m/s]	[-]
v_A	72.89	3.8	15.24	3.16
v_G	42.82	-1.5	-15.24	-0.27
v_{D+}	151.74	3.8	7.62	3.25
v_{D-}	151.74	-1.5	7.62	-1.25
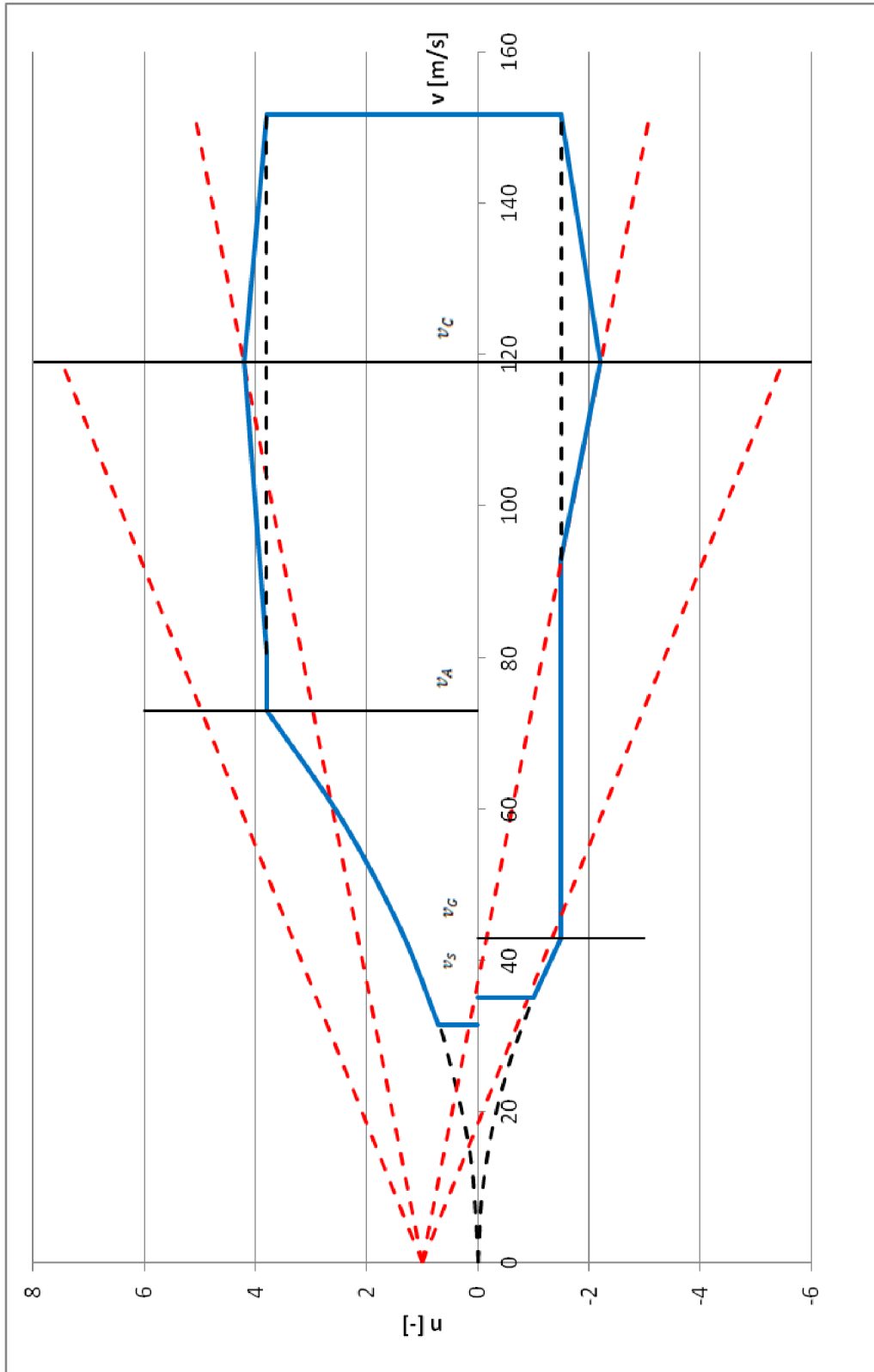
Figure 7.1: Flight envelope

8 CONCEPTUAL DESIGN OF MAIN AIRCRAFT'S PARTS

As part of new design, it is good to present basic referential models.

8.1 Aircraft's model

Aircraft's model represent basic configuration of inner structure. Only the main parts are represented here: fuselage, wing and vertical tail. Engine and engine pod, and canards are not in this draft mentioned.
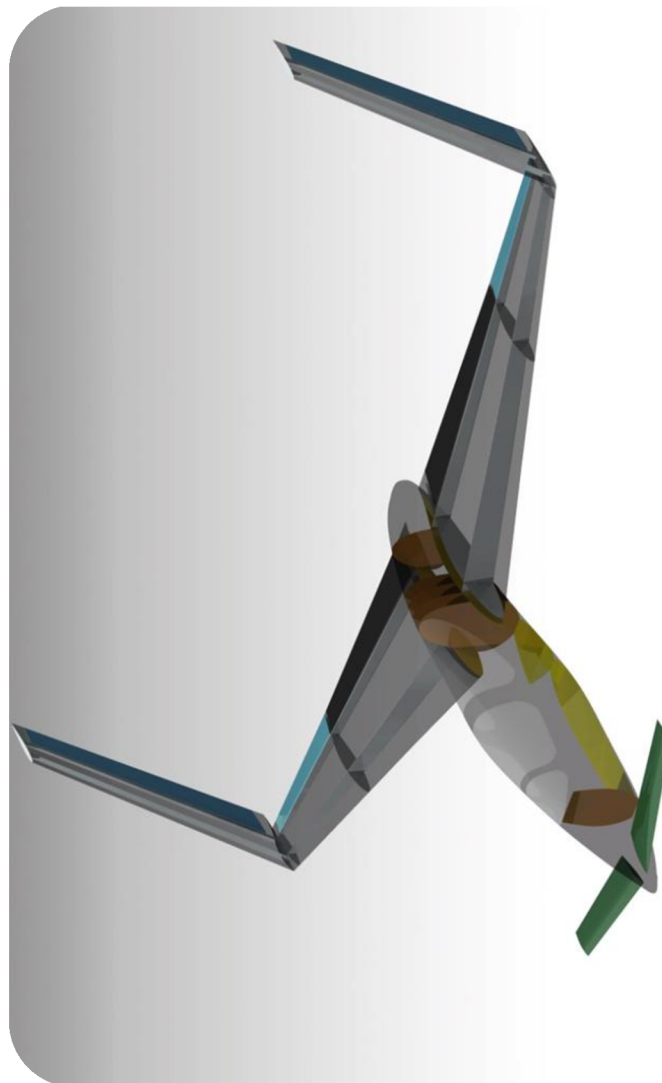
Figure 8.1: Aircraft's reference model

8.2 Wing design

Wing is consisted from two spars and four ribs. Space between main spar and rear spar is in the inner part of the wing filled with landing gear mechanism. Also between leading edge and main spar is placed fuel. The other fuel tanks are placed in space around main landing gear.

Figure 8.2: Wing's referential model

8.3 Vertical tail design

Vertical tail consists from two main ribs and two spars. Stabilizer is connected to the rear spar.
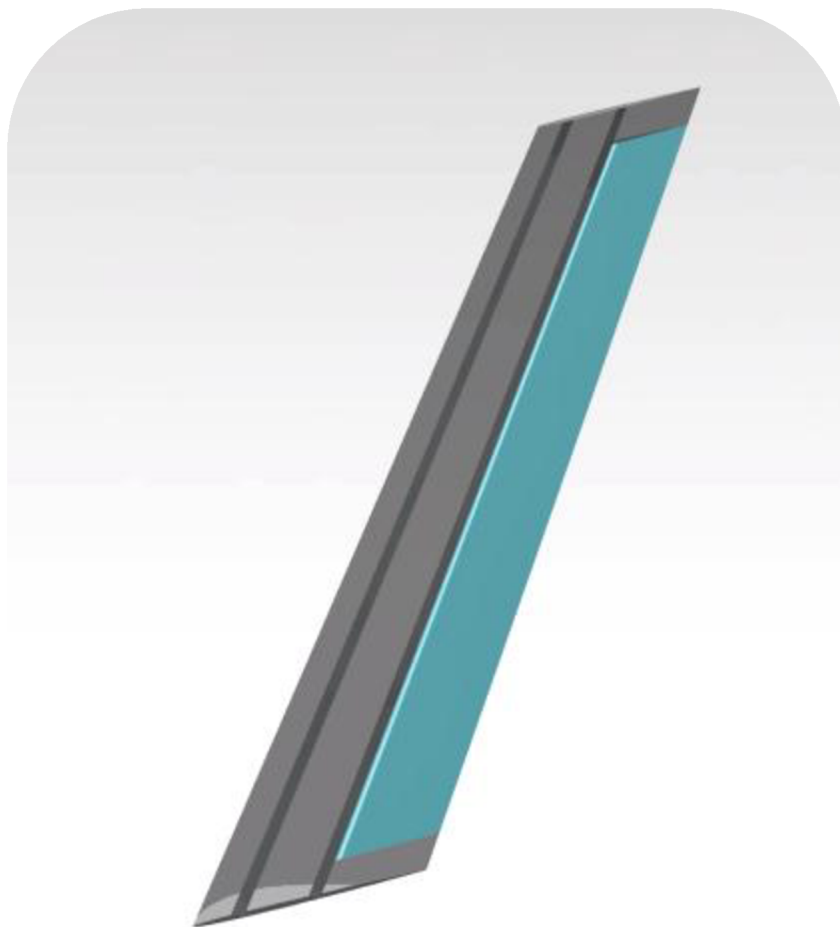
Figure 8.3: Vertical stabilizer's referential model

8.4 Fuselage design

In the fuselage pre-design is visible system of ribs which should provide enough support to all parts connected to them. The first one behind cockpit is working also as fire protection. Area behind cockpit, where the wing and engine are connected is strengthened with ribs. Floor is divided in two parts, where the bigger one is mostly in cockpit, and the second part works as baggage space floor.
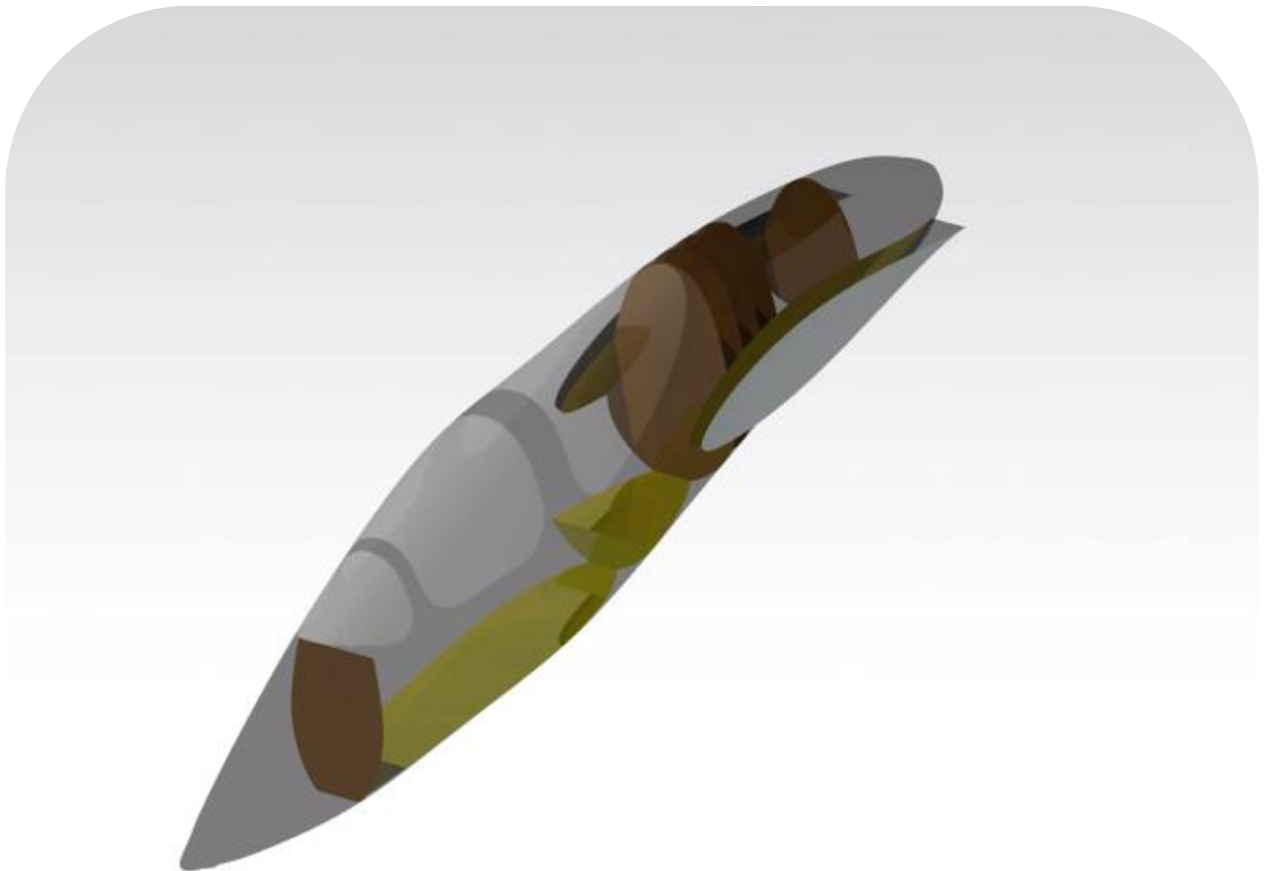
Figure 8.4: Fuselage's referential model

9 DETERMINATION AND ANALYSIS OF DEVELOPMENT COSTS

For costs analysis combination of the literatures [3, 6] was used. For determining it certain preconditions must be met. At first all the calculations are based on cost in 1970's constant dollars, thus in this case inflation is not added.

9.1 Development support

Development support is defined as the nonrecurring manufacturing effort undertaken in support of engineering during DT&E phase of an aircraft program. The cost of the development support is the cost of manufacturing labor and material required to produce mock-ups, test parts, static test items, and other items of hardware that are needed for airframe design and development work.

$$D = 0.008325 \cdot A^{0.873} \cdot V_H^{1.89} \cdot Q_D^{0.346} \tag{9.1}$$

where

A is airframe weight in pounds: $\qquad\qquad A = 1109 lbs$

V_H is maximum speed in knots: $\qquad\qquad V_H = 66 kts$

Q_D is development quantity (number of flight test aircraft): $\qquad Q_D = 2$

9.2 Flight test operations

The flight test operation cost element includes all costs incurred by the aircraft builder to carry out flights tests except the cost of the flight test aircraft. It includes flight test engineering planning and data reduction, manufacturing support, instrumentation, spares, fuel and oil, pilot's pay, facilities rental and insurance. The flight test established the operating envelope of the aircraft, its flying and handling qualities, general airworthiness, initial maintainability features and compatibility with ground support equipment.

$$F = 0.001244 \cdot A^{1.16} \cdot V_H^{1.371} \cdot Q_D^{1.281} \tag{9.2}$$

9.3 Tooling

Tools are the jigs, fixtures, dies, and special equipment used in the fabrication of an aircraft. Tooling hours are defined as the hours charged for tool design, tool planning, tool fabrication, production test equipment, checkout of tools, and maintenance of tooling, normal changes and production planning.

$$T = 4.0127 \cdot A^{0.764} \cdot V_H^{0.899} \cdot Q^{0.178} \cdot R^{0.066} \tag{9.3}$$

where

R is production rate (deliveries per month): $\qquad R = 4$

Q is cumulative quantity: $\qquad Q = Q_D + Q_P$

Q_P is production quantity (number of production aircraft)

Tooling hours are determined between engineers and labors. This determination's balance ratio is 20% engineer's work and 80% labor work.

Therefore:

$$T_E = 0.2 \cdot T \tag{9.4}$$

$$T_L = 0.8 \cdot T \tag{9.5}$$

The costs for engineers and labors for tooling are:

$$T_{Ec} = E_h \cdot T_E \tag{9.6}$$

$$T_{Lc} = L_h \cdot T_L \tag{9.7}$$

where

E_h is engineer's salary: $\qquad E_h = 25 USD/hr$

L_h is labor's salary: $\qquad L_h = 15 USD/hr$

9.4 Manufacturing labor

Manufacturing labor hours include those hours necessary to machine, process, fabricate, and assemble the major structure of an aircraft, and to install purchased parts, government furnished equipment and off-site manufactured assemblies.

$$L = 28.984 \cdot A^{0.74} \cdot V_H^{0.543} \cdot Q^{0.524} \tag{9.8}$$

The cost for the manufacturing is:

$$L_c = L_h \cdot L \tag{9.9}$$

9.5 Quality control

Quality control is the task of inspecting fabricated and purchased parts, subassemblies and assembled items against material and process standards, drawing and/or specifications. Quality control is an extremely important activity in the manufacture of aircraft because of their complexity.

$$QC = 0.13 \cdot L \tag{9.10}$$

The cost for the manufacturing is:

$$QC_c = E_h \cdot QC \tag{9.11}$$

9.6 Manufacturing material and equipment

The material and equipment includes the raw material, hardware and purchased parts required for the fabrication and assembly of the airframe.

$$M = 25.672 \cdot A^{0.689} \cdot V_H^{0.624} \cdot Q^{0.792} \tag{9.12}$$

9.7 Engine and avionics costs

The engine production cost is considered.

$$P = P_E \cdot n \cdot Q \tag{9.13}$$

where

P_E is engine price: $\qquad\qquad P_E = 100{,}000 USD$

n is number of engines: $\qquad\quad n = 2$

9.8 Airframe engineering hours and costs

The engineering activities involved in the DT&E are e.g.: design studies and integration, engineering for wind tunnel models, mock-ups and engine tests, test engineering, laboratory work on subsystems and static test items, development testing and so on.

$$E = 0.0396 \cdot A^{0.791} \cdot V_H^{1.526} \cdot Q^{0.183} \tag{9.14}$$

where

Q is for development number of prototypes, and for production number of prototyped + number of production aircraft

Thus developing hours can be estimated from:

$$E_d = 0.0396 \cdot A^{0.791} \cdot V_H^{1.526} \cdot Q^{0.183} \tag{9.15}$$

And production hours can be estimated from:

$$E_p = 0.0396 \cdot A^{0.791} \cdot V_H^{1.526} \cdot (Q_D + Q_P)^{0.183} \tag{9.16}$$

The costs of engineers for developing hours are:

$$E_{dc} = E_h \cdot E_d \tag{9.17}$$

The costs of engineers for production hours are:

$$E_{pc} = E_h \cdot E_p \tag{9.18}$$

9.9 Overall costs

For sustainable business plan, let us assume we are able to produce 4 aircrafts per month. Then we can split our goal to build 50, 100, 150, and 200 aircraft in series. This prediction will give some data to work with and see what goal we can reach. Margin added to cost of one piece is 10 per cent.

Table 9.1: Costs table

the number of planned aircraft	QP	pcs	50	100	150	200
overall costs	TC	USD	35 632 516	54 436 506	71 391 724	87 379 102
costs for 1 piece	PC	USD	712 650	544 365	475 945	436 896
cost for 1 piece + margin	PC	USD	783 915	598 802	523 539	480 585

Table 9.1 shows how the price for one plane drops with increasing amount of produced aircrafts. The difference between price for 50 pieces and 200 is 63% (almost 303,330USD).
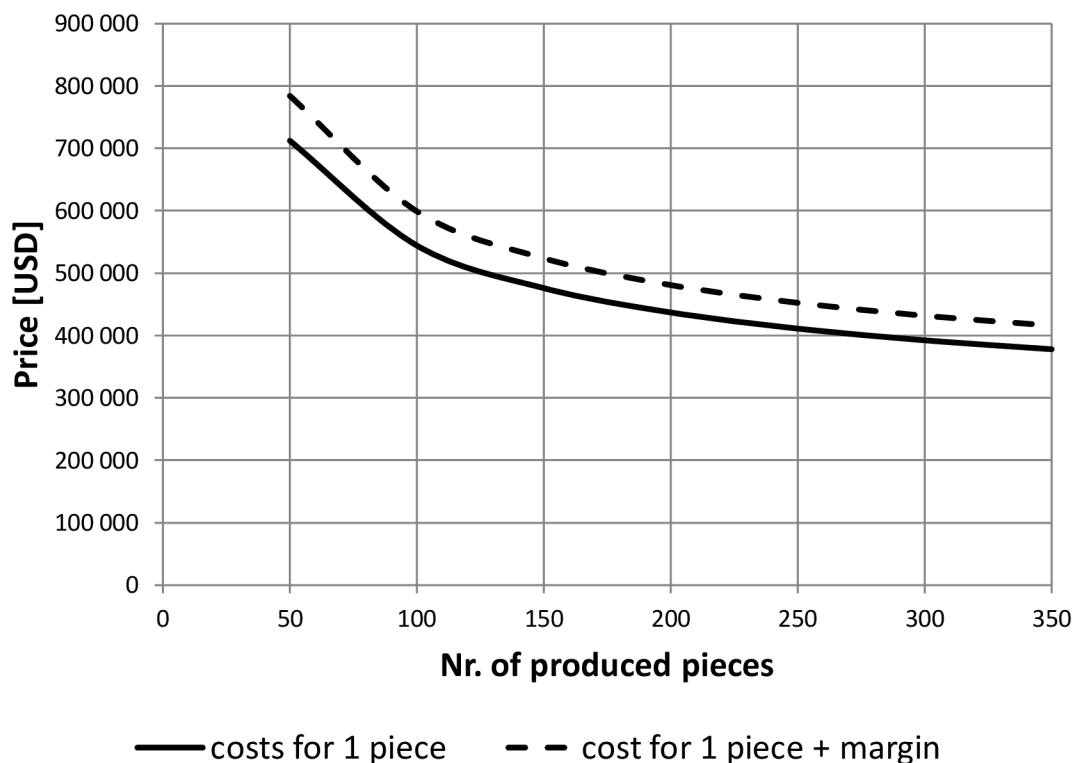
Figure 9.1 Average price of aircraft

Next step is to show how it affect company's budget. One of the assumptions is that the development will take at least five year without any major income from selling aircrafts. After that the company will profit from selling their product.
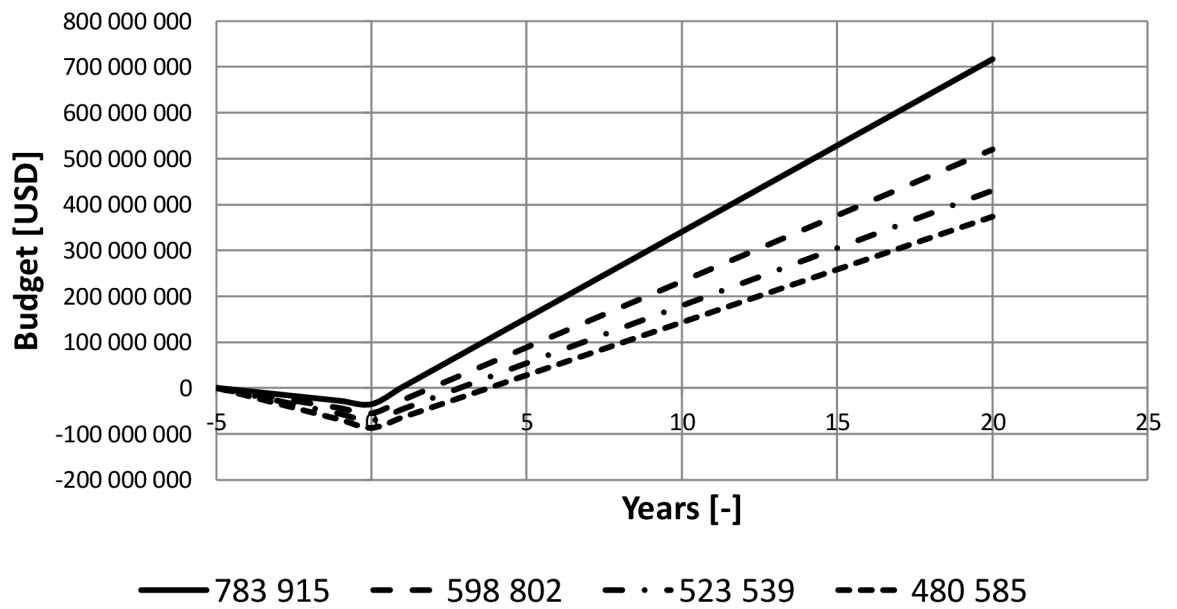
Figure 9.2: Course of loss and profits

All the tables with data are in Appendix 4.

10 CONCLUSION

The main goal of the thesis was to calculate basic mass and aerodynamics characteristics, design main parts and do cost analysis.

In the theoretical part are showed current very light jet aircrafts and their used engines and also their comparison. As it is possible to see there, the market is growing and new aircrafts in this category are producing. Crucial for this design was engine choosing. The French DGEN 380 was chosen, because for small plane like this looks like the best option.

In the practical part are at first calculated basic wing aerodynamics characteristics, which are necessary for other calculations. Next step was to calculate mass distribution over the plane. Due its canard design there were some issues with proper placement of centre of gravity andsubsequent positions of front and rear limits of static margin. Values are higher than in typical aircraft construction design, therefore it should be verified before further steps. The drag polar came next and it is calculate from simple airfoil to the wing in the landing configuration. There is important to say, that aircraft does not need flaps for taking-off, but for landing it must be pulled down to 60° due to the comply with the CS-23 regulation for maximal landing speed. One of the most important parts is performance characteristics. Engines with thrust at 71% were presumed. This give us some interesting values which none of the competitors can fulfill, e.g. rate of climb. The take-off distance is impressively short, but it is done due to the powerful engines. I have to mention that the cause of the failure of one engine was not calculated. From these calculations was created the flight envelope. The last two steps were to design main parts of the aircraft and then calculate development costs for whole process.

11 REFERENCES

[1]: EASA, CS-23 Normal, Utility, Aerobatic and Commuter Aeroplanes, CS-23/ Initial issue

[2]: Jackson, Paul. Jane's: All the World's Aircraft 2004-2005. Coulsdon: Jane's Information Group Limited, 2004. ISBN 0710626142

[3]: Raymer, Daniel P. Aircraft design : a conceptual approach. Third edition. Reston, Virginia: AIAA, 1999. ISBN 1-56347-281-0

[4]: Torenbeek, Egbert. Synthesis of Subsonic Airplane Design. Delft: Delft University Press, 1982. ISBN 90-247-2724-3

[5]: Roskam, Jan. Airplane design: Preliminary calculation of aerodynamic, thrust and power characteristics. Lawrence, Kansas: The University of Kansas. 1987

[6]: Nicolai, Leland and Carichner, Grant. Fundamentals of Aircaft and Airship Design. AIAA. 2010. ISBN 978-1600867514

[7]: Daněk, Vladimír. Projektování letadel. Brno: Nakladatelství VUT Brno. 1991. ISBN 80-214-0373-X

[8]: Daněk, Vladimír. Mechanika letu I: Letové výkony. První vydání. Brno: Nakladatelství VUT Brno. 1994. ISBN 80-214-0476-0

[9]: Daněk, Vladimír. Mechanika letu II: Letové vlastnosti. První vydání. Brno: Nakladatelství VUT Brno. 2011. ISBN 978-80-7204-761-1

[10]: Florián, J. Aerodynamické charakteristiky letounu I.; [s.l.]: VAAZ, 1963

[11]: National Business Aviation Association [online]. [cit. 2015-2-10] Available from: http://www.nbaa.org/ops/safety/vlj/

[12]: Price Induction [online]. [cit. 2014-3-20] Available from: http://www.price-induction.com/

[13]: Price Induction [online]. [cit. 2015-4-17] Available from: http://www.price-induction.com/

[14]: Cirrus Aircraft [online]. [cit. 2015-3-22] Available from: http://cirrusaircraft.com/aircraft/vision-sf50/

[15]: Flaris [online]. [cit. 2015-3-22] Available from: http://www.flaris.pl/

[16]: Diamond Aircraft [online]. [cit. 2015-3-22] Available from:
http://www.diamondaircraft.com/aircraft/djet/

[17]: Aircraft Compare [online]. [cit. 2015-3-22] Available from:
http://www.aircraftcompare.com/aircraft-specification/Epic-Victory/340/spec

[18]: Sport Jet [online]. [cit. 2015-3-22] Available from: http://sportjetair.com/

[19]: Stratos [online]. [cit. 2015-3-22] Available from: http://www.stratosaircraft.com/

[20]: Kewljets [online]. [cit. 2015-3-22] Available from:
http://www.kewljets.com/Jet/Adam-A700

[21]: One Aviation [online]. [cit. 2015-3-22] Available from:
http://oneaviation.aero/eclipse/

[22]: HondaJet [online]. [cit. 2015-3-22] Available from: http://www.hondajet.com/

[23]: Textron Aviation [online]. [cit. 2015-3-22] Available from:
http://cessna.txtav.com/en/citation/mustang

[24]: Embraer [online]. [cit. 2015-3-22] Available from:
http://www.embraerexecutivejets.com/en-us/jets/phenom-
100e/pages/overview.aspx

[25]: Minijets [online]. [cit. 2015-3-19] Available from:
http://www.minijets.org/index.php?id=19

[26]: Pratt&Whitney [online]. [cit. 2015-3-21] Available from:
http://www.pwc.ca/en/engines/pw600

[27]: GE Honda [online]. [cit. 2015-3-21] Available from:
http://gehonda.com/engine/explore.html

[28]: Willams [online]. [cit. 2015-3-21] Available from: http://www.williams-
int.com/products

[29]: Richard Ferriere [online]. [cit. 2015-4-5] Available from:
http://richard.ferriere.free.fr/

[30]: Forum Valka [online]. [cit. 2015-4-5] Available from:
http://forum.valka.cz/topic/view/1231/Northrop-Grumman-B-2A-Spirit

12 LIST OF APPENDIXES

Appendix 1 – The center of gravity drawing

Appendix 2 – Drag polar calculation

Appendix 3 – Performance calculations

Appendix 4 – Costs calculation

Appendix 5 – 3 view drawing

APPENDIX 1

The center of gravity drawing
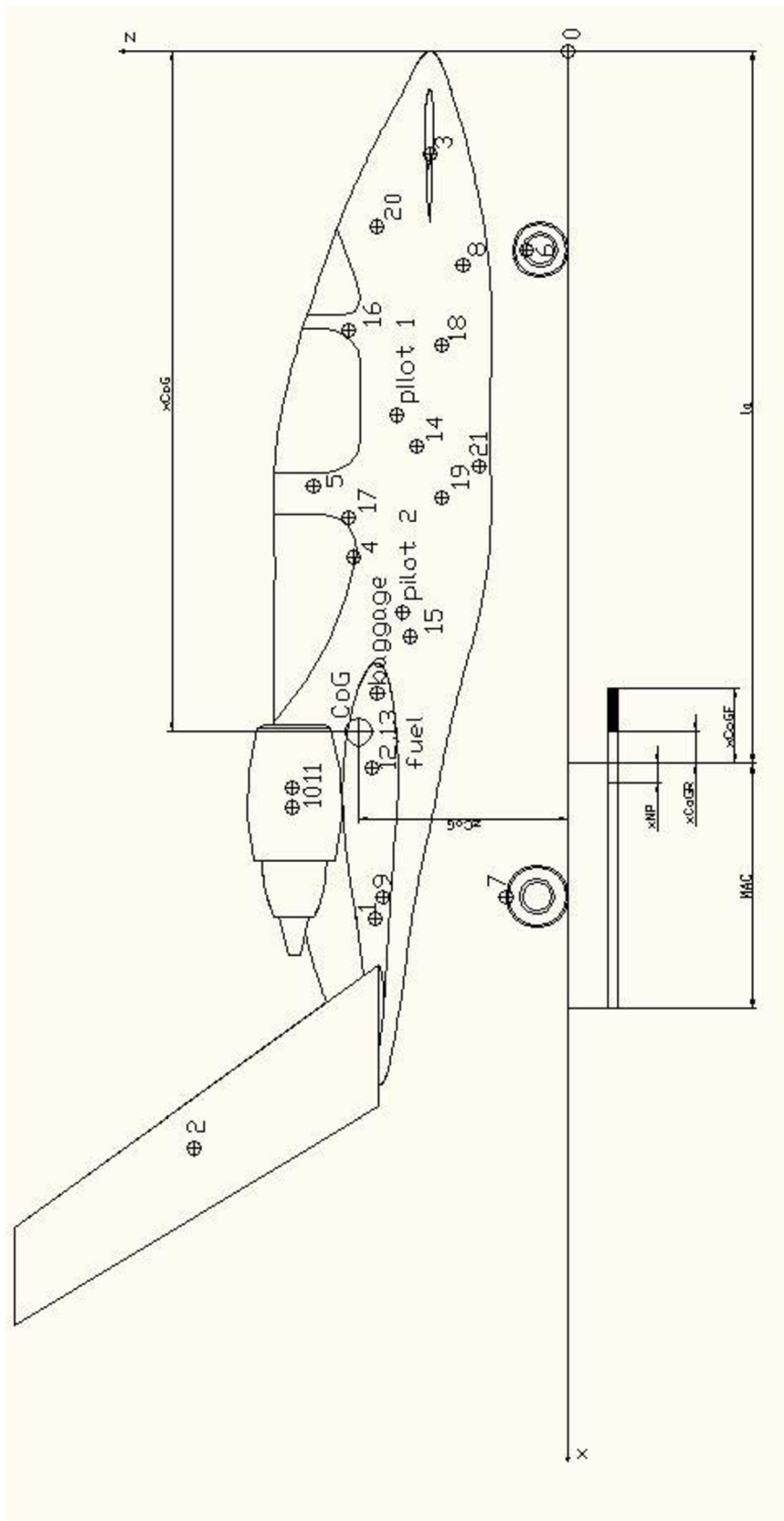
Figure 12.1: Center of gravity drawing

APPENDIX 2

Drag polar calculation

Figure 12.2: Wing polar
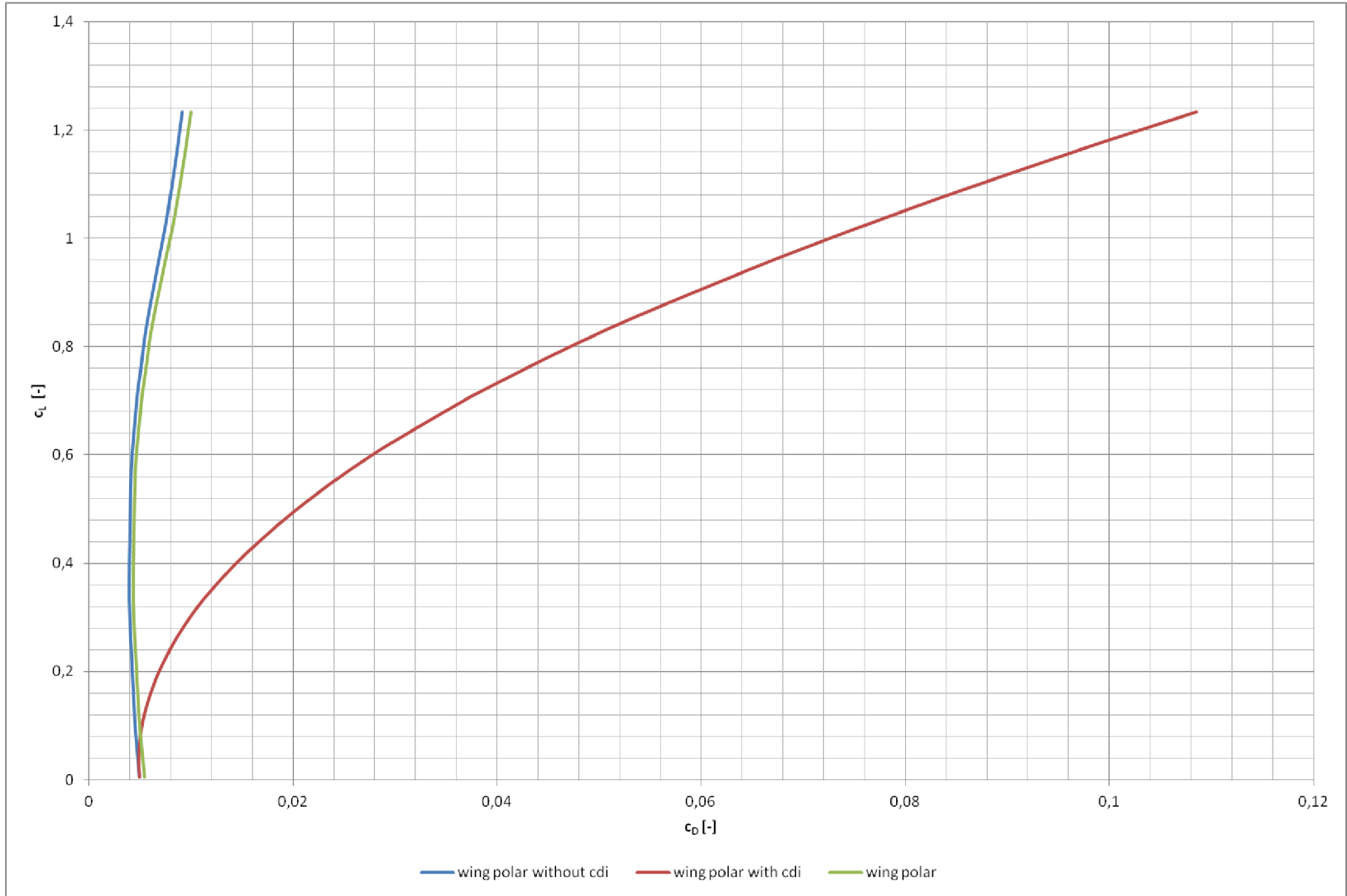
Table 12.1: Drag polar calculation

c_L	c_{Dwing}	c_{Dfus}	c_{Demp}	c_{Dnac}	c_{Dpyl}	c_D
[-]	[-]	[-]	[-]	[-]	[-]	[-]
0,005223	0,004918	0,003839	0,004574	0,000981	0,002880	0,019768
0,030883	0,004863	0,003024	0,004509	0,000713	0,002369	0,018055
0,056702	0,004884	0,003487	0,004455	0,000783	0,001936	0,018121
0,082402	0,005005	0,003498	0,004410	0,000783	0,001582	0,017855
0,108262	0,005225	0,003500	0,004376	0,000783	0,001307	0,017768
0,134022	0,005571	0,003501	0,004351	0,000783	0,001108	0,017891
0,159822	0,005996	0,003501	0,004335	0,000783	0,000985	0,018177
0,185622	0,006508	0,003501	0,004328	0,000783	0,000931	0,018629
0,211481	0,007120	0,003501	0,004331	0,000783	0,000949	0,019261
0,237341	0,007809	0,003501	0,004343	0,000784	0,001045	0,020057
0,263160	0,008576	0,003501	0,004364	0,000784	0,001218	0,021020
0,288980	0,009454	0,003501	0,004396	0,000784	0,001469	0,022180
0,314799	0,010434	0,003501	0,004437	0,000784	0,001797	0,023530
0,340559	0,011506	0,003501	0,004488	0,000784	0,002203	0,025059
0,391839	0,013971	0,003501	0,004620	0,000784	0,003245	0,028698
0,417480	0,015352	0,003501	0,004700	0,000785	0,003886	0,030801
0,443120	0,016819	0,003501	0,004791	0,000785	0,004605	0,033077
0,468780	0,018362	0,003501	0,004891	0,000785	0,005396	0,035511
0,494480	0,020003	0,003501	0,004999	0,000785	0,006260	0,038125
0,520020	0,021721	0,003501	0,005117	0,000785	0,007196	0,040897
0,545520	0,023534	0,003501	0,005244	0,000785	0,008204	0,043845
0,571001	0,025433	0,003501	0,005382	0,000785	0,009296	0,046974
0,596162	0,027426	0,003501	0,005529	0,000786	0,010464	0,050283
0,620846	0,029496	0,003501	0,005684	0,000786	0,011693	0,053736
0,694879	0,036207	0,003501	0,006166	0,000786	0,015525	0,064763
0,719202	0,038591	0,003501	0,006328	0,000786	0,016813	0,068596
0,767152	0,043591	0,003501	0,006701	0,000786	0,019772	0,076929
0,791415	0,046217	0,003502	0,006908	0,000786	0,021412	0,081402
0,815556	0,048911	0,003502	0,007129	0,000787	0,023173	0,086078
0,862365	0,054466	0,003502	0,007605	0,000787	0,026954	0,095891
0,954457	0,066343	0,003502	0,008667	0,000787	0,035387	0,117263
1,000322	0,072681	0,003502	0,009248	0,000787	0,039996	0,128791
1,023174	0,075938	0,003502	0,009554	0,000787	0,042425	0,134783
1,046304	0,079275	0,003502	0,009866	0,000788	0,044906	0,140913
1,069574	0,082688	0,003502	0,010185	0,000788	0,047437	0,147176
1,092703	0,086154	0,003502	0,010505	0,000788	0,049982	0,153508
1,162635	0,097016	0,003502	0,011502	0,000788	0,057892	0,173277
1,186229	0,100801	0,003502	0,011845	0,000788	0,060619	0,180132
1,209583	0,104628	0,003502	0,012190	0,000788	0,063359	0,187045
1,232896	0,108521	0,003502	0,012532	0,000789	0,066070	0,193991

Table 12.2: Drag polar with stopped engines

c_L	c_{Dwing}	c_{Dfus}	c_{Demp}	c_{Dnac}	c_{Dpyl}	c_D
[-]	[-]	[-]	[-]	[-]	[-]	[-]
0,005223	0,004918	0,003839	0,008167	0,016334	0,032667	0,022040
0,030883	0,004863	0,003024	0,007352	0,014704	0,029409	0,020410
0,056702	0,004884	0,003487	0,007815	0,015629	0,031259	0,021335
0,082402	0,005005	0,003498	0,007826	0,015653	0,031306	0,021359
0,108262	0,005225	0,003500	0,007828	0,015657	0,031313	0,021363
0,134022	0,005571	0,003501	0,007829	0,015658	0,031315	0,021364
0,159822	0,005996	0,003501	0,007829	0,015658	0,031316	0,021364
0,185622	0,006508	0,003501	0,007829	0,015658	0,031316	0,021364
0,211481	0,007120	0,003501	0,007829	0,015658	0,031317	0,021364
0,237341	0,007809	0,003501	0,007829	0,015658	0,031317	0,021364
0,263160	0,008576	0,003501	0,007829	0,015658	0,031317	0,021364
0,288980	0,009454	0,003501	0,007829	0,015658	0,031317	0,021364
0,314799	0,010434	0,003501	0,007829	0,015658	0,031317	0,021364
0,340559	0,011506	0,003501	0,007829	0,015658	0,031317	0,021364
0,391839	0,013971	0,003501	0,007829	0,015658	0,031317	0,021364
0,417480	0,015352	0,003501	0,007829	0,015658	0,031317	0,021364
0,443120	0,016819	0,003501	0,007829	0,015658	0,031317	0,021364
0,468780	0,018362	0,003501	0,007829	0,015658	0,031317	0,021364
0,494480	0,020003	0,003501	0,007829	0,015658	0,031317	0,021364
0,520020	0,021721	0,003501	0,007829	0,015658	0,031317	0,021364
0,545520	0,023534	0,003501	0,007829	0,015658	0,031317	0,021364
0,571001	0,025433	0,003501	0,007829	0,015658	0,031317	0,021364
0,596162	0,027426	0,003501	0,007829	0,015659	0,031317	0,021365
0,620846	0,029496	0,003501	0,007829	0,015659	0,031317	0,021365
0,694879	0,036207	0,003501	0,007829	0,015659	0,031317	0,021365
0,719202	0,038591	0,003501	0,007829	0,015659	0,031317	0,021365
0,767152	0,043591	0,003501	0,007829	0,015659	0,031318	0,021365
0,791415	0,046217	0,003502	0,007829	0,015659	0,031318	0,021365
0,815556	0,048911	0,003502	0,007830	0,015659	0,031318	0,021365
0,862365	0,054466	0,003502	0,007830	0,015659	0,031318	0,021365
0,954457	0,066343	0,003502	0,007830	0,015659	0,031318	0,021365
1,000322	0,072681	0,003502	0,007830	0,015659	0,031319	0,021365
1,023174	0,075938	0,003502	0,007830	0,015659	0,031319	0,021365
1,046304	0,079275	0,003502	0,007830	0,015660	0,031319	0,021366
1,069574	0,082688	0,003502	0,007830	0,015660	0,031320	0,021366
1,092703	0,086154	0,003502	0,007830	0,015660	0,031320	0,021366
1,162635	0,097016	0,003502	0,007830	0,015660	0,031320	0,021366
1,186229	0,100801	0,003502	0,007830	0,015660	0,031321	0,021366
1,209583	0,104628	0,003502	0,007830	0,015660	0,031321	0,021366
1,232896	0,108521	0,003502	0,007830	0,015661	0,031321	0,021367

Table 12. 3: Drag polar in landing configuration

| c_L	c_{Dwing}	c_{Dfus}	c_{Demp}	c_{Dnac}	c_{Dpyl}	c_{Dflap}	c_D
[-]	[-]	[-]	[-]	[-]	[-]	[-]	[-]
0,805223	0,042406	0,003839	0,004574	0,000981	0,002880	0,173126	0,230382
0,830883	0,045152	0,003024	0,004509	0,000713	0,002369	0,176109	0,234453
0,856702	0,048002	0,003487	0,004455	0,000783	0,001936	0,179206	0,240445
0,882402	0,050925	0,003498	0,004410	0,000783	0,001582	0,182382	0,246157
0,908262	0,053953	0,003500	0,004376	0,000783	0,001307	0,185673	0,252169
0,934022	0,057057	0,003501	0,004351	0,000783	0,001108	0,189045	0,258422
0,959822	0,060253	0,003501	0,004335	0,000783	0,000985	0,192518	0,264951
0,985622	0,063536	0,003501	0,004328	0,000783	0,000931	0,196085	0,271740
1,011481	0,066913	0,003501	0,004331	0,000783	0,000949	0,199755	0,278809
1,037341	0,070378	0,003501	0,004343	0,000784	0,001045	0,203520	0,286147
1,063160	0,073925	0,003501	0,004364	0,000784	0,001218	0,207374	0,293743
1,088980	0,077560	0,003501	0,004396	0,000784	0,001469	0,211323	0,301609
1,114799	0,081281	0,003501	0,004437	0,000784	0,001797	0,215367	0,309744
1,140559	0,085081	0,003501	0,004488	0,000784	0,002203	0,219495	0,318129
1,191839	0,092903	0,003501	0,004620	0,000784	0,003245	0,227995	0,335625
1,217480	0,096944	0,003501	0,004700	0,000785	0,003886	0,232385	0,344778
1,243120	0,101070	0,003501	0,004791	0,000785	0,004605	0,236869	0,354198
1,268780	0,105286	0,003501	0,004891	0,000785	0,005396	0,241449	0,363884
1,294480	0,109594	0,003501	0,004999	0,000785	0,006260	0,246131	0,373847
1,320020	0,113961	0,003501	0,005117	0,000785	0,007196	0,250876	0,384014
1,345520	0,118407	0,003501	0,005244	0,000785	0,008204	0,255707	0,394425
1,371001	0,122934	0,003501	0,005382	0,000785	0,009296	0,260626	0,405100
1,396162	0,127488	0,003501	0,005529	0,000786	0,010464	0,265574	0,415918
1,420846	0,132035	0,003501	0,005684	0,000786	0,011693	0,270515	0,426791
1,494879	0,146153	0,003501	0,006166	0,000786	0,015525	0,285855	0,460564
1,519202	0,150948	0,003501	0,006328	0,000786	0,016813	0,291065	0,472018
1,567152	0,160627	0,003501	0,006701	0,000786	0,019772	0,301582	0,495547
1,591415	0,165639	0,003502	0,006908	0,000786	0,021412	0,307029	0,507852
1,615556	0,170703	0,003502	0,007129	0,000787	0,023173	0,312530	0,520401
1,662365	0,180738	0,003502	0,007605	0,000787	0,026954	0,323434	0,545597
1,754457	0,201318	0,003502	0,008667	0,000787	0,035387	0,345796	0,598034
1,800322	0,211981	0,003502	0,009248	0,000787	0,039996	0,357383	0,625474
1,823174	0,217396	0,003502	0,009554	0,000787	0,042425	0,363267	0,639508
1,846304	0,222948	0,003502	0,009866	0,000788	0,044906	0,369299	0,653884
1,869574	0,228603	0,003502	0,010185	0,000788	0,047437	0,375444	0,668535
1,892703	0,234294	0,003502	0,010505	0,000788	0,049982	0,381628	0,683276
1,962635	0,251927	0,003502	0,011502	0,000788	0,057892	0,400788	0,728976
1,986229	0,258021	0,003502	0,011845	0,000788	0,060619	0,407409	0,744761
2,009583	0,264124	0,003502	0,012190	0,000788	0,063359	0,414041	0,760582
2,032896	0,270288	0,003502	0,012532	0,000789	0,066070	0,420738	0,776496
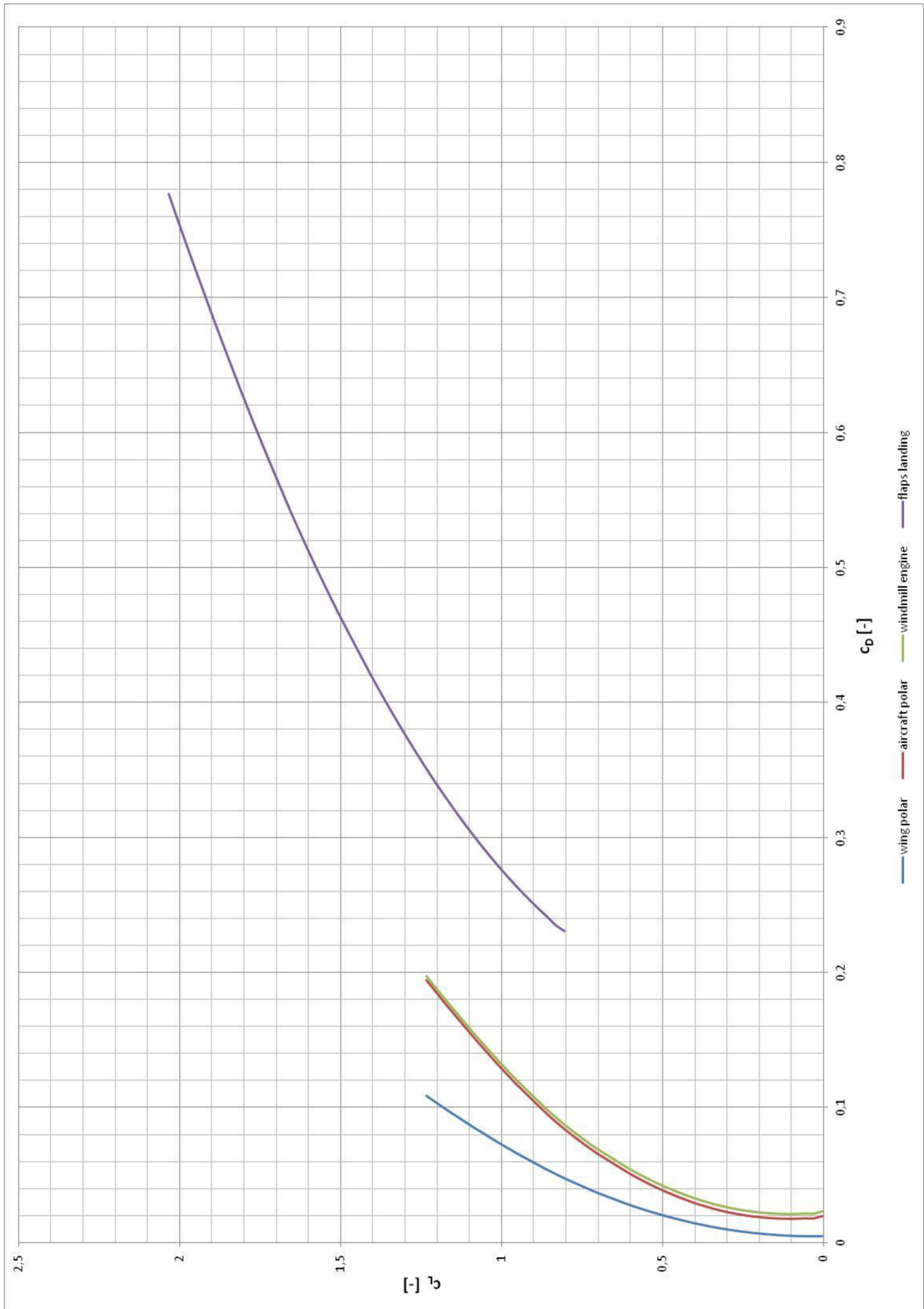
Figure 12.3: Aircraft drag polar

APPENDIX 3

Performance calculations

Table 12.4: Values for rate of climb and angle of climb calculation

c_L	c_D	v	v	D	F	P_p	P_v	ΔP	$\overline{V}_z$	Y
[-]	[-]	[m/s]	[km/h]	[N]	[N]	[kW]	[kW]	[kW]	[m/s]	[°]
0,13402	0,01789	116,97	421,10	1535,59	1770,34	179,62	207,08	27,46	8,59	4,21
0,15982	0,01818	107,11	385,61	1308,30	1893,76	140,14	202,85	62,71	19,63	10,50
0,18562	0,01863	99,39	357,81	1154,44	1999,23	114,74	198,71	83,97	26,28	15,15
0,21148	0,01926	93,12	335,22	1047,70	2091,96	97,56	194,80	97,24	30,43	18,72
0,23734	0,02006	87,90	316,43	972,12	2174,54	85,45	191,14	105,69	33,08	21,56
0,26316	0,02102	83,47	300,51	918,82	2248,74	76,70	187,71	111,02	34,74	23,85
0,28898	0,02218	79,66	286,77	882,92	2316,05	70,33	184,49	114,16	35,73	25,70
0,31480	0,02353	76,32	274,76	859,82	2377,49	65,62	181,46	115,83	36,25	27,21
0,34056	0,02506	73,38	264,16	846,42	2433,77	62,11	178,59	116,48	36,45	28,46
0,39184	0,02870	68,41	246,27	842,48	2533,35	57,63	173,30	115,67	36,20	30,32
0,41748	0,03080	66,27	238,59	848,68	2577,90	56,25	170,85	114,60	35,87	31,01
0,44312	0,03308	64,33	231,58	858,67	2619,48	55,24	168,51	113,27	35,45	31,57
0,46878	0,03551	62,54	225,16	871,39	2658,44	54,50	166,27	111,77	34,98	32,04
0,49448	0,03812	60,90	219,23	886,91	2695,06	54,01	164,12	110,11	34,46	32,42
0,52002	0,04090	59,38	213,78	904,68	2729,33	53,72	162,07	108,35	33,91	32,72
0,54552	0,04385	57,98	208,72	924,55	2761,61	53,60	160,11	106,51	33,33	32,94
0,57100	0,04697	56,67	204,01	946,32	2792,13	53,63	158,23	104,60	32,74	33,10
0,59616	0,05028	55,46	199,66	970,23	2820,70	53,81	156,44	102,63	32,12	33,18
0,62085	0,05374	54,35	195,65	995,64	2847,34	54,11	154,74	100,63	31,49	33,20
0,69488	0,06476	51,37	184,93	1072,10	2920,07	55,07	150,00	94,93	29,71	33,14
0,71920	0,06860	50,49	181,78	1097,15	2941,90	55,40	148,55	93,15	29,15	33,08
0,76715	0,07693	48,89	176,01	1153,53	2982,35	56,40	145,81	89,41	27,98	32,79
0,79142	0,08140	48,14	173,29	1183,17	3001,63	56,95	144,48	87,53	27,39	32,61
0,81556	0,08608	47,42	170,70	1214,11	3020,08	57,57	143,20	85,63	26,80	32,38
0,86236	0,09589	46,11	166,01	1279,10	3053,95	58,98	140,83	81,84	25,61	31,82
0,95446	0,11726	43,83	157,79	1413,27	3114,18	61,95	136,50	74,55	23,33	30,50
1,00032	0,12879	42,82	154,13	1481,03	3141,44	63,41	134,50	71,09	22,25	29,77
1,02317	0,13478	42,33	152,40	1515,32	3154,42	64,15	133,54	69,39	21,72	29,39
1,04630	0,14091	41,86	150,71	1549,21	3167,18	64,86	132,59	67,73	21,20	29,01
1,06957	0,14718	41,41	149,06	1582,87	3179,65	65,54	131,66	66,12	20,69	28,63
1,09270	0,15351	40,97	147,47	1616,03	3191,70	66,20	130,75	64,55	20,20	28,25
1,16264	0,17328	39,71	142,97	1714,42	3226,17	68,09	128,12	60,04	18,79	27,11
1,18623	0,18013	39,32	141,54	1746,80	3237,19	68,68	127,28	58,60	18,34	26,72
1,20958	0,18704	38,94	140,17	1778,80	3247,81	69,26	126,46	57,20	17,90	26,34
1,23290	0,19399	38,57	138,84	1809,98	3258,15	69,80	125,65	55,85	17,48	25,97

Table 12.5: Values for descent and lift-to-drag ratio calculation

c_L	c_D	v	v	v_z	K
[-]	[-]	[m/s]	[km/h]	[m/s]	[-]
0,10826	0,01777	130,15	468,52	21,36	6,09
0,13402	0,01789	116,97	421,10	15,61	7,49
0,15982	0,01818	107,11	385,61	12,18	8,79
0,18562	0,01863	99,39	357,81	9,97	9,96
0,21148	0,01926	93,12	335,22	8,48	10,98
0,23734	0,02006	87,90	316,43	7,43	11,83
0,26316	0,02102	83,47	300,51	6,67	12,52
0,28898	0,02218	79,66	286,77	6,11	13,03
0,31480	0,02353	76,32	274,76	5,70	13,38
0,34056	0,02506	73,38	264,16	5,40	13,59
0,39184	0,02870	68,41	246,27	5,01	13,65
0,41748	0,03080	66,27	238,59	4,89	13,55
0,44312	0,03308	64,33	231,58	4,80	13,40
0,46878	0,03551	62,54	225,16	4,74	13,20
0,49448	0,03812	60,90	219,23	4,70	12,97
0,52002	0,04090	59,38	213,78	4,67	12,72
0,54552	0,04385	57,98	208,72	4,66	12,44
0,57100	0,04697	56,67	204,01	4,66	12,16
0,59616	0,05028	55,46	199,66	4,68	11,86
0,62085	0,05374	54,35	195,65	4,70	11,55
0,69488	0,06476	51,37	184,93	4,79	10,73
0,71920	0,06860	50,49	181,78	4,82	10,48
0,76715	0,07693	48,89	176,01	4,90	9,97
0,79142	0,08140	48,14	173,29	4,95	9,72
0,81556	0,08608	47,42	170,70	5,00	9,47
0,86236	0,09589	46,11	166,01	5,13	8,99
0,95446	0,11726	43,83	157,79	5,39	8,14
1,00032	0,12879	42,82	154,13	5,51	7,77
1,02317	0,13478	42,33	152,40	5,58	7,59
1,04630	0,14091	41,86	150,71	5,64	7,43
1,06957	0,14718	41,41	149,06	5,70	7,27
1,09270	0,15351	40,97	147,47	5,75	7,12
1,16264	0,17328	39,71	142,97	5,92	6,71
1,18623	0,18013	39,32	141,54	5,97	6,59
1,20958	0,18704	38,94	140,17	6,02	6,47
1,23290	0,19399	38,57	138,84	6,07	6,36

Table 12.6: Values for descent and lift-to-drag ratio calculation with stopped engine

c_L	c_D	v	v	V_z	K
[-]	[-]	[m/s]	[km/h]	[m/s]	[-]
0,00522	0,02290	130,15	468,52	25,12	5,18
0,03088	0,02118	116,97	421,10	18,35	6,38
0,05670	0,02125	107,11	385,61	14,28	7,50
0,08240	0,02098	99,39	357,81	11,65	8,53
0,10826	0,02090	93,12	335,22	9,86	9,45
0,13402	0,02102	87,90	316,43	8,59	10,24
0,15982	0,02131	83,47	300,51	7,66	10,90
0,18562	0,02176	79,66	286,77	6,98	11,42
0,21148	0,02239	76,32	274,76	6,46	11,81
0,23734	0,02319	73,38	264,16	6,07	12,08
0,26316	0,02415	68,41	246,27	5,56	12,31
0,28898	0,02531	66,27	238,59	5,39	12,30
0,31480	0,02666	64,33	231,58	5,26	12,24
0,34056	0,02819	62,54	225,16	5,16	12,13
0,39184	0,03183	60,90	219,23	5,08	11,99
0,41748	0,03393	59,38	213,78	5,03	11,81
0,44312	0,03621	57,98	208,72	4,99	11,61
0,46878	0,03864	56,67	204,01	4,97	11,40
0,49448	0,04125	55,46	199,66	4,97	11,16
0,52002	0,04403	54,35	195,65	4,98	10,92
0,54552	0,04697	51,37	184,93	5,02	10,24
0,57100	0,05010	50,49	181,78	5,04	10,03
0,59616	0,05341	48,89	176,01	5,10	9,58
0,62085	0,05687	48,14	173,29	5,14	9,36
0,69488	0,06789	47,42	170,70	5,19	9,14
0,71920	0,07173	46,11	166,01	5,29	8,71
0,76715	0,08006	43,83	157,79	5,53	7,93
0,79142	0,08453	42,82	154,13	5,65	7,58
0,81556	0,08921	42,33	152,40	5,71	7,42
0,86236	0,09902	41,86	150,71	5,76	7,26
0,95446	0,12039	41,41	149,06	5,82	7,12
1,00032	0,13192	40,97	147,47	5,87	6,98
1,02317	0,13791	39,71	142,97	6,03	6,59
1,04630	0,14404	39,32	141,54	6,07	6,47
1,06957	0,15031	38,94	140,17	6,12	6,36
1,09270	0,15664	38,57	138,84	6,17	6,25

Table 12.7: Values for take-off length calculation

v	F	a_{xa}	v/a_{xa}	dl
[kmh]	[N]	[m/s^{-2}]	[1/s]	[m]
0	5024,70	3,7933	0,0000	0,0000
20	5018,03	3,7862	1,4673	4,0759
40	5011,36	3,7764	2,9423	12,2594
60	5004,70	3,7638	4,4282	20,5008
80	4998,06	3,7484	5,9285	28,8189
100	4991,42	3,7303	7,4466	37,2330
120	4984,79	3,7094	8,9863	45,7634
130	4978,17	3,6950	9,7728	26,1027

Table 12.8: Values for range and endurance calculation

c_L	c_D	v	v	v	SFC	R	R	T
[-]	[-]	[m/s]	[km/h]	[kts]	[kg/N·h]	[km]	[nm]	[h]
0,10826	0,01777	130,15	468,52	253,00	0,614	658,73	355,71	2,31
0,13402	0,01789	116,97	421,10	227,39	0,594	752,39	406,29	2,75
0,15982	0,01818	107,11	385,61	208,23	0,579	829,64	448,01	3,15
0,18562	0,01863	99,39	357,81	193,22	0,568	889,32	480,23	3,50
0,21148	0,01926	93,12	335,22	181,02	0,558	934,52	504,64	3,79
0,23734	0,02006	87,90	316,43	170,87	0,55	964,55	520,86	4,02
0,26316	0,02102	83,47	300,51	162,28	0,543	981,65	530,09	4,20
0,28898	0,02218	79,66	286,77	154,86	0,537	985,74	532,30	4,32
0,31480	0,02353	76,32	274,76	148,37	0,532	978,94	528,63	4,40
0,34056	0,02506	73,38	264,16	142,65	0,527	965,16	521,19	4,43
0,39184	0,02870	68,41	246,27	132,99	0,521	914,41	493,78	4,40
0,41748	0,03080	66,27	238,59	128,84	0,517	886,22	478,56	4,33
0,44312	0,03308	64,33	231,58	125,06	0,514	855,15	461,78	4,26
0,46878	0,03551	62,54	225,16	121,58	0,512	822,48	444,14	4,18
0,49448	0,03812	60,90	219,23	118,38	0,509	791,45	427,38	4,08
0,52002	0,04090	59,38	213,78	115,44	0,506	761,10	410,99	3,98
0,54552	0,04385	57,98	208,72	112,71	0,505	728,56	393,42	3,88
0,57100	0,04697	56,67	204,01	110,17	0,502	699,89	377,94	3,77
0,59616	0,05028	55,46	199,66	107,82	0,501	669,42	361,49	3,67
0,62085	0,05374	54,35	195,65	105,65	0,499	641,80	346,57	3,56
0,69488	0,06476	51,37	184,93	99,86	0,494	569,09	307,31	3,28
0,71920	0,06860	50,49	181,78	98,16	0,493	547,71	295,77	3,19
0,76715	0,07693	48,89	176,01	95,04	0,491	506,46	273,49	3,03
0,79142	0,08140	48,14	173,29	93,58	0,49	487,13	263,05	2,94
0,81556	0,08608	47,42	170,70	92,18	0,489	468,60	253,04	2,86
0,86236	0,09589	46,11	166,01	89,64	0,487	434,32	234,53	2,71
0,95446	0,11726	43,83	157,79	85,21	0,484	375,96	203,02	2,43
1,00032	0,12879	42,82	154,13	83,23	0,482	351,90	190,02	2,31
1,02317	0,13478	42,33	152,40	82,30	0,481	340,78	184,02	2,26
1,04630	0,14091	41,86	150,71	81,38	0,481	329,62	177,99	2,21
1,06957	0,14718	41,41	149,06	80,49	0,48	319,74	172,66	2,16
1,09270	0,15351	40,97	147,47	79,64	0,479	310,50	167,67	2,11
1,16264	0,17328	39,71	142,97	77,20	0,478	284,33	153,54	1,98
1,18623	0,18013	39,32	141,54	76,43	0,477	276,85	149,50	1,94
1,20958	0,18704	38,94	140,17	75,69	0,476	269,80	145,69	1,90
1,23290	0,19399	38,57	138,84	74,97	0,475	263,19	142,12	1,87

APPENDIX 4

Costs calculation

Table 12.9: Development costs table

the number of planned aircraft	QP	[pcs]	50	100	150	200
engineering hours for development	Ed	[hr]	48 125	48 125	48 125	48 125
engineering hours for production	Ep	[hr]	87 359	98 822	106 306	111 985
tooling hours	T	[hr]	255 975	288 589	309 826	325 913
engineering tooling hours	Te	[hr]	51 195	57 718	61 965	65 183
labor tooling hours	Tw	[hr]	204 780	230 872	247 861	260 731
labor hours	L	[hr]	827 617	1 178 013	1 451 876	1 685 185
quality control hours	QC	[hr]	107 590	153 142	188 744	219 074
development support	D	[USD]	147 075	147 075	147 075	147 075
flight test operations	F	[USD]	18 443	18 443	18 443	18 443
manufacturing material and equipment	M	[USD]	2 224 320	3 792 574	5 201 670	6 515 698
engine price	P	[USD]	10 400 000	20 400 000	30 400 000	40 400 000
costs for engineering work development	Edc	[USD]	1 203 117	1 203 117	1 203 117	1 203 117
costs for engineering work production	Edp	[USD]	2 183 976	2 470 547	2 657 643	2 799 616
costs of engineering tooling hours	Tec	[USD]	1 279 877	1 442 947	1 549 129	1 629 567
costs of labor's tooling hours	Tdc	[USD]	3 071 704	3 463 073	3 717 911	3 910 960
costs of labor's hours	Lc	[USD]	12 414 250	17 670 190	21 778 139	25 277 775
quality control costs	QCc	[USD]	2 689 754	3 828 541	4 718 597	5 476 851
overall costs	TC	[USD]	35 632 516	54 436 506	71 391 724	87 379 102
costs for 1 piece	PC	[USD]	712 650	544 365	475 945	436 896
cost for 1 piece + margin	PC	[USD]	783 915	598 802	523 539	480 585

Table 12.10: Income table

Qo	50	100	150	200
year	Income [USD]			
1	37 627 936	28 742 475	25 129 887	23 068 083
2	75 255 873	57 484 950	50 259 773	46 136 166
3	112 883 809	86 227 425	75 389 660	69 204 249
4	150 511 746	114 969 900	100 519 547	92 272 332
5	188 139 682	143 712 375	125 649 433	115 340 415
6	225 767 619	172 454 850	150 779 320	138 408 497
7	263 395 555	201 197 325	175 909 207	161 476 580
8	301 023 492	229 939 800	201 039 094	184 544 663
9	338 651 428	258 682 275	226 168 980	207 612 746
10	376 279 365	287 424 751	251 298 867	230 680 829
11	413 907 301	316 167 226	276 428 754	253 748 912
12	451 535 238	344 909 701	301 558 640	276 816 995
13	489 163 174	373 652 176	326 688 527	299 885 078
14	526 791 111	402 394 651	351 818 414	322 953 161
15	564 419 047	431 137 126	376 948 300	346 021 244
16	602 046 984	459 879 601	402 078 187	369 089 327
17	639 674 920	488 622 076	427 208 074	392 157 409
18	677 302 857	517 364 551	452 337 961	415 225 492
19	714 930 793	546 107 026	477 467 847	438 293 575
20	752 558 730	574 849 501	502 597 734	461 361 658

Table 12.11: Budget table

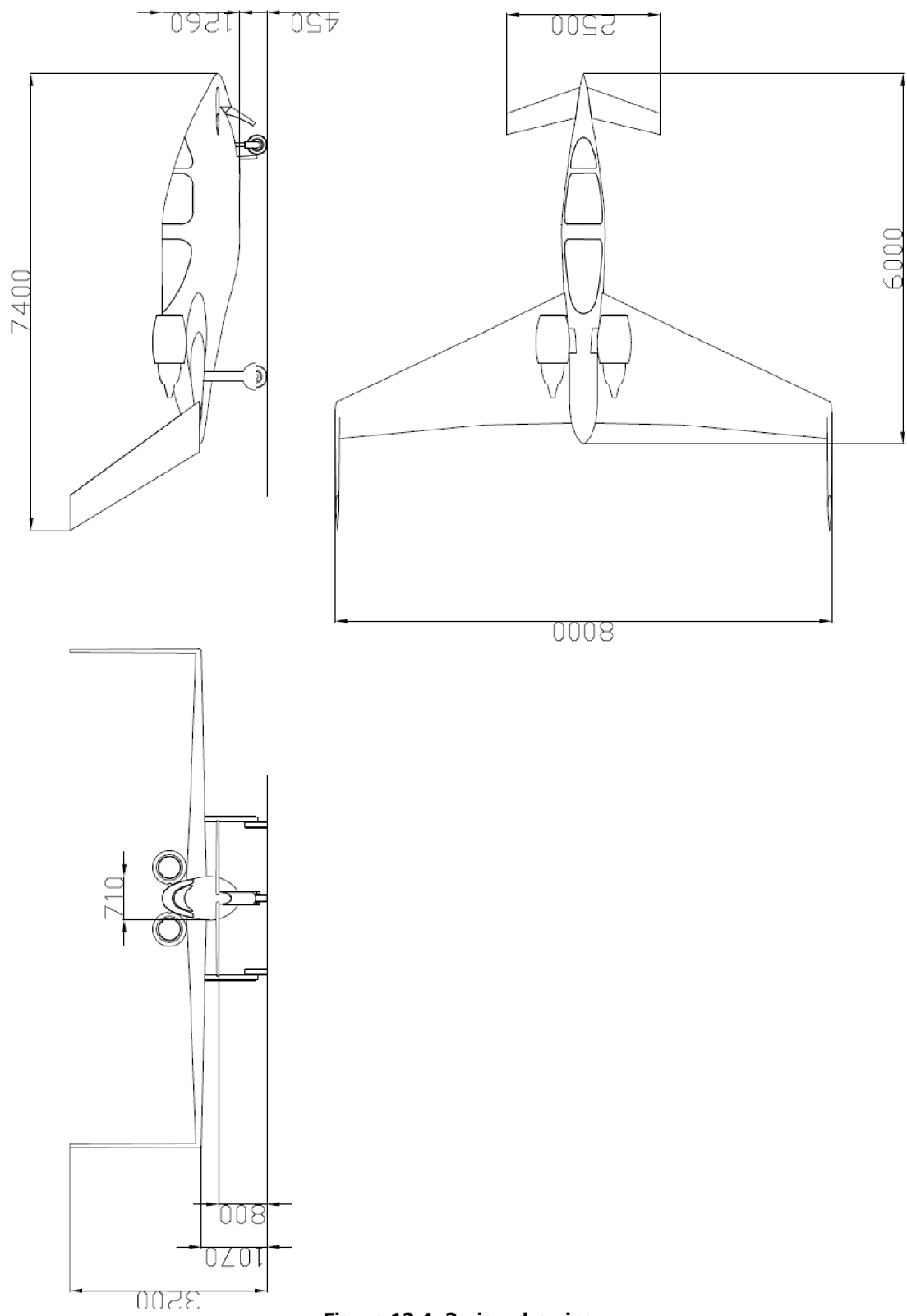| year	budget for nr. of produced aircraft [USD]			
	50	100	150	200
-5	0	0	0	0
-4	-7 126 503	-10 887 301	-14 278 345	-17 475 820
-3	-14 253 006	-21 774 602	-28 556 689	-34 951 641
-2	-21 379 509	-32 661 903	-42 835 034	-52 427 461
-1	-28 506 012	-43 549 205	-57 113 379	-69 903 282
0	-35 632 516	-54 436 506	-71 391 724	-87 379 102
1	1 995 421	-25 694 031	-46 261 837	-64 311 019
2	39 623 357	3 048 444	-21 131 950	-41 242 936
3	77 251 294	31 790 919	3 997 937	-18 174 853
4	114 879 230	60 533 394	29 127 823	4 893 230
5	152 507 167	89 275 869	54 257 710	27 961 313
6	190 135 103	118 018 345	79 387 597	51 029 396
7	227 763 040	146 760 820	104 517 483	74 097 478
8	265 390 976	175 503 295	129 647 370	97 165 561
9	303 018 913	204 245 770	154 777 257	120 233 644
10	340 646 849	232 988 245	179 907 143	143 301 727
11	378 274 786	261 730 720	205 037 030	166 369 810
12	415 902 722	290 473 195	230 166 917	189 437 893
13	453 530 659	319 215 670	255 296 803	212 505 976
14	491 158 595	347 958 145	280 426 690	235 574 059
15	528 786 532	376 700 620	305 556 577	258 642 142
16	566 414 468	405 443 095	330 686 464	281 710 225
17	604 042 405	434 185 570	355 816 350	304 778 308
18	641 670 341	462 928 045	380 946 237	327 846 390
19	679 298 278	491 670 520	406 076 124	350 914 473
20	716 926 214	520 412 995	431 206 010	373 982 556

APPENDIX 5

3 view drawing

Figure 12.4: 3-view drawing